Universitätsklinikum Essen

Relevance of the oncogene DJ-1, the tight junction protein claudin-1 and the thyroid hormone transporter MCT8 for follicular thyroid carcinogenesis

Inaugural-Dissertation

zur

Erlangung des Doktorgrades

Dr. rer. nat.

der Fakultät für Biologie

an der

Universität Duisburg-Essen

vorgelegt von

M.Sc. Julia Badziong

aus Wesel

März 2018

Die der vorliegenden Arbeit zugrunde liegenden Experimente wurden in der Klinik für Endokrinologie und Stoffwechselerkrankungen am Universitätsklinikum Essen durchgeführt.

1. Gutachter: Prof. Dr. Dagmar Führer-Sakel

2. Gutachter: Prof. Dr. Elke Cario

Vorsitzender des Prüfungsausschusses: Prof. Dr. Matthias Gunzer

Tag der mündlichen Prüfung: 22.08.2018

„Es gibt Gezeiten für der Menschen Treiben, nimmt man die Flut wahr,
führt sie uns zum Glück, versäumt man sie, so muß die ganze Reise des Lebens sich durch Not und Klippen winden. Wir sind nun flott auf solcher hohen See und müssen, wenn der Strom uns hebt, ihn nutzen, wo nicht, verlieren, was zur See wir wagten.“

(William Shakespeare)

Meinen Eltern und Kevin

in Liebe und Dankbarkeit

Table of contents

Abbreviations

°C – Degree Celsius

µ - Micro

Aa – Amino acids

ALK - Anaplastic lymphoma kinase

Amp – Ampicillin

ATC – Anaplastic thyroid carcinoma

BCA – Bicinchoninic acid assay

Bp – Base pairs

BrdU – 5-Bromo-2'-Deoxyuridine

BSA – Bovine serum albumin

Cld1 – Claudin-1

CO_2 – Carbon dioxide

d - Day

DAPI – 4',6-diamidino-2-phenylindole

DJ-1 - Parkinson disease protein 7

DMSO - Dimethyl sulfoxide

DNA – Deoxyribonucleic acid

DTT – Dithiothreitol

EDTA - Ethylenediaminetetraacetic acid

FA – Follicular adenoma

FACS – Fluorescence activated cell sorting

FAK – Focal adhesion kinase

FBS – Fetal bovine serum

Fig – Figure

For – Forward

FOXO3a – Forkhead box O3

FTC – Follicular thyroid carcinoma

FTC-133 – Follicular thyroid carcinoma cell line 133

G418 – Geneticin ®

GD – Graves' disease

h – Hour

H_2O – Water

H_2O_2 – Hydrogen peroxide

HBSS - Hank's Balanced Salt Solution

HPT – Hypothalamic-pituitary-thyroid

H-RAS – Harvey rat sarcoma

Kb – Kilo base

kDa – Kilo Dalton

KLF17 – Krüppel like transcription factor 17

l – Liter

LAT2 – L-type amino acid transporter 2

LAT3 – L-type amino acid transporter 3

LAT4 – L-type amino acid transporter 4

LB - Lysogeny broth

m – Milli

mAb – Monoclonal antibody

MCT8 – Monocarboxylate transporter 8

MEN2 – Multiple endocrine neoplasia type 2

min – Minutes

MMI - Methimazole

mRNA - Messenger RNA

MTC – Medullary thyroid carcinoma

NaCl – Sodium chloride

NIS – Sodium iodide symporter

Oatp – Organic anion-transporting polypeptide gene family

P70S6K – Ribosomal protein S6 kinase beta-1

pAb – Polyclonal antibody

PARK7 – Parkinson disease protein 7

PAX8 – Paired box gene 8

PBS – Phosphate buffered saline

pCR – Pathological complete remission

PCR – Polymerase chain reaction

PFA - Paraformaldehyde

PMA – Phorbol-12-myristate-13-acetate

PPARγ - Peroxisome proliferator-activated receptor gamma

PPFP – PAX8/PPARγ rearrangement

PTC – Papillary thyroid carcinoma

PTEN – Phosphatase and tensin homolog

PVDF – Polyvinylidene fluoride

qRT-PCR – Quantitative real time PCR

RAI - Radioiodine

Rev – Reverse

RIPA – Radioimmunoprecipitation assay buffer

RNA – Ribonucleic acid

Rpm – Revolutions per minute

SDS – Sodium docecyl sulfate

siRNA – Small interfering RNA

SOC – Super optimal broth with catabolite repression

T2 - 3,5-diiodo-L-thyronine

T3 – Triiodothyronine

T4 - Levothyroxine

TAE– Tris-acetate-EDTA

TERT – Telomerase reverse transcriptase

TBS – Tris buffered saline

TBS-T – Tris buffered saline Tween 20

TE – Tris-EDTA

TG - Thyroglobulin

TG buffer– Tris/Glycin buffer

TH – Thyroid hormones

TPO – Thyroid peroxidase

TRH – Thyrotropin-releasing hormone

TSH – Thyroid stimulating hormone

TTF-1 - Thyroid transcription factor 1

UV – Ultraviolet

V – Volt

WHO – World Health Organization

Chapter 1: The thyroid – An overview

1 Structure, function and dysfunction

The thyroid is a small endocrine gland which synthesizes, stores and secretes thyroid hormones into the circulation. It is located in the front part of the neck below the voice box and at the front and side face of the trachea (Fig. 1). The thyroid is part of the hypothalamic-pituitary-thyroid (HPT) axis. Synthesis of thyroid hormones (TH) is regulated by the hypothalamus via the thyrotropin-releasing hormone (TRH) and the pituitary by the thyroid-stimulating hormone (TSH) (Pape *et al*., 2010). TRH stimulates the pituitary to produce and secrete TSH while TSH in turn stimulates the thyroid to produce THs. TSH secretion itself can be blocked by negative feedback due to the most important THs thyroxine (T4) and triiodothyronine (T3) (Fig. 2). TH are required for growth, metabolism and a normal function of nearly all tissues (Yen, 2001).

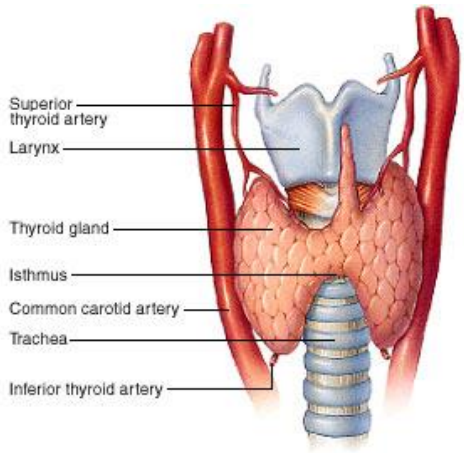

Figure 1: Localization of the human thyroid gland. The human thyroid consists of two lobes and is located in the front part of the neck below the voice box and the side face of the trachea. Source: www.mhhe.com/biosci/esp/2001_saladin/folder_structure/in/m5/s4/assets/images/inm5s4_1.jpg

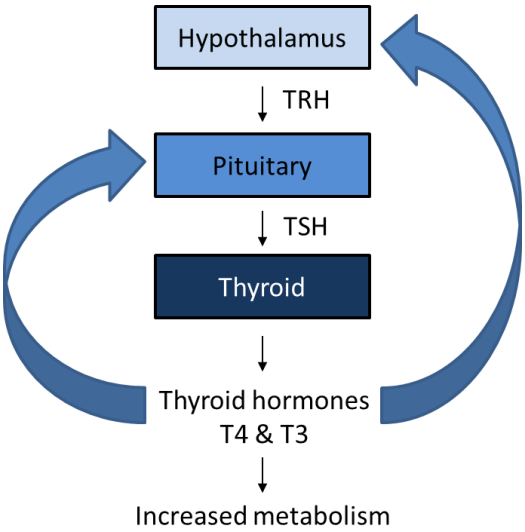

Figure 2: Overview of thyroid homeostasis due to the hypothalamic-pituitary-thyroid (HPT) axis. Hypothalamus releases TRH which stimulates the pituitary to release TSH. TSH stimulates the thyroid to produce thyroid hormones thyroxine (T4) and triiodothyronine (T3) which leads to an increased metabolism. Negative feedback of T4 and T3 regulate a balanced TH amount in the bloodstream.

Thyroid dysfunction is among the most common endocrine disorder (Pape *et al.*, 2010). One type is an overactive thyroid which produces too many thyroid hormones. This status, when the energy metabolism speeds up, is called hyperthyroidism. Patients who suffer from hyperthyroidism have symptoms like sweating, trembling, weight and hair loss, nervousness, palpitations and restlessness. The most frequent causes of hyperthyroidism are a thyroid autonomy or an autoimmune disease called Graves' disease (GD). The HPT axis is

disturbed and there is an inappropiate secretion of THs. To treat hyperthyroidism, antithyroid agents (propythiouracil, methimazol), which block thyroid hormone synthesis, can be used (Girgis *et al*., 2011). Other possibilities to treat hyperthyroidism are surgery or radioiodine (RAI) therapy. The other type of thyroid dysfunction is called hypothyroidism and is usually due to lack of TH production and hence an underactive thyroid. Untreated hypothyroidism in newborns leads to impaired mental development as well as a delayed growth (Williams, 2009). In adults, all body functions slow down and patients have loss of energy, slower metabolism, overweight, tiredness, bradycardia, dry skin and sensitivity to cold (Pape *et al*., 2010; Bensenor *et al*., 2012). The most frequent cause in adulthood is a Hashimoto's thyroiditis (autoimmune disease). To treat hypothyroidism the synthetic thyroid hormone levothyroxine (L-thyroxine) is used.

2 Thyroid cancer

Nodular thyroid diseases are the most common endocrine-related diseases. The prevalence of thyroid nodules in Germany is around 20-25 % (Meisinger *et al*., 2012) and the frequency of nodular thyroid disease increases with age (Führer and Schmid, 2010).

Thyroid tumours are classified by their function and their morphology. Classification of thyroid tumours can be performed by different methods e.g. sonography (Fig. 3) and scintigraphy. Both methods offer the physicians the opportunity to make statements on the accurate size as well as a functional classification of the nodule (hot/ cold) (Führer and Schmid, 2010).

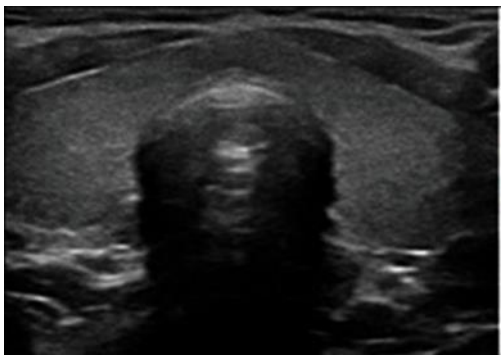

Figure 3: Normal thyroid gland. Gray scale ultrasound, transverse scan showing normal thyroid anatomy (Chaudhary *et al*., 2013)

Thyroid cancer in contrast is rare and accounts for only 0.1 % of all thyroid nodules (Führer and Schmid, 2010). Pathologists divide thyroid cancers into those with a follicle cell differentiation (differentiated carcinomas, poorly differentiated carcinomas and anaplastic carcinomas) and those with a C-cell differentiation (medullary carcinomas) (Fig. 4).

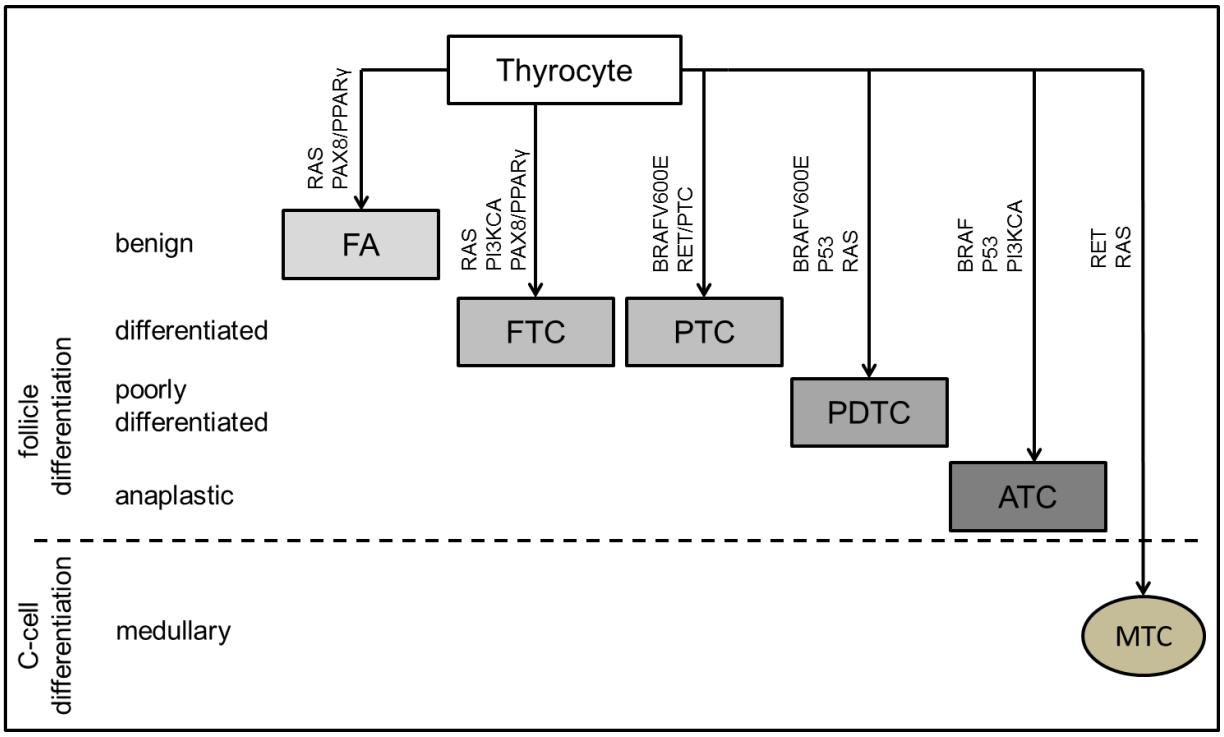

Figure 4: Schematic overview of the different types of thyroid cancer. Thyroid cancers are divided into those with follicle cell differentiation (benign, differentiated, poorly differentiated, anaplastic) and those with a C-cell differentiation (MTC).

The most common thyroid malignancy (incidence of ~80 %) is papillary thyroid carcinoma (PTC) (Nikiforova and Nikiforov, 2008; Giordano *et al*., 2014). The PTC belongs to the differentiated carcinomas and is well characterized. It shows somatic point mutations in the *BRAF* gene (Xu *et al.*, 2003) which is the most frequent molecular defect in sporadic PTCs. PTCs are also characterized by e.g. the RET/PTC rearrangement which occurs in 10-20 % of the cases (Nikiforova and Nikiforov, 2008). Taken together, in PTC a high frequency (~ 70 %) of activating alterations of genes encoding effectors of the MAPK signaling pathway can be found. However, mutations in members of the RAS pathway have also been reported *(PTEN*, *PI3KCA*, *Akt1*) (Giordano *et al*., 2014). PTCs are commonly curable with a 5 year survival of over 95 % (Hay *et al*., 2002) and current treatment includes surgery and radioactive iodine therapy (Giordano *et al*., 2014) followed by TH replacement or TH therapy. Follicular thyroid carcinoma (FTC) also belongs to the differentiated thyroid carcinomas. Today, we know about two molecular defects in FTC. First, mutations in the *RAS* genes occur in 30-50 % of all FTC but also in ~13-48 % of benign follicular adenoma (FA) (Nikiforova *et al.*, 2003). The second defect is the PAX8/PPARγ rearrangement (PPFP) which occurs in 25-56 % of FTC but also in up to 13 % of FA (Nikiforova *et al.*, 2003). Both

defects are not specific for FTC. The last two thyroid malignancies with a follicle differentiation are the poorly differentiated thyroid carcinoma (PDTC) and the undifferentiated anaplastic thyroid carcinoma (ATC). PDTC and ATC represent 5-10 % of all thyroid cancers. Both tumours show a high prevalence for *TERT* (telomerase reverse transcriptase) promotor mutations and also *RAS* or *BRAF* mutations (Landa *et al*., 2016). PDTC and ATC have a very poor prognosis. ATC is a very aggressive and fast growing tumour of the thyroid. The cause is an inactivation of Tp53 and an activation of multiple tyrosine kinase cascades, in particular the PI3K pathway (Schmid, 2010). Medullary thyroid carcinoma (MTC) is the only thyroid carcinoma with a C-cell differentiation. The incidence of MTC is 1-3 % of all thyroid carcinoma (Führer and Schmid, 2010). In 20-30 % of the cases the MTC is hereditary and germline mutations in the *RET* proto-gene are the cause. More often MTC occur sporadically (70-80 %). These MTCs are characterized by somatic mutations in the *RET* gene as well as *RAS* genes (Tiedje et al., 2015).

3 Open questions and working hypothesis for this thesis

Down to the present day we are able to classify thyroid nodules by their function as well as their morphology. We know increasingly about somatic mutations which occur with a high frequency in thyroid tumours. In some cases activating mutations affect the MAPK pathway, in some cases preferable the PI3K pathway. However, it is yet unclear which mechanisms influence the tumour biology in terms of invasiveness and metastasis. Besides, we are still unable to distinguish between a benign follicular adenoma and a malignant follicular thyroid carcinoma using cytology and it is yet open, whether FA and FTC evolve sequentially.

In this thesis we investigated the putative oncogene DJ-1 as a player of the PI3K pathway and claudin-1 as an important tight junction protein. We have choosen DJ-1 as it showed already an upregulation in FTC compared to FA (Krause *et al*., 2011) and was found to influence tumour biology in e.g. breast cancer. We choose claudin-1 because it plays an important role in development of the epithelial integrity of cell structure and an altered claudin-1 expression was observed in other human malignancies. Moreover, we addressed thyroid hormone transporters (MCT8, LAT2

and LAT4) as they facilitate the transport of TH into target tissues but are also expressed on the thyroid. We investigated if TH transporters are still expressed in thyroid malignancies and which role they play in states of altered thyroid function.

4 References

Bensenor IM, Olmos RD, Lotufo PA 2012 Hypothyroidism in the eldery: diagnosis and management. *Clinicial interventions in aging* **7**, 97-11

Führer D, Schmid KW 2010 Benigner Schilddrüsenknoten oder Schilddrüsenmalignom? *Der Internist* **51** 611–619.

Girgis CM, Champion BL, Wall JR 2011 Current concepts in graves' disease. *Therapeutic advances in endocrinology and metabolism* **3** 135-144.

Giordano TJ et al. 2014 Integrated genomic characterization of papillary thyroid carcinoma. *Cell* **3** 676-690.

Hay ID, Thompson GB, Grant CS, Bergstralh EJ, Dvorak CE, Gorman CA, Maurer MS, McIver B, Mullan BP, Oberg AL, Powell CC, van Heerden JA, Goellner JR 2002 Papillary thyroid carcinoma managed at the Mayo Clinic during six decades (1940-1999): temporal trends in initial therapy and long-term outcome in 2444 consecutively treated patients. *World journal of surgery* **8** 879-885.

Landa I, Ibrahimpasic T, Boucai L, Sinha R, Knauf JA, Shah RH, Dogan S, Ricarte-Filho JC, Krishnamoorthy GP, Xu B, Schultz N, Berger MF, Sander C, Taylor BS, Ghossein R, Ganly I, Fagin JA 2016 Genomic and transcriptomic hallmarks of poorly differentiated and anaplastic thyroid cancers. *The Journal of clinical investigation* 3 1052-1066.

Meisinger C, Ittermann T, Wallaschofski H, Heier M, Below H, Kramer A, Doring A, Nauck M, Volzke H 2012 Geographic variations in the frequency of thyroid disorders and thyroid peroxidase antibodies in persons without former thyroid disease within Germany. *European journal of endocrinology* **3** 363-371.

Nikiforova MN, Lynch RA, Biddinger PW, Alexander EK, Dorn GW, Tallini G, Kroll TG, Nikiforov YE 2003 RAS point mutations and PAX8-PPAR gamma rearrangement in thyroid tumours: evidence for distinct molecular pathways in thyroid follicular carcinoma. *The Journal of clinical endocrinology and metabolism* **88** 2318–2326.

Nikiforova MN, Nikiforov YE 2008 Molecular genetics of thyroid cancer: implications for diagnosis, treatment and prognosis. *Expert review of molecular diagnostics* **8** 83–95.

Pape, Klinke, Silbernagl 2010 Physiologie (Book), *Thieme* 547-554.

Reiners C, Wegscheider K, Schicha H, Theissen P, Vaupel R, Wrbitzky R, Schumm-Draeger PM 2004 Prevalence of thyroid disorders in the working population of Germany: ultrasonography screening in 96,278 unselected employees. *Thyroid : official journal of the American Thyroid Association* **14** 926–932.

Schmid KW 2010 Molekularpathologie von Schilddrüsentumouren. *Der Pathologe* **31** 229–233.

Tiedje V, Ting S, Dralle H, Schmid KW, Führer D 2015 Medullary Thyroid Carcinoma. *Internist* **56** 1019-31.

Willliams GR 2009 Actions of thyroid hormones in bone. *Endokrynologia Polska* **60** 380-388.

Xu X, Quiros RM, Gattuso P, Ain KB, Prinz RA 2003 High prevalence of BRAF gene mutation in papillary thyroid carcinomas and thyroid tumor cell lines. *Cancer research* **63** 4561–4567.

Yen PM 2001 Physiological and molecular basis of thyroid hormone action. *Physiological reviews* **81** 1097–1142.

Chapter 2: Impact of DJ-1 on follicular thyroid carcinogenesis

1 Introduction

1.1 DJ-1 and its relevance in vitro

The protein DJ-1 consists of 189 amino acids and is linked to Parkinson's disease (Bonifati *et al.*, 2003) and also human cancer (Davidson *et al.*, 2008; He *et al.*, 2012; Kawate *et al.*, 2013). DJ-1 is also called Parkinson disease protein 7 (PARK7). The human *DJ-1* gene is located in the distal part of the short arm of chromosome 1 (1p36.12-1p36.33) (Taira *et al.*, 2001) and is found in the cytoplasm and to a lesser extent in the nucleus and mitochondria of the cells. The structure of DJ-1 was investigated by X ray crystallography showing a monomer structure of DJ-1 with a α/β-fold containing of 11 β-strands and 8 α-helices (Tao and Tong, 2003) (Fig. 5).

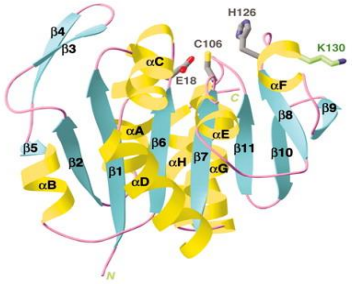

Figure 5: *Schematic* drawing of the structure of DJ-1. The β-strands are shown in *cyan*, α-helices are in *yellow*, and the loops are in *magenta*. Conserved cysteine in position 106 in the center (Tao and Tong, 2003).

In 1997, DJ-1 was first described as a putative oncogene due to its role in tumour growth and cell transformation. Thus it was demonstrated that DJ-1 transfected mouse embryonic fibroblast cells (NIH-3T3) showed an increase in proliferation and colony formation rate. Additionally, it was shown that the DJ-1 transforming activity was enhanced by co-transfected H-Ras and that the transforming activity of DJ-1 was efficiently, almost fully enhanced by H-Ras (Nagakubo *et al.*, 1997). In 2005, DJ-1 was described as a suppressor of the phosphatase and tensin homolog (PTEN) function in the flye eye (Kim *et al.*, 2005). It was shown that the DJ-1 expression level in different thyroid carcinoma cell lines (anaplastic carcinoma cell line (FRO), poorly differentiated papillary thyroid carcinoma cell lines (KTC1, KTC2, KTC3), follicular thyroid carcinoma cell line (FTC-133)) is positively correlated to Akt activity (Zhang *et al.*, 2008). Furthermore, it was shown that DJ-1 promotes migration and invasion of glioma cells by increasing focal adhesion kinase (FAK) phosphorylation. Moreover, pancreatic cancer cell lines (BxPC-2 and SW1990) were investigated and DJ-1 was found to be significantly upregulated and knockdown experiments in these cells showed that DJ-1 regulates pancreatic cancer cell migration and invasion properties (He *et al.*, 2012).

Furthermore, it was demonstrated that DJ-1 overexpression increases the invasion capacity and that a *DJ-1* knockdown downregulates cell invasion of breast cancer cell lines (Ismail *et al.*, 2014).

1.2 DJ-1 in human cancer

DJ-1 has a role in human cancer. Particulary breast cancer patients have elevated levels of DJ-1 protein in the serum as compared to healthy women (Le Naour *et al.*, 2001). Also mRNA expression of DJ-1 was found to be increased in breast cancer tissues (Tsuchiya *et al.*, 2012). Low DJ-1 protein expression after neoadjuvant therapy in breast cancer cells was found, associated with pathological complete remission (pCR) of DJ-1 (Kawate *et al.*, 2013). Furthermore, DJ-1 protein level was increased in primary non-small lung cancer samples and was associated with a poor prognosis in these patients (MacKeigan *et al.*, 2003). Therefore, the group of Han et al. marked DJ-1 as a potential biomarker for early diagnosis and monitoring of lung cancer metastasis (Han et al., 2017). A significant correlation between DJ-1 and phosphorylated PKB/Akt immunoreactivity was found in lung cancer patients (Kim *et al.*, 2005) which is in line with observations in breast cancer patients. DJ-1 expression was associated with a more aggressive disease in ovarian carcinoma patients (Davidson *et al.*, 2008). In gastric carcinoma (GC) a higher expression of DJ-1 was found to be significantly correlated with lymph node metastasis, distant metastasis and an advanced clinical stage. Moreover, a higher DJ-1 expression in gastric tumour cells was negatively correlated with PTEN expression (Li *et al.*, 2013). Higher DJ-1 serum levels were also found in endometrial cancer patients and DJ-1 serum amounts were significantly increased in parallel with the worsening of the neoplastic grade of the endometrial tumour (Di Cello et al., 2017). For the thyroid it was demonstrated that normal or benign thyroid tissues express no or little DJ-1 protein whereas malignant thyroid tissues like PTC, FTC, MTC and ATC highly express DJ-1 (Zhang *et al.*, 2008). In 2011 Krause *et al.* showed an up-regulation of DJ-1 in FTC compared with normal thyroid tissue (Krause *et al.*, 2011).

1.3 Aims & working hypothesis

DJ-1 is presumed to play a pivotal role in the PI3K/Akt driven carcinogenesis pathway particulary as a negative regulator of the tumour suppressor PTEN. In line with this, high DJ-1 expression is significantly correlated with tumour invasiveness itself, likewise DJ-1 overexpression is associated with a poor prognosis in different types of cancer (lung cancer, supraglotic squamous cancer, gastric carcinoma, urothelial carcinoma). Taken together this could make DJ-1 a novel prognostic marker in thyroid carcinogenesis.

It is still unknown how a follicular thyroid carcinoma develops. By clonality analysis we know that thyroid carcinomas as well as about 60 % of the benign nodules have a monoclonal origin which means that the tumours most likely develop from the expansion of a progenitor cell. Since previously described FA and FTC show no specific genotype but a RAS/PI3K activation, DJ-1 can be an interesting driver for follicular tumourigenesis.

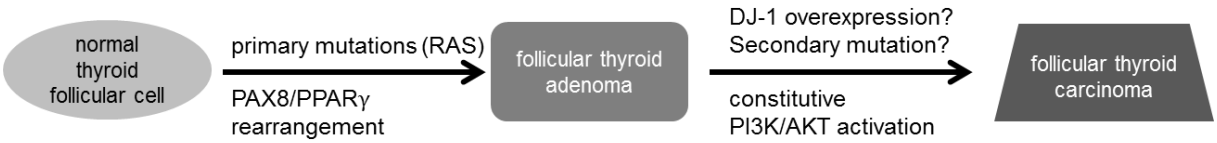

Figure 6: Hypothesis of DJ-1 dependent cell transformation of thyrocytes. A primary mutation in the *RAS* gene or the PAX8/PPARγ rearrangement leads to a neoplastic change of a normal follicular cell to a benign follicular adenoma. A secondary change due to a DJ-1 overexpression leads to a constitutive activation of the PI3K/Akt pathway and to transformation of the thyrocyte.

In view of the proposed impact of DJ-1 on Akt signaling, we asked whether DJ-1 plays a role in follicular thyroid carcinogenesis and/or impacts behaviour of FTC. In this thesis we show that DJ-1 expression is stepwise increased on mRNA and protein level from normal thyroid tissues to FA and FTC and exhibits cytoplasmic localization. Furthermore, we demonstrate that downregulation of DJ-1 diminishes migration and invasion capacity in follicular thyroid cancer cells (FTC-133), while overexpression of DJ-1 enhances proliferation and adds to tumourigenicity particulary in RASV12 and less in PPFP co-expressing rat PCCL3 cells and human FTC-133 cells.

2 Material and Methods

2.1 Material

All compositions of buffers, used substances and manufactures of used products are represented in detail in Appendix C (Material).

2.2 Methods

2.2.1 Immunohistochemistry

Thyroid samples from 116 patients were investigated. Histological classification of tissue specimens, according to World Health Organization (WHO) criteria, was obtained by certified pathologist. The following paraffin-embedded tissue sections were studied: 27 normal thyroid tissues (NT), 44 follicular adenoma (FA) and 45 follicular thyroid carcinoma (FTC) tissues.

Paraffin-embedded tissue sections were incubated with an anti-DJ-1 antibody. Tissue sections were deparaffinized and rehydrated through graded series of alcohols (70 %-/96 %-/100 % ethanol). Pretreatment was performed for 20 min in citrate buffer (pH 6.0) at 95 °C. Tissue sections were blocked in an aqueous hydrogen peroxide solution (3% H_2O_2). Primary antibodies were incubated for 30 min at RT. Immunoreactivity was demonstrated using a classical polymer system. Cell nuclei were stained with Haematoxylin (1:8) for 5 min and sections were mounted in Entellan®. All steps were performed in a semi-automated fashion using the Dako Autostainer. Human normal breast tissue was used as positive control. Negative controls (without primary antibody) were included in the experimental set-up. The Olympus BX51 upright microscope was used for light microscopy. Staining intensities were evaluated by calculating the hybrid (H) score of cytoplasmic DJ-1 expression (Detre et al., 1995; Mazières et al., 2013; Ting *et al.*, 2013):

$$H - Score = (strong\ staining\ (\%) * 3) + (medium\ staining(\%) * 2) + (weak\ staining\ (\%) * 1)$$

2.2.2 Cell culture

For cell culture experiments the human follicular thyroid carcinoma cell line FTC-133 (Hoelting *et al.*, 1997), which is derived from a lymph node metastasis near the primary tumour, was used. Cells were used between passages 5 and 15. FTC-133 cells were cultured in normal growth medium containing Ham's F12 medium supplemented with 10 % fetal bovine serum (FBS). FTC-133 starvation medium contained Ham's F12 and 2 % FBS. In addition, the rat follicular thyroid cell line PCCL3 (Fusco *et al.* 1987) was used between passages 5 and 10. Cells were cultured in Ham's F12 medium with 5 % FBS, 5 µg/ml Transferrin, 10 µg/ml Insulin, 10 ng/ml Somatostatin, 1 mU/ml thyroid stimulating hormone (TSH) and 10 nM Hydrocortison. PCCL3 starving medium contained Ham's F12, 5 % FBS, 5 µg/ml Transferrin, 10 ng/ml Somatostatin and 10 nM Hydrocortison. Cells were grown at 37 °C and 5 % CO_2.

Both cell lines were re-authenticated by mRNA expression profiling of the following markers: *TG*, *TPO*, *NIS*, *THOX1, PAX8* and *TTF-1* for FTC-133 cells and *rTg*, *rTpo*, *rNis* and *rThox1* for PCCL3 cells. For the mRNA expression profile of PCCL3 cells, mRNA of a thyroid from a 8 month old male rat was used as a control.

2.2.3 siRNA transfection

FTC-133 cells (25.000 cells/ml) were plated in six-well plates and cultured until 70-80 % confluency. Transfection with control (ctrl.) siRNA-A and DJ-1 siRNA was performed by following manufacturers' instructions. Briefly, transfection reagent and DJ-1-siRNA or ctrl. siRNA-A were diluted into transfection medium, incubated for 30 min at RT and added to the cells. After 6 h of incubation 1 ml of normal growth medium with two times FBS was added. After another 18 h the medium was replaced by fresh growth medium. Then proteins were isolated by using RIPA buffer or cells were used for migration and invasion assays.

2.2.4 Plasmids

The following constructs were generated: pcDNA3.1/Hygro-DJ-1 and pcDNA3.1/Hygro-RASV12. DJ-1 and RASV12 plasmids were restricted from their

donor vector (pcDNA3.1-DJ-1 and pcDNA3.1-RASV12) and cloned into the vector pcDNA3.1/Hygro (EV) by using recognition sites. Single base mutations were generated by site-directed mutagenesis using the Quickchange site-directed mutagenesis kit. Transformation was carried out in TOP10 chemically-competent *E.coli* followed by incubation at 37°C overnight on lysogeny broth (LB)-agar-plates containing 100 µg/ml ampicillin. Single clones were selected and incubated in LB medium overnight at 37°C. Expression vectors were extracted with QiaPrep® Spin Miniprep Kit and positive clones were detected by sequencing. The constructs pcDNA3.1/Hygro and pcDNA3.1-PAX8/PPARγ (PPFP) (Kroll et al., 2000) were available in our lab.

2.2.5 Transfection

The following stable PCCL3 cell lines were generated: PCCL3+EV, PCCL3+DJ-1, PCCL3+RASV12, PCCL3+PPFP, PCCL3+DJ-1-RASV12 and PCCL3+DJ-1-PPFP. For transfection 6 µl of the transfection reagent Lipofectamine® 2000 was diluted in 150 µl Opti-MEM and added to 14 µg of the DNA in 700 µl Opti-MEM and incubated for 5 min at RT. An amount of 150 µl of both solutions was added to the cells in a six well plate and incubated for 24 h at 5 % CO_2 and 37 °C. Subsequently the medium was replaced and cells were cultured for 72 h in normal growth medium. Selection of cells was performed with either 500 µg/ml Hygromycin B or 500 µg/ml G418 over 21-28 days. For generation of DJ-1-RASV12 and DJ-1-PPFP co-expression cell lines, the single transfected PCCL3+DJ-1 or PCCL3+PPFP cells were co-transfected with RASV12 or DJ-1 plasmid as described above. Selection of double transfected cells was performed with 500 µg/ml Hygromycin B and 500 µg/ml G418 over 21-28 days.

Transfection of FTC-133 cells was performed after manufactures manuel (JetPrime). The following transient transfected cells lines were generated: FTC133+EV, FTC133+DJ-1, FTC133+RASV12, FTC133+PPFP, FTC133+DJ-1-RASV12 and FTC133+DJ-1-PPFP. For transfection 2 µg DNA was diluted into 200 µl jetPRIME® buffer and mixed by vortexing. Then 4 µl jetPRIME® were added and gently vortexed for 10 s. The solution was incubated for 10 min at RT. Then 200 µl of the transfection

mix were added to 200.000 cells/ml and seeded into 6-well plates. Cells were incubated for 24 h and then analyzed.

2.2.6 Immunoblot

The following antibodies were used: anti-DJ-1 (1:1000), anti-phospho-Akt S473 (1:1000), anti-phospho-P70S6K (1:1000), anti-Akt (1:1000), anti-phopho-P44/42 MAPK (pArk1/2, 1:1000), anti-P44/42 MAPK (Ark1/2, 1:1000), anti-β-Actin (1:1000), anti-GAPDH (1:1000), anti-Lamin A/C (1:1000), anti-alpha 1 Sodium Potassium ATPase (1:1000), anti-rabbit IgG HRP-linked antibody (1:2000) and anti-rabbit IgG DyLight 488 (1:15000). Whole protein lysates were extracted by RIPA-buffer. In addition a phosphatase and protease inhibitor cocktail was added to the buffer. Protein fractionation was performed using the subcellular protein fractionation kit for cultured cells. Extracted proteins were quantified by BCA protein assay. Aliquots of proteins (10-20 µg) were separated on a 10 % SDS gel, blotted onto a polyvinylidene difluoride (PVDF) membrane using the wet-blot technique at 4 °C overnight. Unspecific binding sides were blocked with 5 % bovine serum albumin (BSA) for 1 h at RT. Primary antibodies were incubated overnight in 5 % BSA at 4 °C. Incubation of the secondary antibody was performed for 2 h at RT in 2.5 % non-fat milk. Visualization of proteins was done by luminescence using the Immun-Star™ WesternC™ Kit or by fluorescence dependent on the secondary antibody. Differences in protein expression levels were quantified by densitometry using the ImageLab™ Software. Relative values of the loading controls β-Actin, Akt and Ark or the target proteins DJ-1, pAkt, pArk or pP70S6K were calculated. The adjusted values were used to calculate the geometric mean of the controls and target proteins followed by calculation of the percent of protein level alteration.

2.2.7 Immunofluorescence

PCCL3 cells (50 000 cells/ml) were seeded on cover slides and incubated at 5 % CO_2 and 37 °C for 48 h. Cells were washed twice with phosphate buffer saline (PBS) for 5 min and then fixed with 4 % paraformaldehyde (PFA) for 15 min at RT. PFA was

aspirated, cells were washed three times with PBS and were permeabilized with 0.1 % TritonTM X-10 in PBS for 10 min at RT. Blocking was performed by using 3 % BSA in PBS for 1 h at RT. Cells were washed three times with 0.1 % BSA/ PBS and a specific primary antibody against DJ-1 (1:1000) was diluted in 0.1% BSA/ PBS. After incubation with the primary antibody (4°C, overnight) cells were washed six times with 0.1 % BSA/ PBS. Then, cells were incubated with the secondary antibody AlexaFluor® 488 goat anti rabbit (1:250) for 1 h at RT in 0.1 % BSA/ PBS. Cells were washed again six times with 0.1 % BSA/ PBS for 5 min and detection of the cytoskeleton was performed by incubation with Phalloidin® 555 (1:60) in 0.1% BSA/ PBS for 20 min at RT. Visualizing of the nuclei was performed with Draq5TM (1:500) for 1 h at RT. Cover slides were embedded in ImmuMount and viewed with an LSM 510 Meta confocal microscope.

2.2.8 In vitro scratch assay

FTC-133 (40.000 cells/ml) or PCCL3 cells (50.000 cells/ml) were seeded in 24-well plates and grown to 70-80 % confluency for 48 h at 5 % CO_2 and 37 °C. Cells were incubated for 24 h in the respective starvation medium before the scratch was performed by cross-scraping the monolayer with a pipette tip. The scratch was monitored by a light microscope with camera system (Olympus CK40 with Olympus C5060 camera) directly after performing the scratch as well as at certain time points. The open wound area was calculated using TScratch Software (Gebäck et al., 2009). The percentage of open wound area at the chosen time points was normalized to the time point directly after performing the scratch.

2.2.9 Trans-well migration assay

FTC-133 cells (50.000 cells/ml) or PCCL3 cells (50.000 cells/ml) were seeded onto the membrane of Cell Culture Inserts in 24-well plates in 300 µl of the respective starvation medium. Each well was filled with 700 µl of normal growth medium. The migration was performed at 5 % CO_2 and 37 °C for 24 h (FTC-133) cells and 48 h (PCCL3). Medium was aspirated and the non-migrated cells were removed from the filter by using a

cotton bud. For counting, cells were detached with 0.25 % trypsin/EDTA, washed, resuspended in medium and analyzed with a cell counter system.

2.2.10 Trans-well invasion assay

Cell Culture Inserts were placed in 24-well plates and coated with Matrigel (200 µg/ml) for 2 h at 37 °C. FTC-133 cells (50.000 cells /well) or PCCL3 cells (50.000 cells /well) were seeded onto the Matrigel coated membrane of the Insert in 300 µl of the respective starvation medium. Each well contained 700 µl of cell line specific normal growth medium. The invasion was performed at 5 % CO_2 and 37 °C for 24 h (FTC-133) and 48 h (PCCL3). Medium was aspirated and the non-invaded cells were removed from the filter by using a cotton bud. For counting, cells were detached with 0.25 % trypsin/EDTA, washed, resuspended in medium and analyzed with a cell counter system.

2.2.11 Growth curves

PCCL3 cells (15.000 cells/ml) were seeded in 6-well plates and cultured in starvation medium. After 5, 10 and 12 days cells were detached with 0.25 % trypsin/EDTA and counted using a cell counter system. The medium was replaced every five days.

2.2.12 Colony formation assay (PCCL3)

PCCL3 cells (500 cells /well) were seeded in 6-well plates. The cells were cultured for 7 days in normal growth medium. Then the medium was aspirated, cells were washed with PBS and stained with 0.5% crystal violet, 1% formaldehyde and 1% methanol in PBS for 20 min. After washing with deionized water the stained colonies were dried and randomly three photos of each well were taken by using a light microscope with camera system (Olympus CK40 with Olympus C5060 camera). The colony size was analyzed using the Image J software. The experiment was performed three times in triplicates. Results of the colony formation assay are presented as box plot graphs.

2.2.13 Caspase-3 activity assay

PCCL3 cells (40 000 cells/ml) were seeded in 6-well plates and cultured until 70-80 % of confluency. For induction of apoptosis cells were incubated with 50 µM Etoposide for 48 h. The assay was performed at 5 % CO_2 and 37 °C. DMSO treated cells (<0.02 %) were used as a control. After the indicated time the medium was collected, attached cells were detached by using Trypsin/EDTA (0.25 %), both parts were merged. Then cells were assayed using the Caspase-3 colorimetric protease assay according to the manufactures manual.

2.2.14 Proliferation assay (BrdU)

For proliferation assay, cells (25.000 cells/ml) were seeded onto 96 well plates and cultured for 24 h at 37 °C and 5 % CO_2. 5-Bromo-2'-Deoxyuridine (BrdU, 10µM) labeling solution was incubated for 2 h at 37 °C and 5 % CO_2. Then cells were washed once with 10 x PBS, fixed with 70 % ethanol/ 0.5M HCl for 30 min at RT, washed three times with PBS/ 10% FBS and nucleases were added for 30 min at 37 °C. Cells were washed three times, incubated with anti-BrdU-POD solution (200 mU/ml) for 30 min at 37 °C, washed again three times and incubated with a peroxidase substrate for 2-30 min at RT. Cells were assayed by an ELISA reader at 405 nm and a reference wavelength of 490 nm. The percentage of proliferating cells normalized to the respective control was determined.

2.2.15 Annexin V assay

Annexin V staining was performed according to the manufactures manual (Biolegend). FTC-133 cells ($1x10^6$ cells/ml) were washed twice with cold BioLegend staining buffer and resuspended in Annexin V binding buffer. Then 100 µl of this suspension were transferred to a 5 ml test tube and 5 µl of FITC Annexin V were added. Addionally 10 µl of PI solution or 7-AAD were added. The suspension was gently vortexed and incubated for 15 min at RT in the dark. Finally 400 µl of Annexin V binding buffer were added to each tube. The cells were analyzed by flow cytometry.

2.2.16 Quantitative RT-PCR

Total RNA was isolated from NT, FA and FTC tissues by using the RNeasy Fibrous Tissue Mini Kit. cDNA was prepared using SuperScript® III First-Strand Synthesis SuperMix for qRT-PCR. Quantitative real-time PCR was performed by the LightCycler® 480 II using SYBR Green Master I for amplification. Oligonucleotides were designed using PrimerBlast and synthesized by Eurofins. Oligonucleotide sequences for h*DJ-1*-for, h*DJ-1*-rev, h*βAct*-for, h*βAct*-rev, *18S*-for, *18S*-rev, h*Ppia*-for and h*Ppia*-rev are presented in Appendix C (Table 18). Results were analyzed by a variant of the delta-delta CT analysis method which takes into account the efficiency of the amplification (Pfaffl, 2001). The mRNA levels of h*DJ-1* were normalized to h*β-ACTIN*, h*PPIA* and *18S*.

2.2.17 Statistical analysis

For immunohistochemistry, the median H-Score was determined. Scratch assay, trans-well migration, trans-well invasion and colony formation assay were performed in triplicates and were repeated in three independent experiments. Growth curves were performed in duplicates and have been repeated six times. qRT-PCR was performed in duplicates. Analysis was performed by the unpaired t-test or One-way ANOVA with Bonferroni's multiple comparison post-hoc test using GraphPad Prism 5 software. Results are shown as mean±SEM. Differences were considered significant if p values were: *$p<0.05$, **$p<0.01$ or ***$p<0.001$. Annexin V staining was performed in three independent experiments. Analysis was performed by One-way ANOVA with Tukey's multiple comparison post-hoc test using GraphPad Prism 5 software. Differences were considered significant if p values were **$p<0.009$ or ****$p<0.0001$.

3 Results

3.1 Cytoplasmic DJ-1 is increased in human follicular thyroid carcinoma tissue

DJ-1 expression and localization was investigated in normal thyroid tissue, follicular adenoma and follicular thyroid carcinomas by qRT-PCR and immunohistochemistry. The mean age of diagnosis of an FA was 50.25 years while the mean age of diagnosis of an FTC was 57.97 years. More woman were diagnosed with either a FA (25 vs 15) or a FTC (22 vs 17) as compared to men (Table 1).

Table 1: Number, age and sex of patients for FA and FTC samples.

Characteristics	**Number**
FA	n=44
mean age of diagnosis (SD)	50.25 (13.75)
age range	18-89
mean age male (SD), n	51.73 (16.07), 15
mean age female (SD), n	49.93 (8.34), 25
not specified	4
FTC	n=45
mean age of diagnosis (SD)	57.97 (16.78)
age range	19-83
mean age male (SD), n	55.47 (18.29), 17
mean age female (SD), n	59.91 (15.07), 22
not specified	6

Significantly higher DJ-1 transcript levels were found in FTC compared to FA and NT (1.58±0.07 for FTC, 0.96±0.04 for FA and 1.00±0.05 for NT; $p<0.001$) (Fig. 7A). To investigate if increased DJ-1 mRNA expression is also reflected on the protein level and to determine DJ-1 localization, immunohistochemistry was performed. DJ-1 was moderately expressed in the cytoplasm of normal thyroid tissues and a significant stepwise increase in DJ-1 protein expression was found in FA ($p<0.01$; 51.59±5.71)

and FTC (p<0.001; 70.33±5.56) as compared to NT (33.75±6.30) (Fig. 7B).

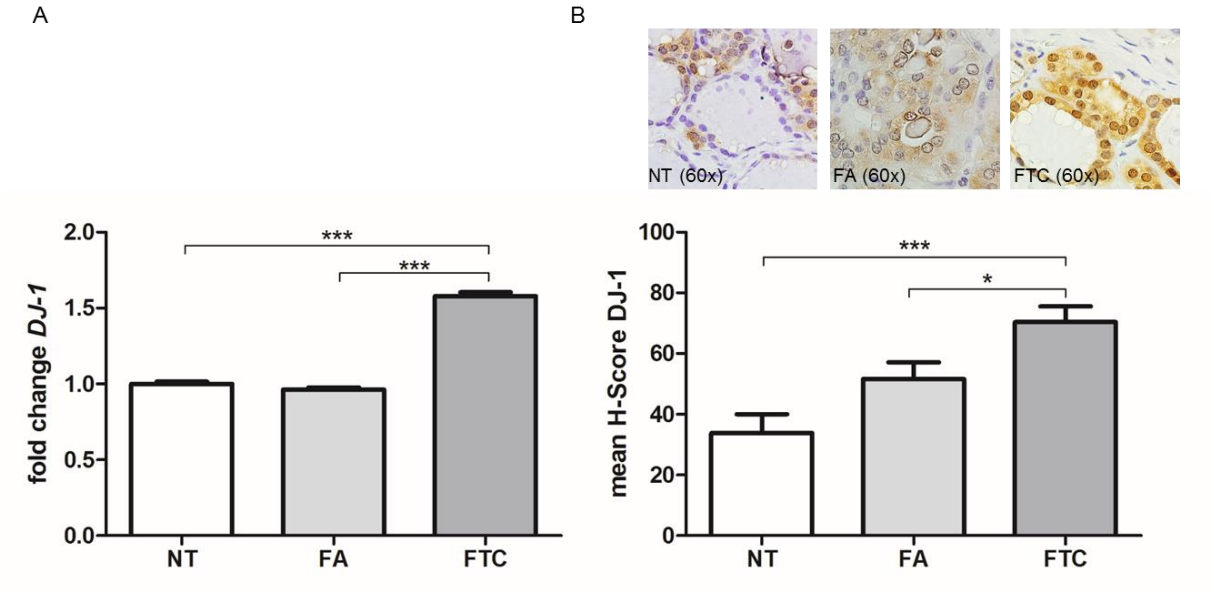

Figure 7: DJ-1 expression is increased in human follicular thyroid carcinoma tissue. DJ-1 expression was investigated in human tissues of normal thyroid (NT), follicular adenoma (FA) and follicular thyroid carcinoma (FTC). (A) Gene expression levels were determined by quantitative real-time PCR. DJ-1 mRNA expression level was significantly increased in FTC compared to NT and FA. 18S, PPIA (peptidylprolyl isomerase A, cyclophilin A) and β-ACTIN (ribosomal protein L13a) were used as reference genes. Data are presented as fold-changes, mean±SEM, n=8, efficiency corrected ΔΔCt method. Values were obtained significant by unpaired t-test and considered statistically significant if ***p<0.001. (B) Protein expression levels were determined by immunohistochemistry of NT (N=27), FA (N=44) and FTC (N=45). DJ-1 was significantly increased in FTC compared to NT and FA. Olympus BX51 upright microscope (magnification of 60x, Olympus). Data are presented as mean H-Scores, mean±SEM, n=27-45, unpaired t-test, *p<0.05, ***p<0.001.

3.2 DJ-1 knockdown decreases migration and invasion in human follicular thyroid carcinoma cells

We performed qRT-PCR to investigate if the FTC-133 cells still express the thyroid specific markers *TG*, *TPO*, *NIS*, *THOX1*, *TTF1* and *PAX8*. Thyroid markers *PAX8* and *TTF1* were expressed on a detectable level in FTC-133 cells. However, no expression was detected for *TG*, *TPO*, *NIS* and *THOX1* (CT values of the qRT-PCR measurements are high around 30) (Table 2).

Table 2: CT values of thyroid mRNA specific target genes

Gene	FTC-133 cells
TG	>35
TPO	>35
NIS	>35
THOX1	>35
PAX8	29
TTF1	30

As the next step the functional relevance of DJ-1 in FTC behaviour was investigated *in vitro*. First, the endogenous expression and localization of DJ-1 in follicular thyroid cancer FTC-133 cells was examined by fractionation and immunoblotting showing that DJ-1 is localized in the cytoplasma (Fig. 8A).

To investigate if modulation of DJ-1 expression influences the functional behaviour of FTC-133 cells, DJ-1 knockdown experiments were performed. Successful DJ-1 knockdown was demonstrated by immunoblotting and as a negative control served FTC-133 cell transfected with non-targeting ctrl. siRNA (Fig. 8B). A DJ-1 knockdown of 50 % was demonstrated. A slower cell invasion and a slower cell migration rate were found in DJ-1 siRNA transfected FTC-133 cells compared to ctrl. siRNA transfected cells by trans-well migration and trans-well invasion assays (Fig. 8C, D). Furthermore, findings of the trans-well migration assay were confirmed by scratch assay, showing a slower reconstitution of an intact cell monolayer in DJ-1 siRNA transfected cells as compared to the ctrl. siRNA transfected cells (Fig. 8E).

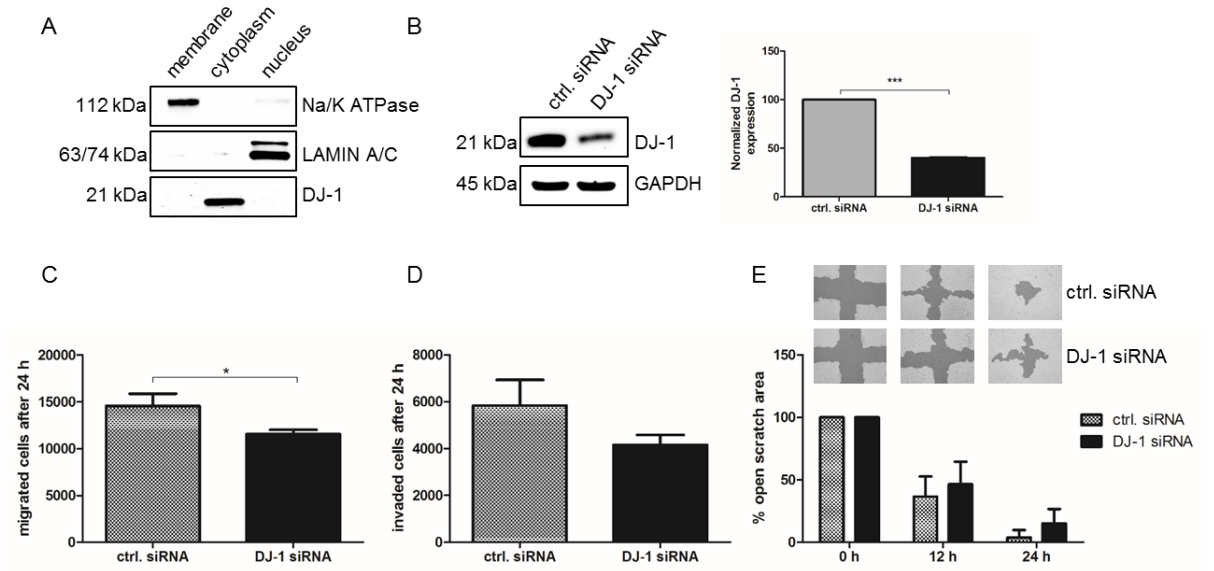

Figure 8: DJ-1 knockdown decreases the aggressiveness of human follicular thyroid carcinomas cells. (A) Western blot analysis of fractionated protein lysates of FTC-133 cells showed cytoplasmic DJ-1 protein expression. The specific cell fraction markers sodium potassium ATPase (membrane) and LAMIN A/C (nucleus) were used as control. (B) Protein expression levels were determined by immunoblotting of FTC-133 wildtype (WT), ctrl. siRNA and DJ-1 siRNA transfected cells. DJ-1 was significantly decreased in DJ-1 siRNA transfected cells as compared to FTC-133 WT and ctrl. siRNA transfected cells. Data are presented as normalized DJ-1 expression, mean±SEM, n=3. Values were obtained significant by unpaired t-test and considered statistically significant if ***$p<0.001$. (C) Knockdown of DJ-1 results in a slower trans-well migration of FTC-133 cells as compared to the control. Values were obtained significant by unpaired t-test and considered statistically significant if *$p<0.05$. (D) Knockdown of DJ-1 results in slower trans-well invasion of FTC-133 cells as compared to ctrl. siRNA transfected cells. (E) Knockdown of DJ-1 results in slower scratch repair of FTC-133 cells as compared to the control. All data are represented as mean±SEM, n=3.

Next we asked, if modulation of the functional behaviour by DJ-1 knockdown involves PI3K/Akt and/or MAPK/Erk signaling. Therefore, the expression and phosphorylation pattern of Akt and Erk were investigated in DJ-1 knockdown and ctrl. siRNA transfected FTC-133 cells. A decrease of pAkt was found in DJ-1 siRNA transfected cells as compared to controls. We investigated also the expression pattern of downstream targets forkhead box O3 (FOXO3a) and ribosomal protein S6 kinase beta-1 (P70S6K). Both targets were significantly downregulated after knockdown of DJ-1. No differences were observed for the phosphorylation of Erk (Fig. 9A, B).

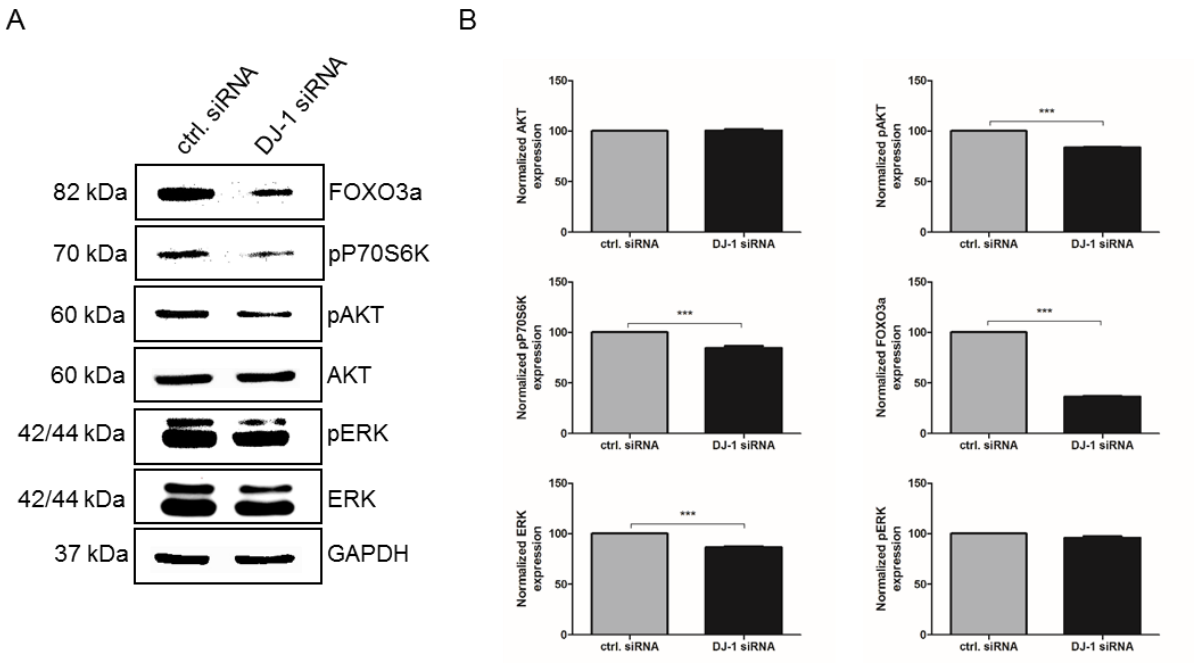

Figure 9: Phosphorylation of Akt and Erk by DJ-1 knockdown in follicular thyroid carcinoma cells. Protein expression levels were determined by immunoblotting of ctrl. siRNA and DJ-1 siRNA transfected cells. (A, B) DJ-1 knockdown revealed no significant differences of Akt expression between ctrl. siRNA and DJ-1 siRNA transfected cells. DJ-1 knockdown decreased protein expression of pAkt as compared to ctrl. siRNA transfected cells. DJ-1 knockdown revealed significant decreased protein expression of pP70S6K and FOXO3a as compared to ctrl. siRNA transfected cells. DJ-1 knockdown significantly decreased Ark expression as compared to ctrl. siRNA transfected cells. DJ-1 knockdown revealed no differences of pErk expression between ctrl. siRNA and DJ-1 siRNA transfected cells. β-ACTIN was used as loading control for Akt and Erk expression and total Akt as well as total Erk for their corresponding phospho-proteins. Data are presented as normalized protein expression, n=3, mean±SEM. Values were obtained significant by One-way ANOVA with Bonferroni's multiple comparison post-hoc test and considered statistically significant if ***p<0.001.

3.3 DJ-1 acts as an additional factor in follicular thyroid tumourigenesis

We performed qRT-PCR to investigate if the PCCL3 cells still express the thyroid specific markers *Tg*, *Tpo, Nis* and *Thox1.* All investigated thyroid specific markers were expressed at a detectable level in PCCL3 cells. The CT values of the qRT-PCR measurements varied between 14-26 (Table 3).

Table 3: CT values of thyroid specific target genes

Gene	Rat thyroid	PCCL3 cells
Tg	14	19
Tpo	21	26
Nis	23	24
Thox1	26	26

We found a significant downregulation of r*Tg* (0.64±0.07) and r*Tpo* (0.46±0.05) compared to the normal rat thyroid gland. However, r*Nis* (0.97±0.06) and r*Thox1* (0.93±0.05) showed comparable expression levels as the rat thyroid (Fig. 10).

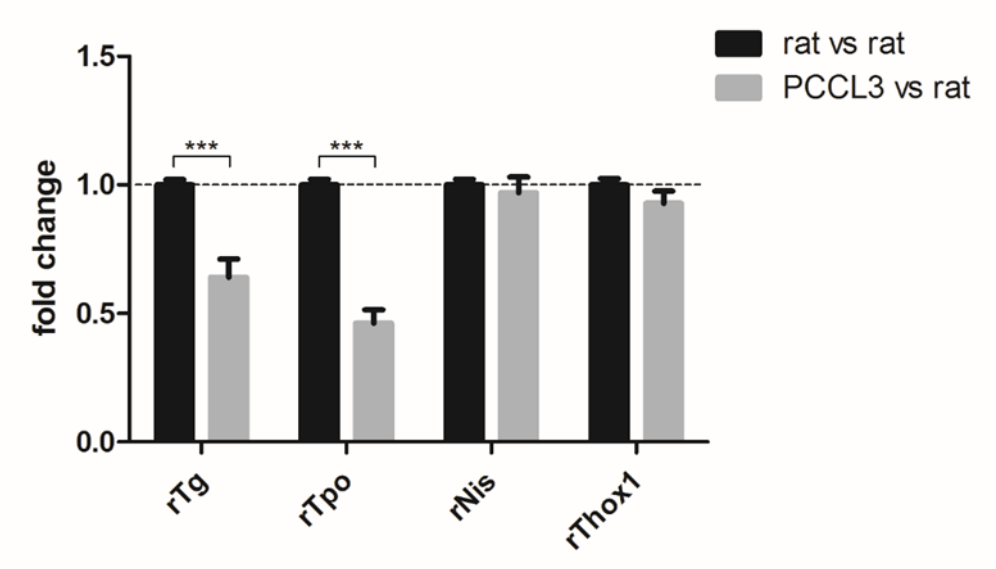

Figure 10: Expression of thyroid specific genes in PCCL3 cells. *Tg*, *Tpo*, *Nis* and *Thox1* expression was investigated in a rat thyroid and rat PCCL3 cells. (A) Gene expression levels were determined by quantitative real-time PCR. mRNA expression level of *Tg* and *Tpo* were decreased in PCCL3 cells but are still on a detectable level. *rNis* and *rThox1* expression were comparable to the rat thyroid. 18S and PPIA (peptidylprolyl isomerase A, cyclophilin A) were used as reference genes. Data are presented as fold-changes, mean±SEM, efficiency corrected ΔΔCt method. Values were obtained significant by unpaired t-test and considered statistically significant if ***p<0.001.

Next, we stably transfected DJ-1, RASV12 and PPFP into PCCL3 cells to investigate their influence on thyroid cell behaviour. To investigate if the plasmids DJ-1, RASV12 and PPFP were incorporated into the cells, we performed PCR (see Appendix C, Table 19) and agarose gel electrophoresis (Fig. 11A, B).

A

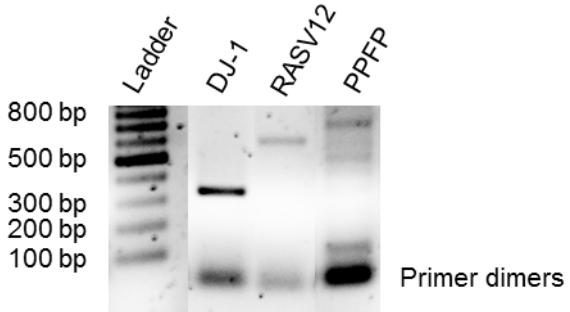

B

construct	size
DJ-1	~ 450 bp
RASV12	~ 650 bp
PPFP	~ 750 bp

Figure 11: Detection of genomic integration of DJ-1, RASV12 and PPFP in PCCL3 cells. A) Agarose gel of construct control PCR. DJ-1, RASV12 and PPFP were amplified by PCR. B) Table show size of the amplified constructs.

Further we investigated the localization of DJ-1 *in vitro* by performing immunofluorescence of PCCL3 WT cells. We found DJ-1 mainly located in the cytoplasm (Fig. 12) like already observed for human thyroid tissue samples.

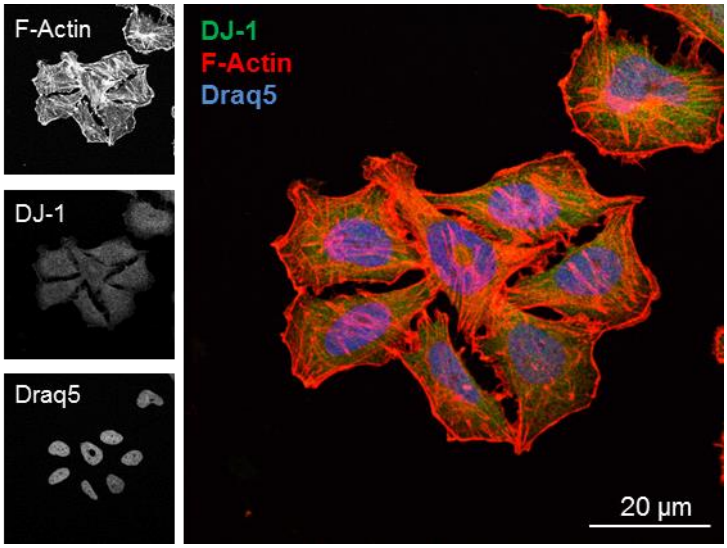

Figure 12: Localization of DJ-1 in PCCL3 cells. PCCL3 cells with predominant DJ-1 (green) localization in the cytoplasm by immuno-fluorescence. Detection of the nucleus was performed with Draq5 (blue), detection of the cytoskeleton with Phalloidin 555 (red). Microscopy was performed with confocal microscopy using the LSM510 (Zeiss, Germany).

To investigate whether DJ-1 impacts follicular thyroid tumourigenesis, PCCL3 cells were stably transfected with DJ-1 or stably co-transfected with DJ-1 and one of the two common oncogenes in follicular tumours RASV12 (Theoharis *et al*. 2012) or PPFP (Kroll *et al*., 2000; Nikiforova *et al*., 2003). In addition, stably single transfected cell lines with RASV12, PPFP and EV were generated and served as controls. Functional behaviour was investigated by proliferation-, migration-, invasion and colony formation assays as well as determination of caspase-3 activity to assess apoptosis.

In general, only minor alterations in functional behaviour of “normal” rat PCCL3 cells with DJ-1 overexpression were found i.e. slightly elevated migration and slightly diminished invasion (Fig. 13B-C, 13E-F). In contrast, significantly increased proliferation was found for DJ-1 overexpressing cells. Furthermore, increased proliferation was observed in double transfected DJ-1-RASV12 PCCL3 cells as compared to single RASV12, DJ-1 or EV transfected cells (Fig. 13A). Moreover, DJ-1-RASV12 PCCL3 cells showed significantly enhanced trans-well migration and trans-well invasion than DJ-1 and RASV12 and EV single transfected cells (Fig. 13B-C). For the DJ-1-PPFP double transfected cells significant differences in proliferation rate were

found as compared to EV PCCL3 cells but not to DJ-1 or PPFP transfected PCCL3 cells (Fig. 13B). However, in the trans-well migration assay, both the DJ-1-PPFP co-transfected and the PPFP single transfected cells showed a significant increase in migration capacity compared to EV PCCL3 cells (Fig. 13E), while in the trans-well invasion assay a significantly slower invasion rate was found for DJ-1-PPFP co-transfected cells compared to the EV and PPFP single transfected cells (Fig. 13F).

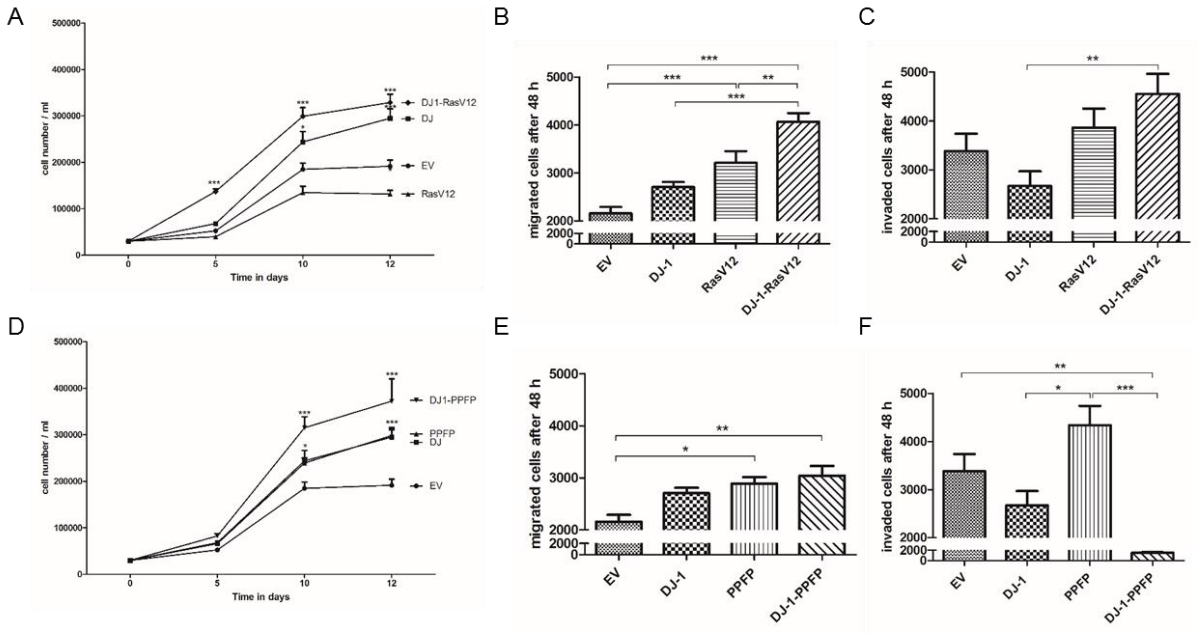

Figure 13: DJ-1 adds to RASV12 conferred tumourigenesis in rat thyroid PCCL3 cells. (A, D) Proliferation was investigated by performing growth curves over 12 days. DJ-1-RASV12 co-transfected cells showed an increased proliferation rate compared to EV, DJ-1 and RASV12 overexpressing cells while DJ-1-PPFP co-transfected cells showed no significant differences compared to EV and PPFP single transfected cells. (B, E) Migration of cells was investigated by using the trans-well migration assay. DJ-1-RASV12 co-transfected cells showed a faster migration rate compared to EV, DJ-1 and RASV12 single transfected cells. DJ-1-PPFP co-transfected cells showed a significant increase in migration compared to EV transfected cells. Also RASV12 and PPFP overexpressing cells showed an increase in migration as compared to EV transfected cells. (C, F) Invasiveness of the cells was investigated by using the trans-well invasion assay. Double mutant DJ-1-RASV12 showed a faster invasion rate compared to DJ-1 overexpressing cells. DJ-1-PPFP co-expressing cells showed a slower invasion rate compared to PPFP and EV single transfected cells. All data are presented as mean±SEM. Growth curves were performed six times in duplicates. All other assays were performed three times in triplicates. Values were obtained significantly by One-way ANOVA with Bonferroni's multiple comparison post-hoc test and considered statistically significant if *p<0.05, **p<0.01, ***p<0.001.

Besides trans-well migration, we performed also scratch assay experiments. DJ-1-RASV12 co-transfected cells showed a faster scratch repair after 48 h as compared to the single transfected cells DJ-1 and RASV12, while the DJ-1-PPFP co-transfected cells showed a slower scratch repair as compared to the DJ-1 single transfected cells and no differences to the PPPF single transfected cells (Fig. 14).

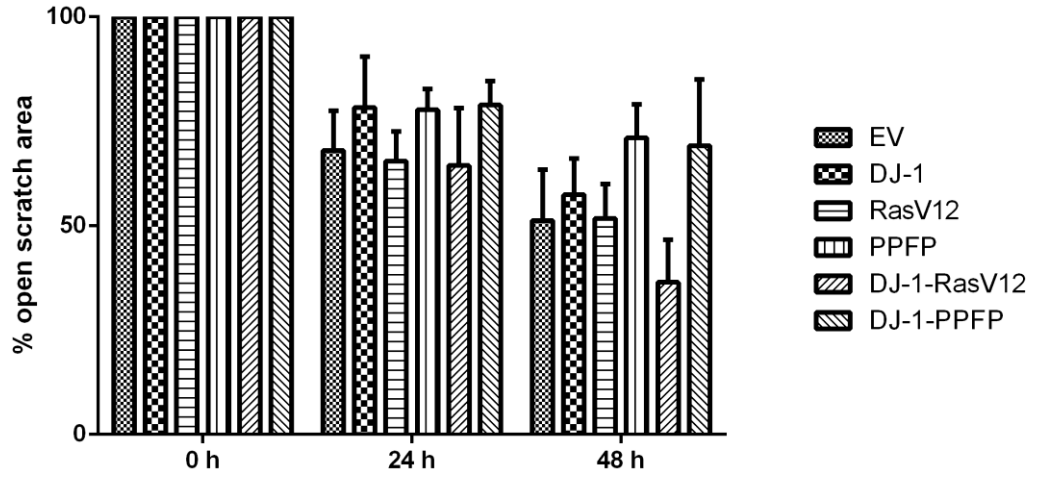

Figure 14: Scratch assay of EV, DJ-1, RASV12, PPFP, DJ-1-RASV12 and DJ-1-PPFP transfected cells. DJ-1-RASV12 co-transfected cells showed a faster scratch repair as compared to the single transfected cells. DJ-1-PPFP co-transfected cells showed a slower sratch repair as compared to the single transfected cells. All data are represented as mean±SEM, n=3.

To further investigate the growth properties of the cells we performed colony formation assays. We found a similar pattern as described for the growth curves. Thus co-transfected DJ-1-RASV12 cells built significantly larger colonies than the EV, DJ-1 and RASV12 overexpressing cells (Fig. 15A). Also DJ-1 overexpressing cells built significant larger colonies than the EV transfected cells. The DJ-1-PPFP co-transfected cells built smaller colonies than the DJ-1 and PPFP single transfected cells (Fig. 15B).

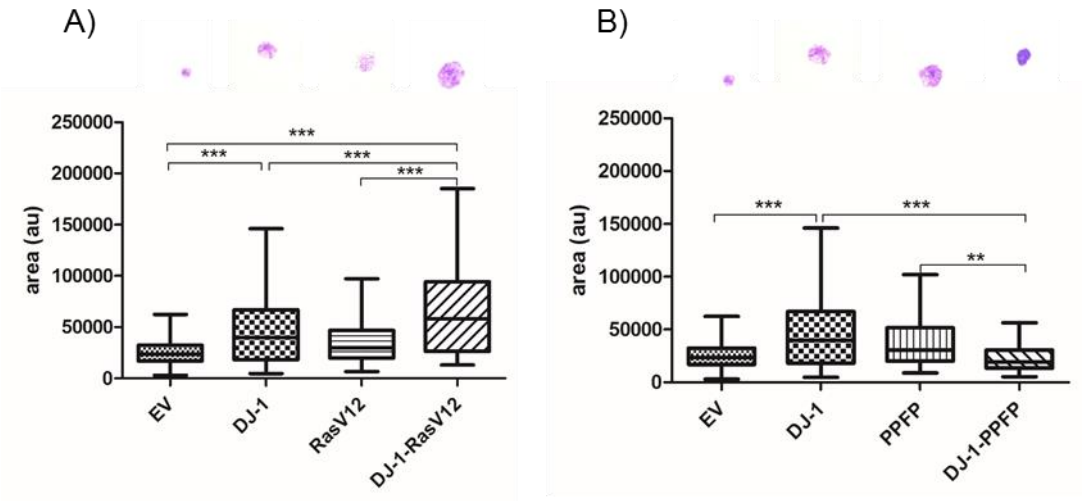

Figure 15: Colony formation assay of PCCL3 transfected cells. A) DJ-1-RASV12 co-transfected cells built significantly larger colonies as compared to the single transfected cells. B) DJ-1-PPFP co-transfceted cells built significantly smaller colonies as compared to the single tranfected cells. All data are represented as mean±SEM, n=3.

At last, we wanted to investigate if DJ-1 influences apoptosis by using a Caspase-3 activity assay. Therefore, we performed tests to find the optimal etoposide concentration for induction of apoptosis (see supplemental data. We were able to show successful induction of apoptosis by using Etoposide (50 µM) (Fig. 16). However, no significant differences in apoptosis rate were found between single and co-transfected PCCL3 cells.

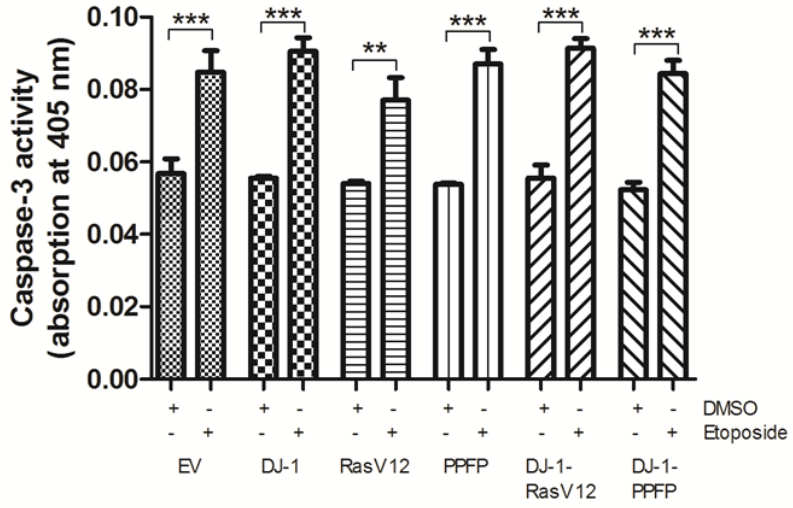

Figure 16: Apoptosis rate investigated by Caspase-3 activity assay. Succesful induction of apoptosis by using etoposide was observed. No significant differences in apoptosis rate was observed between DJ-1, RASV12 and PPFP single transfected or DJ-1-RASV12 and DJ-1-PPFP co-transfected cells. Values were obtained significant by One-way ANOVA with Bonferroni's multiple comparison post-hoc test and considered statistically significant if **p<0.01, ***p<0.001.

To further investigate which signaling pathways are activated by DJ-1 overexpression we analyzed the expression pattern of the following targets in PCCL3 cells: For the PI3K/Akt signaling pathway, total Akt, pAkt, Pten and pP70S6K expression levels were determined. For the MAPK/Erk signaling pathway, total Erk and pErk expression levels were investigated. Overexpression of DJ-1 resulted in significantly increased protein expression of total Akt and Erk in PCCL3 cells, whereas pAkt and pP70S6K expression levels were significantly reduced as compared to EV transfected PCCL3 cells. However, phosphorylation of Akt was strongly enhanced in RASV12 single transfected cells as well as in the DJ-1-RASV12, PPFP and DJ-1-PPFP co-transfected cells. Furthermore, we found an enhanced expression of Pten in DJ-1 overexpressing cells and diminished Pten expression in RASV12 and PPFP single transfected cells as well as DJ-1-RASV12 and DJ-1-PPFP co-transfected cells. Moreover, phosphorylation of P70S6K was significantly diminished in RASV12 and PPFP single transfected cells as

well as DJ-1-RASV12 and DJ-1-PPFP co-transfected cells as compared to the EV transfected cells. No difference in pErk expression was found in DJ-1 overexpressing PCCL3 cells compared to EV transfected cells, in contrast to a 3-fold increased pErk level in RASV12 overexpressing PCCL3 cells but not PPFP, DJ-1-RASV12 or DJ-1-PPFP transfected cells (Fig. 17).

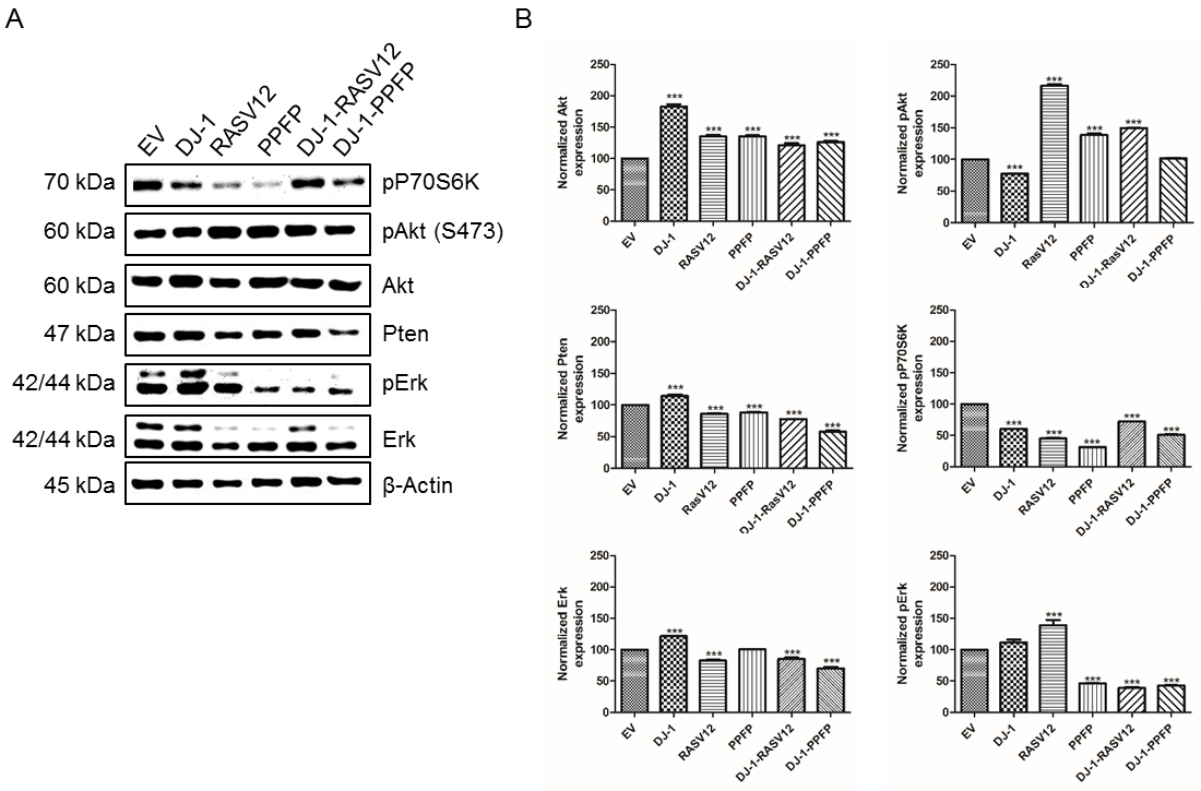

Figure 17: DJ-1 and RASV12 as well as PPFP overexpression in normal rat thyroid cells have distinct impact on PI3K/AK and MAPK/Erk signaling. Basal expression of Akt, pAkt (S473), Pten, pP70S6K, Erk and pErk was investigated in EV, DJ-1, RASV12 and PPFP single transfected cells as well as DJ-1-RASV12 and DJ-1-PPFP co-transfected PCCL3 cells. A, B) DJ-1 overexpressing cells showed an increase of Pten expression while the expression of pAkt and pP70S6K was diminished as compared to the EV transfected cells. β-Actin was used as a loading control for Pten, p-P70S6K, Akt and Erk. Total Akt and total Erk were used as loading control for the corresponding phospho-proteins. Data are presented as normalized protein expression, n=3, mean±SEM. Values were obtained significant One-way ANOVA with Bonferroni's multiple comparison post-hoc test and considered statistically significant if ***p<0.0

3.4 Impact of DJ-1 overexpression on tumour aggressiveness

To investigate the impact of DJ-1 on tumour aggressiveness, FTC-133 cells were transiently transfected with DJ-1, RASV12, PPFP as well as DJ-1-RASV12 and DJ-1-

PPFP plasmids. We performed qRT-PCR to investigate the mRNA expression. FTC-133 wildtype cells and HEK-293T cells were used as control. We found an overexpression of the transfected oncogenes in FTC-133 cells (Fig. 18).

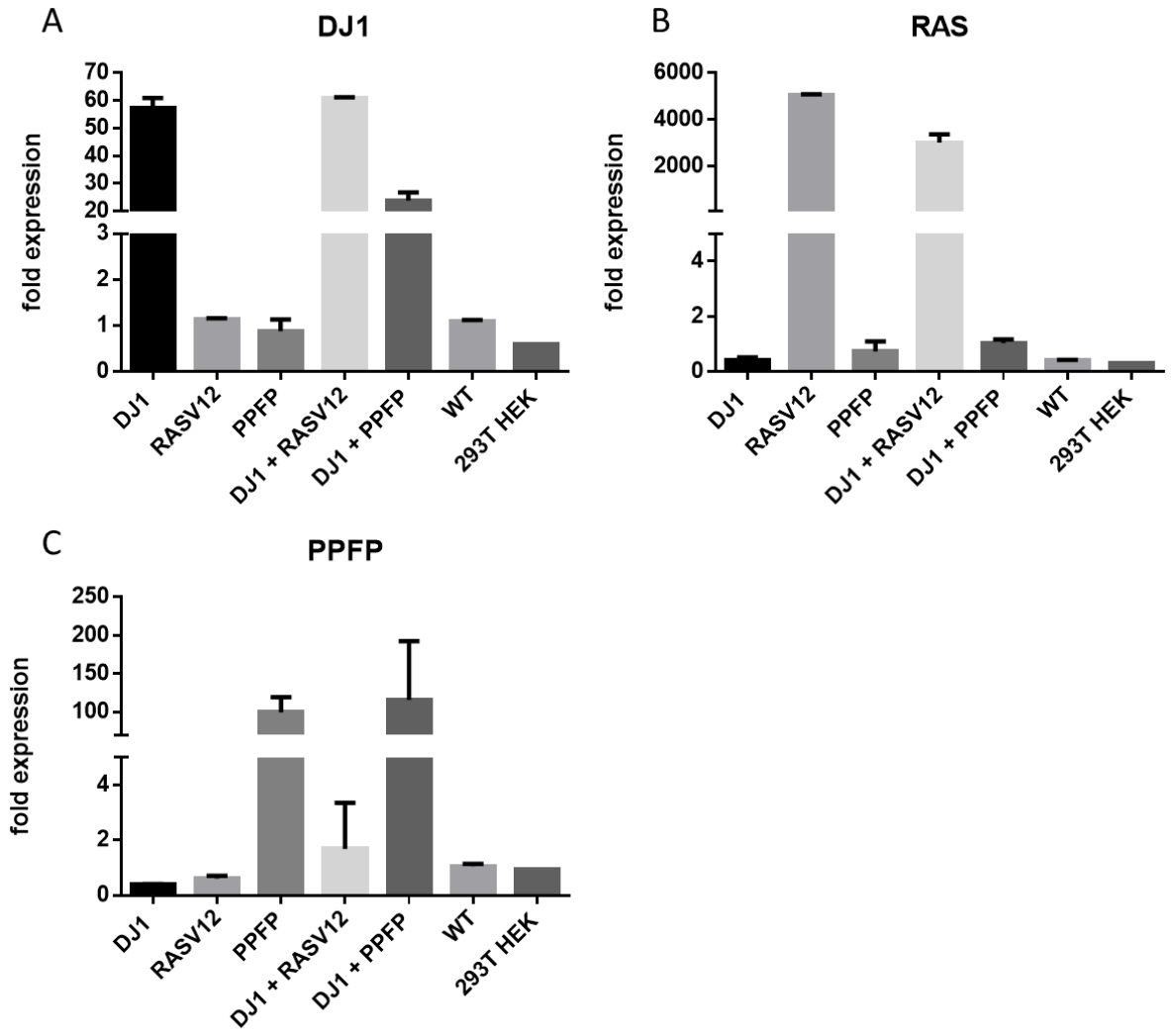

Figure 18: Expression of DJ-1, RASV12 and PPFP in transiently transfected FTC-133 cells. DJ-1, RASV12 and PPFP expression was investigated in DJ-1, RASV12, PPFP, DJ-1-RASV12, DJ-1-PPFP transfected FTC-133 cells, FTC-133 wildtype cells and HEK293T cells. Gene expression levels were determined by quantitative real-time PCR. (A) mRNA expression of DJ-1 was increased in DJ-1, DJ-1-RASV12 and DJ-1-PPFP tranfected cells. (B) mRNA expression of RASV12 was increased in RASV12 and DJ-1-RASV12 transfected cells. (C) mRNA expression of PPFP was increased in PPFP and DJ-1-PPFP tranfected cells.

Next we investigated expression pattern of DJ-1, RASV12, PPFP as well as DJ-1-RASV12 and DJ-1-PPFP transfected cells on protein level. We obtained similar results for protein expression as for mRNA expression. DJ-1 protein expression was increased in DJ-1, DJ-1-RASV12 and DJ-1-PPFP transfected cells. RASV12 protein expression

levels were increased in RASV12 and DJ-1-RASV12 transfected cells and PPFP expression was increased in PPFP and DJ-1-PPFP transfected cells (Fig. 19).

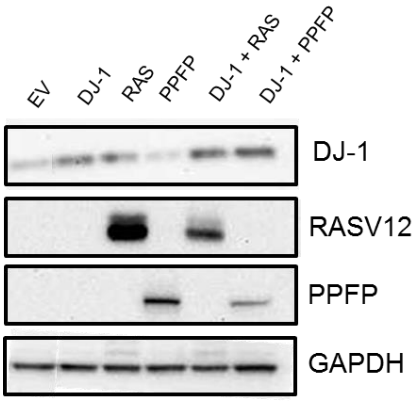

Figure 19: Analysis of DJ-1, RASV12 and PPFP expression on protein level. DJ-1, RASV12 and PPFP protein expression was investigated in EV, DJ-1, RASV12, PPFP, DJ-1-RASV12 and DJ-1-PPFP transfected FTC-133 cells. GAPDH was used as loading control. DJ-1 overexpression was obtained in DJ-1, DJ-1-RASV12 and DJ-1-PPFP transfected cells. An increased expression of RASV12 was found in RASV12 and DJ-1-RASV12 transfected cells and PPFP overexpression was observed in PPFP and DJ-1-PPFP transfected cells.

Furthermore, we wanted to investigate if DJ-1 expression leads to a constitutive activation of PI3K/Akt pathway in thyreocytes. Therefor we investigated the expression and phosphorylation of Akt, pP70S6K and Erk in EV, DJ-1, RASV12, PPFP, DJ-1-RASV12 and DJ-1-PPFP transfected FTC-133 cells. We found no other significant activitation of the PI3K/Akt pathway due to DJ-1 overexpression. In PPFP transfected FTC-133 cells we found an effect on phosphorylation of P70S6K and in RASV12 transfected FTC-133 cells on Erk activation as expected (Fig. 20).

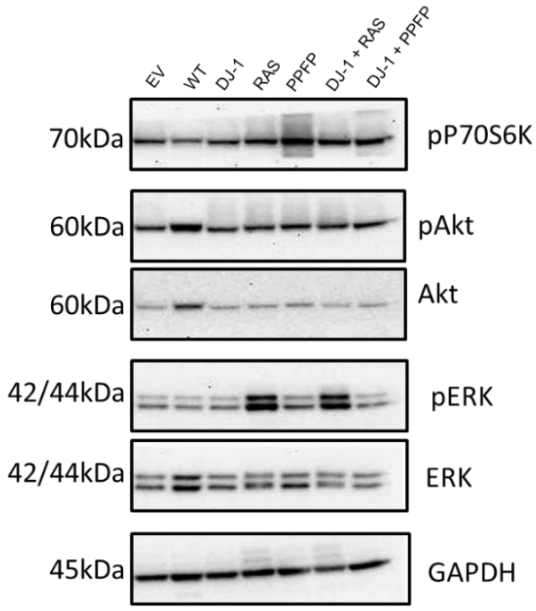

Figure 20: Impact of DJ-1 overexpression on PI3K/Akt and Erk pathway. Western blot analysis of Akt, Erk and pP70S6K activation in FTC-133 cells. DJ-1 overexpression showed no effect on phosphorylation of P70S6K. FTC-133 cells with RAS overexpression show a strong phosphorylation of Erk and FTC-133 cells with an overexpression of PPFP show a strong phosphorylation of P70S56K.

To investigate the proliferation of EV, DJ-1, RASV12, PPFP, DJ-1-RASV12 and DJ-1-PPFP transfected FTC-133 cells we used a BrdU-Assay. It was striking that only DJ-1 transfected FTC-133 cells showed a significantly higher proliferation rate compared to EV transfected cells. All other FTC-133 cells showed only a slight increase in proliferation as compared to the EV transfected FTC-133 cells (Fig. 21).

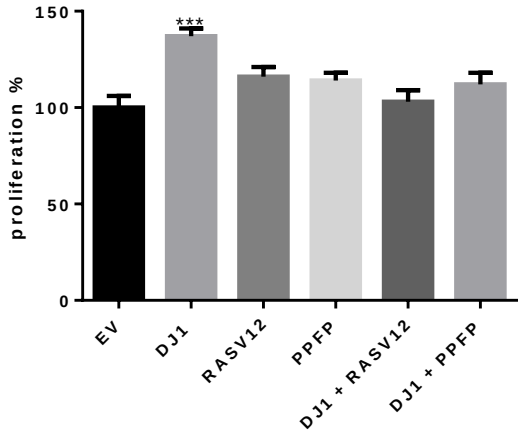

Figure 21: DJ-1 increases proliferation in FTC-133 cells. DJ-1 transfected FTC-133 cells showed a significant increase in proliferation as compared to the EV transfected cells. However, neither RASV12 or PPFP single transfected FTC-133 cells nor DJ-1-RASV12 or DJ-1-PPFP co-transfected FTC-133 cells showed significant

differences in proliferation behaviour as compared to the EV transfected cells. Values were obtained significant by One-way ANOVA with Bonferroni's multiple comparison post-hoc test and considered statistically significant if ***p<0.003.

To answer the question if DJ-1 leads to a more aggressive behaviour of follicular thyroid carcinomas we performed migration as well as invasion assay with DJ-1, RASV12, PPFP, DJ-1-RASV12 and DJ-1-PPFP transfected FTC-133 cells. Compared to EV transfected cells we found a significantly higher migration capacity in DJ-1 and RASV12 transfected FTC-133 cells. In PPFP transfected FTC-133 cells we found no change in migration capacity compared to the EV transfected control cells. However, additional expression of DJ-1 and RASV12 as well as PPFP transfected FTC-133 cells showed also a higher migration capacity (Fig. 22A). In contrast we found no effect of DJ-1 expression in invasion assays (Fig. 22B).

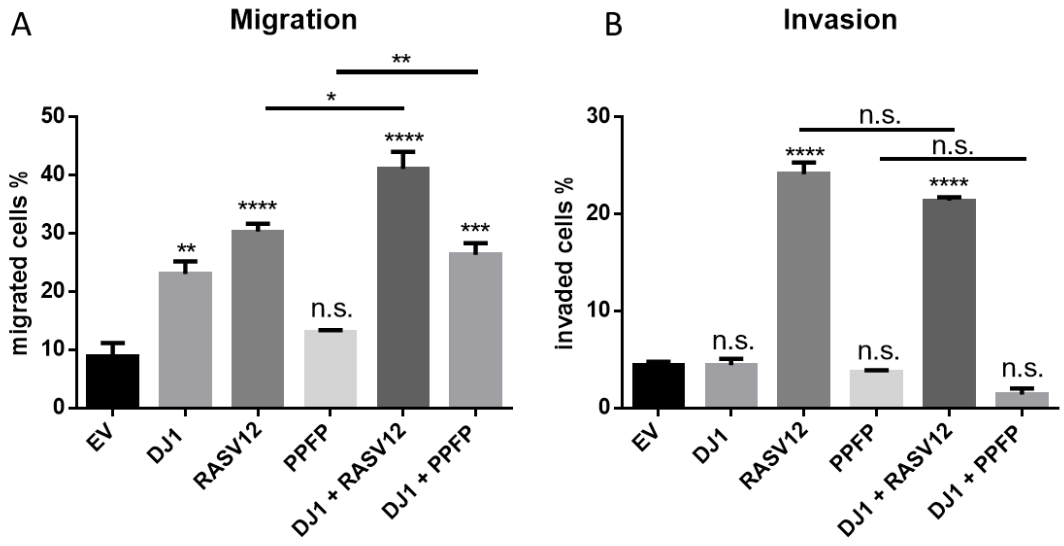

Figure 22: Co-expression of DJ-1 and RASV12 or DJ-1 and PPFP leads to an increased migration capacity in FTC-133 cells. (A) DJ-1 as well as RASV12 transfected FTC-133 cells show a significant increased migration capacity as compared to the EV transfected control cells. DJ-1-RASV12 transfected cells show the strongest effect on migration capacity. (B) Only RASV12 transfected FTC-133 cells show an increased invasion capacity in FTC-133 cells. Values were obtained significant by One-way ANOVA with Tukey's multiple comparison post-hoc test and considered statistically significant if *p<0.05, **p<0.005, ***p<0.0006, ****p<0.0001.

Subsequently we investigated apoptosis in FTC-133 transfected cells. Compared to EV transfected FTC-133 cells we found a significantly decreased apoptosis rate in DJ-1, RASV12 and PPFP transfected cells, whereat DJ-1 showed no additive effect on apoptosis rate in RASV12 and PPFP transfected FTC-133 cells (Fig. 23).

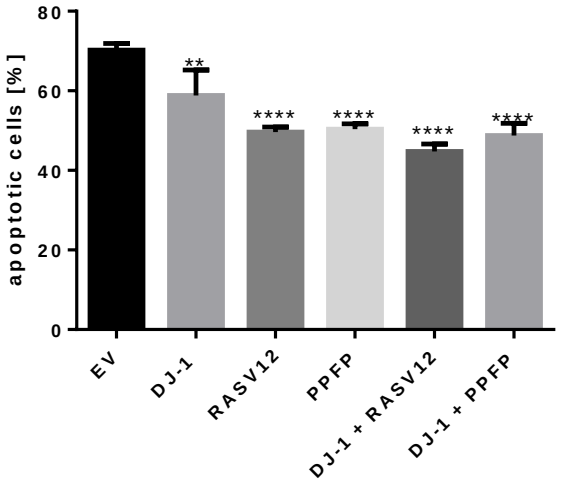

Figure 23: Apoptosis rate in FTC-133 transfected cells. Compared to EV transfected FTC-133 cells, DJ-1 and the oncogenes RASV12 and PPFP exert an anti-apoptotic effect. No differences between the oncogenes were found. DJ-1 has no additive effect on apoptose evasion in follicular thyroid carcinoma cells with an activation of the classical oncogenes RAS and PPFP. Values were obtained significant by One-way ANOVA with Tukey's multiple comparison post-hoc test and considered statistically significant if *p<0.009 or ****p<0.0001.

01.

4 Discussion

To our knowledge, this is the first study investigating the impact of DJ-1 on FTC behaviour and DJ-1 role in follicular thyroid tumourigenesis.

First, we performed qRT-PCR of human normal thyroid tissue, follicular adenoma and follicular thyroid carcinoma tissues and found a significant upregulation of DJ-1 in FTC compared to NT and FA tissue. By immunohistochemistry we observed a significant stepwise increase in DJ-1 protein expression from NT to FA and FTC and showed that DJ-1 is mainly located in the cytoplasm. This is in line with other studies showing e.g. in gastric carcinoma, urothelial carcinoma and breast cancer specimens that DJ-1 is expressed in the cytoplasm (Li *et al*. 2013, Lee *et al*. 2012, Kim *et al*. 2005).

To investigate whether DJ-1 impacts FTC behavior, FTC-133 cells were chosen and it was demonstrated that FTC-133 cells exhibit endogenous DJ-1 expression with cytoplasmic localization. *DJ-1* knockdown was performed in FTC-133 cells and resulted in approximately 60% reduced DJ-1 protein expression compared to ctrl. siRNA transfected cells. Since the ability to migrate and to invade surrounding tissues e.g. blood or lymphatic vessels, is a hallmark of cancer, we performed trans-well migration, scratch-assay and trans-well invasion experiments. We found a significantly slower trans-well migration and scratch repair capacity in addition to a slower trans-well invasion with downregulation of *DJ-1* in FTC-133 cells. This is in agreement with studies on human pancreatic cancer cell lines (BxPC-2 and SW1990) where authors showed a significant decrease in cell migration and invasion by *DJ-1* knockdown (He *et al*. 2012). Next, we asked if DJ-1 impact on FTC behavior is conferred through altered signaling via PI3K/Akt or MAPK/Erk pathway. We observed that DJ-1 downregulation resulted in decreased pAkt, and unchanged pErk levels. Downregulation of pAkt is in line with previous findings from Kim *et al*. where decreased phosphorylation of Akt in response to *DJ-1* knockdown was shown in the human lung carcinoma cell line A549 and in breast cancer tissues (Kim *et al*. 2005). Since DJ-1 may act as a negative regulator of PTEN, we investigated if PTEN expression is altrered after *DJ-1* knockdown in FTC-133 cells. However, FTC-133 cells do not express PTEN (Weng *et al*., 2001; Morani *et al*., 2014) and we found no PTEN expression after *DJ-1* knockdown.

Next, we investigated whether DJ-1 has an impact on follicular thyroid tumourigenesis. We started cultivation of conserved FRTL-5 transfected cells (from former studies, University Hospital Leipzig) but were not successful in the laboratory in Essen. Therefore, we decided to use the rat thyroid cell line PCCL3 as an alternative system and stably transfected them with EV, DJ-1, RASV12, PPFP, DJ-1-RASV12 and DJ-1-PPFP plasmids. We characterized stably transfected cells for changes in proliferation, migration, invasion, apoptosis rate and signal transduction pathways (see 3.3). Overall two methodical caveats appeared: 1) We were able to show expression of DJ-1, RASV12 and PPFP only on mRNA level but not on protein level; 2) Functional characterization of RASV12 transfected PCCL3 cells showed discrepant results for proliferation behaviour and Akt activation to reported results from the literature. For this reason we chose a new strategy to investigate the role of DJ-1 in follicular thyroid carcinogenesis and performed several experiments in DJ-1, RASV12, PPFP, DJ-1-RASV12 and DJ-1-PPFP transfected FTC-133 cells (see 3.4).

Nevertheless analysis of DJ-1 in PCCL3 cells showed several interesting findings: As DJ-1 alone could be a key regulator of thyroid follicular carcinoma we expected a significant faster proliferation, migration and invasion rate as compared to the EV control in PCCL3 cells. However, DJ-1 overexpression resulted only in marginal alteration of migration and a slower invasion capacity but in an enhanced proliferation. The results of proliferation and migration are in line with our hypothesis and the higher migration rate of DJ-1 in PCCL3 cells is also in line with DJ-1 overexpression in pancreatic cancer cell lines (BxPC-3 and SW1990) showing an increased migration rate (He *et al*., 2012). In contrast, the slower invasion rate neither fits with the literature (He *at al*., 2012) nor to our obtained results from *DJ-1* knockdown in FTC-133 cells. We can be sure, due to analysis of genomic integration, that the stable transfection of PCCL3 cells with DJ-1 was successful. We were also careful using stably transfected cells just between passages 5-10. We performed trans-well invasion assays according to the manufactures' instructions but it might be due to the size and profile of the PCCL3 cells that there were systematic problems.

For analysis of DJ-1-RASV12 and DJ-1-PPFP co-transfected cells, we found that once DJ-1 overexpression was combined with expression of a classical thyroid oncogene, this resulted in augmented tumourigenicity compared with the impact of the oncogene

per se. This additive effect of DJ-1 was most pronounced with the oncogene RASV12 and DJ-1-RASV12 transfected PCCL3 cells showed higher proliferation, faster scratch repair, faster trans-well migration as well as faster trans-well invasion compared to single DJ-1 or RASV12 transfected PCCL3 cells. They built also bigger colonies in colony formation assay contributing to a more aggressive behaviour of the cells. Mutations in the *RAS* gene are frequently observed in human carcinomas (Takashima and Faller, 2013) and are characteristics of follicular thyroid adenoma and follicular thyroid carcinoma (Nikiforova et al., 2003; Nikiforova and Nikiforov, 2008). Furthermore, it was previously shown that DJ-1 in cooperation with H-RAS was able to transform mouse NIH-3T3 cells (Nagakubo et al., 1997). Based on our findings we suggest that DJ-1 acts as an additional factor in thyroid tumourigenesis. The faster trans-well migration and trans-well invasion of RASV12 transfected PCCL3 cells was expected as it is one of the most prominent oncogenes but the slower proliferation rate contradicts our results in RASV12 transient transfected FTC-133 cells where a significantly faster proliferation was found in RASV12 transfected FTC-133 cells (see 3.4). However, different studies showed that RAS is able to activate senescence in cells by upregulation of the cyclin-dependent kinase inhibitor p161NK4A (Benanti and Galloway, 2004; Sebastian and Johnson, 2009). So, it is not impossible that the RASV12 transfected PCCL3 cells underwent senescence and therefore showed a decreased proliferation rate. In comparison to our studies in FTC-133 cells it could also be a species dependent mechanism that RASV12 transfected PCCL3 cells showed a slower proliferation rate as compared to the EV control. To investigate proliferation in PCCL3 cells we performed growth curves, while we used a proliferation assay using 5-Bromo-2'-Deoxyuridine (BrdU) incorperation for the FTC-133 cells. So, the choice of method could also play a role in investigation of proliferation. Moreover, all investigated proliferative effects of RASV12 (chapter 3.4 and literature) were performed in transient transfected cells and here we used stable transfected cells.

DJ-1-PPFP co-transfected PCCL3 cells showed a significantly faster proliferation rate, faster trans-well migration, but slower trans-well invasion and slower scratch repair capacity compared to EV, DJ-1 and PPFP single transfected cells. However, the proliferation, migration and invasion of PPFP overexpressing cells was enhanced as compared to the EV and DJ-1 transfected cells. This is in line with former results where

PPFP transfected human thyroid cells (Nthy-ori-3-1) showed also an increased cell growth and invasion rate as compared to the control (Reddi *et al*., 2010). Nothing is known about a connection between DJ-1 and the PAX8/PPARγ rearrangement. It might be a possible explanation for the obtained results that DJ-1 in cooperation with PPFP inhibits cell invasion as well as the scratch repair capacity. To investigate this possible behaviour of the DJ-1-PPFP co-transfected cells, further experiments will be necessary e.g. different invasion experiments. Since all experiments were performed three times in triplicates a failure in the experimental set up is unlikely but it might be that the trans-well invasion and scratch assay per se are no suitable methods for the cells.

To take a closer look on underlying mechanisms *in vitro*, we analyzed the expression pattern of proteins involved in the PI3K/Akt and MAPK/Erk pathway in DJ-1, RASV12 and PPFP overexpressing and DJ-1-RASV12 and DJ-1-PPFP co-transfected PCCL3 cells. We observed a strong increase of pAkt expression in RASV12 and PPFP single transfected cells which is no surprise due to their oncogenic potential and effect on the PI3K pathway. We observered a dimished expression of pAkt expression in DJ-1 transfected cells but elevated expression levels of pAkt in DJ-1-RASV12 and DJ-1-PPFP co-transfected cells. Activation of Akt in co-transfected cells was not as pronounced as in the RASV12 and PPFP single transfected cells but a 50 % stronger activation compared to the EV control could be observed. This dimished activation might be due to a inhibitory effect of DJ-1 on protein level which was seen in the single transfected cells. Furthermore, the diminished pAkt expression of DJ-1 overexpressing cells is in contrast to previous experiments in human breast cancer patients, where elvated DJ-1 levels were found in relation to strong Akt activation (Kim *et al*., 2005). Besides pAkt we investigated also the activation of the downstream target P70S6K of the PI3K/Akt pathway. We found a decreased phosphorylation of P70S6K in DJ-1, RASV12, PPFP, DJ-1-RASV12 and DJ-1-PPFF overexpressing cells as compared to the EV transfected cells. As a DJ-1 overexpression activates the PI3K pathway, as expression of PI3K downstream targets should be strongly elevated. We could also observe differences in the expression of Pten. In DJ-1 overexpressing cells we found an enhanced expression of Pten as compared to the EV transfected cells and a decreased expression in all other transfected PCCL3 cells. This is in contrast to

previous studies where it was shown that DJ-1 acts as a negative regulator of PTEN. However, it was also described that enhanced PTEN expression reduces the phosphorylation of Akt (Kim et al., 2005) which can be observed in our analysis. Due to the fact that none of the previous described associations between DJ-1 and PTEN were performed in thyroid tissue or thyroid cell lines, it might be that the correlation between DJ-1 and PTEN is tissue and/or species specific. Moreover, we observed a slightly stronger phosphorylation of Akt in DJ-1 and RASV12 overexpressing cells as compared to the EV transfected control. However, pAkt expression was dimished in DJ-1-RASV12 co-transfected cells which is surprising. If DJ-1 and RASV12 overexpression alone elevate the phosphorylation status of Akt we expected the same or even a stronger phosphorylation for DJ-1-RASV12 co-transfected cells.

Since the finding in PCCL3 cells were partially contradictory to the literature and known thyroid signaling, we repeated experiments in FTC-133 cells. We were able to show elevated levels of DJ-1 mRNA in DJ-1, DJ-1-RASV12 and DJ-1-PPFP transfected cells. Moreover, we confirmed expression on protein level. For this reason we can be sure that transfection of FTC-133 was successful and that the cells overexpress the introduced oncogenes and DJ-1.

Migration of DJ-1 transfected FTC-133 cells was significantly enhanced as was migration of RASV12 transfected cells. This is in line with previous described enhanced migration of DJ-1 overexpressing cells in pancreatic cancer. Analysis of migration of DJ-1-RASV12 and DJ-1-PPFP transfected cells showed a significantly faster migration compared to the RASV12 and PPFP single transfected cells. So, it is safe to say that this strong effect is mediated by DJ-1. Invasion experiments showed significantly higher invasion capacities of RASV12 and DJ-1-RASV12 cells as compared to the EV control. However, this effect was mediated by RASV12 and not DJ-1. We can conclude that DJ-1 seems to have no effect on the invasion capacity. Next, we investigated proliferation of FTC-133 transfected cells. We found a significantly faster proliferation of DJ-1 compared to the EV transfected control cells which we could also observe in PCCL3 cells. But neither DJ-1-RASV12 nor DJ-1-PPFP showed a faster proliferation as compared to DJ-1 transfected cells. Furthermore, we showed that DJ-1, RASV12, PPFP, DJ-1-RASV12 and DJ-1-PPFP transfected cells lead to more apoptotic cells as

compared to the EV transfected control cells. However, DJ-1-RASV12 transfected cells show the most prominent effect.

Taken together, our data show that DJ-1 contributes to more aggressive behaviour of follicular thyroid cancer cells. Furthermore, these findings suggest that DJ-1 per se has influence on thyroid tumorigenesis but additively propels tumourigenesis in presence of an oncogene. Thereby modulation of behaviour appears to depend on the involved oncogene and is reflected in activation of PI3K/Akt and/or MAPK/Erk signaling.

.

5 References

Bonifati V, Rizzu P, Squitieri F, Krieger E, Vanacore N, van Swieten JC, Brice A, van Duijn CM, Oostra B, Meco G, *et al.* 2003 DJ-1(PARK7), a novel gene for autosomal recessive, early onset Parkinsonism. *Neurological sciences: official journal of the Italian Neurological Society and of the Italian Society of Clinical Neurophysiology* **24** 159–160.

Benanti JA and Galloway DA 2004 The normal response RAS: senescence or transformation? *Cell Cylce* **3** 715-7.

Davidson B, Hadar R, Schlossberg A, Sternlicht T, Slipicevic A, Skrede M, Risberg B, Flørenes VA, Kopolovic J & Reich R 2008 Expression and clinical role of DJ-1, a negative regulator of PTEN, in ovarian carcinoma. *Human pathology* **39** 87–95.

Detre S, Saclani Jotti G, Dowsett M 1995 A "quickscore" method for immunohistochemical semiquantitation: validation for oestrogen receptor in breast carcinomas. *Journal of clinical pathology* **48** 876–8.

Di Cello A, Di Sanzo M, Perrone FM, Santamaria G, Rania E, Angotti E, Venturella R, Mancuso S, Zullo F, Cuda G and Costanzo F 2017 DJ-1 is a reliable serum biomarker for discriminating high-risk endometrial cancer. *Tumour Biology* **39** 1-9

Fusco A, Berlingieri MT, Di Fiore PP, Portella G, Grieco M & Vecchio G 1987 One- and two-step transformations of rat thyroid epithelial cells by retroviral oncogenes. *Molecular and cellular biology* **7** 3365–3370.

Gebäck T, Schulz MMP, Koumoutsakos P, Detmar M 2009 TScratch: a novel and simple software tool for automated analysis of monolayer wound healing assays. *BioTechniques* **46** 265–274.

Han B, Wang J, Gao J, Feng S, Zhu Y, Li X, Xiao T, Qi J and Cui W 2017 DJ-1 as a potential biomarker for the early diagnosis in lung cancer patients. Tumour Biology **39** 1-7.

He X, Zheng Z, Li J, Ben Q, Liu J, Zhang J, Ji J, Yu B, Chen X, Su L, Zhou L, Liu B & Yuan Y 2012 DJ-1 promotes invasion and metastasis of pancreatic cancer cells by activating SRC/Ark/uPA. *Carcinogenesis* **33** 555–562.

Hod Y 2004 Differential control of apoptosis by DJ-1 in prostate benign and cancer cells. *Journal of cellular biochemistry* **92** 1221–1233.

Hoelting T, Duh QY, Clark OH & Herfarth C 1997 Invasion of metastatic human follicular thyroid cancer is inhibited via antagonism of protein kinase C. *Cancer letters* **119** 1–5.

Hou P, Ji M & Xing M 2008 Association of PTEN gene methylation with genetic alterations in the phosphatidylinositol 3-kinase/Akt signaling pathway in thyroid tumors. *Cancer* **113** 2440–2447.

Kawate T, Iwaya K, Kikuch, R, Kaise H, Oda M, Sato E, Hiroi S, Matsubara O & Kohno N 2013 DJ-1 protein expression as a predictor of pathological complete remission after neoadjuvant chemotherapy in breast cancer patients. *Breast cancer research and treatment* **139** 51–59.

Kim RH, Peters M, Jang Y, Shi W, Pintilie M, Fletcher GC, DeLuca C, Liepa J, Zhou L, Snow B *et al.* 2005 DJ-1, a novel regulator of the tumor suppressor PTEN. *Cancer cell* **7** 263–273.

Krause K, Prawitt S, Eszlinge M, Ihling C, Sinz A, Schierle K, Gimm O, Dralle H, Steinert F, Sheu SY *et al.* 2011 Dissecting molecular events in thyroid neoplasia provides evidence for distinct evolution of follicular thyroid adenoma and carcinoma. *The American journal of pathology* **179** 3066–3074.

Kroll TG, Sarraf P, Pecciarini L, Chen CJ, Mueller E, Spiegelman BM, Fletcher JA 2000 PAX8-PPARgamma1 fusion oncogene in human thyroid carcinoma [corrected]. *Science* 289 1357–1360.

Lee H, Choi SK & Ro JY 2012 Overexpression of DJ-1 and HSP90α, and loss of PTEN associated with invasive urothelial carcinoma of urinary bladder: Possible prognostic markers. *Oncology letters* **3** 507–512.

Le Naour F, Misek DE, Krause MC, Deneux L, Giordano TJ, Scholl S & Hanash SM 2001 Proteomics-based identification of RS/DJ-1 as a novel circulating tumour antigen in breast cancer. Clinical cancer research : *an official journal of the American Association for Cancer Research* **7** 3328–3335.

Li Y, Cui J, Zhang CH, Yang DJ, Chen JH, Zan WH, Li B, Li Z & He Yl 2013 High-expression of DJ-1 and loss of PTEN associated with tumour metastasis and correlated with poor prognosis of gastric carcinoma. *International journal of medical sciences* **10** 1689–1697.

MacKeigan JP, Clements CM, Lich JD, Pope RM, Hod Y & Ting JPY 2003 Proteomic profiling drug-induced apoptosis in non-small cell lung carcinoma: identification of RS/DJ-1 and RhoGDIalpha. *Cancer research* **63** 6928–6934.

Mazières J, Brugger W, Cappuzzo F, Middel P, Frosch A, Bara I et al 2013 Evaluation of EGFR protein expression by immunohistochemistry using H-score and the magnification rule: re-analysis of the SATURN study. *Lung cancer (Amsterdam, Netherlands)* **82** 231–7.

Nagakubo D, Taira T, Kitaura H, Ikeda M, Tamai K, Iguchi-Ariga SM & Ariga H 1997 DJ-1, a novel oncogene which transforms mouse NIH3T3 cells in cooperation with ras. *Biochemical and biophysical research communications* **231** 509–513.

Nikiforova MN, Lynch RA, Biddinger PW, Alexander EK, Dorn GW, Tallini G, Kroll TG & Nikiforov YE 2003 RAS point mutations and PAX8-PPAR gamma rearrangement in thyroid tumours: evidence for distinct molecular pathways in thyroid follicular carcinoma. *The Journal of clinical endocrinology and metabolism* **88** 2318–2326.

Nikiforova MN & Nikiforov YE 2008 Molecular genetics of thyroid cancer: implications for diagnosis, treatment and prognosis. *Expert review of molecular diagnostics* **8** 83–95.

Pfaffl MW 2001 A new mathematical model for relative quantification in real-time RT-PCR. *Nucleic acids research* **29** e45.

Reddi HV, Madde P, Marlow LA, Copland JA, McIver B, Grebe SKG, Eberhardt NL 2010 Expression of the PAX8/PPARγ Fusion Protein Is Associated with Decreased Neovascularization In Vivo: Impact on Tumorigenesis and Disease Prognosis. *Genes & cancer* **1** 480–492.

Sebastian T and Johnson PF 2009 RasV12-mediated down-regulation of CCAAT/enhancer binding protein beta in immortalized fibroblasts requires loss of

p19Arf and facilitates bypass of oncogene-induced senescence. *Cancer research* **69** 2588-98.

Taira T, Takahashi K, Kitagawa R, Iguchi-Ariga SM & Ariga H 2001 Molecular cloning of human and mouse DJ-1 genes and identification of Sp1-dependent activation of the human DJ-1 promoter. *Gene* **263** 285–292.

Takashima A & Faller DV 2013 Targeting the RAS oncogene. *Expert opinion on therapeutic targets* **17** 507–531.

Theoharis C, Roman S & Sosa JA 2012 The molecular diagnosis and management of thyroid neoplasms. *Current opinion in oncology* **24** 35–41.

Weng, L.P., Gimm, O., Kum, J.B., Smith, W.M., Zhou, X.P., Wynford-Thomas, D., Leone, G., Eng, C. 2001 Transient ectopic expression of PTEN in thyroid cancer cell lines induces cell cycle arrest and cell type-dependent cell death. *Human molecular genetics* **10** 251–258.

Xing M 2010 Genetic alterations in the phosphatidylinositol-3 kinase/Akt pathway in thyroid cancer. *Thyroid: official journal of the American Thyroid Association* **20** 697-706

Zhang HY, Wang HQ, Liu HM, Guan Y & Du ZX 2008 Regulation of tumour necrosis factor-related apoptosis-inducing ligand-induced apoptosis by DJ-1 in thyroid cancer cells. *Endocrine-related cancer* **15** 535–544.

Chapter 3: The impact of claudin-1 on follicular thyroid cancer

1 Introduction

1.1 The tight junction protein claudin-1

Tight junction (TJ) proteins are transmembrane proteins which regulate the movement of solutes across the epithelium by forming a continuous intercellular barrier between epithelial cells which is required to separate tissue spaces (Anderson and Van Itallie, 2009). Another key role of tight junction proteins is the maintance of the cell polarity throught the fence function (Krause *et al.*, 2008; Feigin and Muthuswamy, 2009). Several studies showed that epithelial TJ proteins are dynamic structures. TJ proteins are involved in modulation of e.g. wound repair (McCartney and Cantu-Crouch, 1992), inflammation (Riehl and Stenson, 1994) and in cell transformation (Madara *et al.*, 1992).

The major tight junction proteins are the occludins and the claudins. Currently, 27 claudin family members are known. Claudin-1 is assumed to be the most important protein responsible for the paracellular barrier integrity of epithelial cells (González-Mariscal *et al.*, 2003). In tumour progression, tight junction assembly is often disrupted resulting in the loss of cell membrane localized tight junction proteins (Resnick *et al.*, 2005).

For claudin-1, an altered protein expression as well as subcellular localization has been observed in common human malignancies including colon, lung and breast cancer and melanoma (Tokés *et al.*, 2005; Chao *et al.*, 2009; Németh *et al.*, 2010). Furthermore, subcellular claudin-1 expression has been associated with a more aggressive tumour behaviour (Miwa *et al.*, 2001). Alterations in different claudin subtypes have also been described in human thyroid cancer tissues (Tzelepi *et al.*, 2008), whereby a weak subcellular expression of claudin-1 in FTC was reported to correlate with disease recurrence and survival. However, the mechanisms behind the possible impact of claudin-1 on FTC biology were not addressed.

1.2 Aims & working hypothesis

We investigated claudin-1 expression and localization in a series of normal thyroid tissues, follicular adenoma, follicular thyroid carcinoma and their metastases. In addition, functional properties of claudin-1 were investigated in two human follicular thyroid carcinoma cell lines: FTC-133 and FTC-238. These cell lines originate from a 42-year-old patient with follicular thyroid carcinoma (Hoelting *et al.*, 1997). The FTC-133 cells are derived from a regional lymph node metastasis and the FTC-238 cells are derived from a lung metastasis. These cell lines are widely used in vitro models to study tumour aggressiveness of human follicular thyroid carcinoma. We modulated the pathogenic character of these cell lines with respect to claudin-1 expression and/or protein kinase C (PKC) activity and characterized them for functional properties by addressing migration, invasion and proliferation.

2 Material and Methods

2.1 Material

All compositions of buffers, used substances and manufactures of used products can be found in detail in Appendix C (Material).

2.2 Methods

2.2.1 Immunohistochemistry

Thyroid samples were obtained from patients undergoing thyroid surgery for nodular thyroid disease or thyroid cancer. For immunohistochemical analysis of claudin-1, paraffin-embedded tissue sections of 40 follicular adenoma, 44 follicular thyroid carcinoma and six distant metastases of follicular thyroid carcinoma (soft tissue and liver metastases) and normal surrounding thyroid tissues were studied. Classification of the thyroid nodules was performed by board-certified pathologists (Institute of Pathology, Essen) according to World Health Organization (WHO) criteria.

For immunohistochemical analysis the following antibody was used: anti-claudin-1 (1:100). Deparaffinization, rehydration and staining of the tissue samples was performed like already described for DJ-1 in chapter 2 (see 2.2.1). Paraffin-embedded skin tissue sections were used as positive control. Negative controls (no primary antibody) were included in the experimental set-up. The Olympus BX51 upright microscope was used for light microscopy. Membranous, cytoplasmic and nuclear tumour staining intensities were evaluated by calculating the ‘hybrid’ (H) (Ting *et al.*, 2013).

2.2.2 Cell culture

For cell culture experiments the human follicular thyroid cell lines FTC-133 and FTC-238 were used (Hoelting *et al.*, 1997). Both FTC cell lines are derived from the same male patient and harbour Tp53 mutation, whereas a homozygous phosphatase and tensin homolog (PTEN) inactivating mutation is only present in FTC-133 cells (Simon *et al*. 1994, Saiselet *et al*. 2012).

Re-authentification of the cell lines was performed by qRT-PCR of thyroid hormone markers (see chapter 2). Cells were used between passages 5 and 15. Follicular thyroid carcinoma cells were cultured in Ham's F12 medium with 10 % FBS and 1 % ZellShield. For migration and invasion studies, cells were cultured in serum-low medium containing Ham's F12 Nutrient Mixture with 2 % FBS and 1 % ZellShield. Cells were grown at 37 °C and 5 % CO_2. Once cells were confluent they were detached by trypsin/EDTA and seeded in new dishes.

2.2.3 Generation of claudin-1 and RASV12 overexpressing constructs

The plasmid peYFP-Cld-1-C2 was kindly provided by I.E. Blasig (Berlin, Germany). To design the claudin-1 overexpressing construct, human claudin-1 was excised from the vector peYFP-C2 with the fast digest enzymes BamHI and HindIII. 1 µg of the plasmid DNA was incubated for 1 h at RT with 1 µl BamHI, 1 µl HindIII, 2 µl restriction buffer and filled up to 20 µl with deionized water. The target vector pcDNA3-YFP-NLS was linearized the same way. After purification by gel electrophoresis, both fragments were ligated with a T4-DNA-Ligase and a ratio of 3:1 (Vector:Insert) for 2 h at RT in a volume of 25 µl. The product was transformed via heat-shock into 50 µl of XL-1 blue chemically competent cells. After incubation of 16-18 h at 37 °C on LB agar plates, colonies were picked, grown in LB medium for 16-18 h and plasmid DNA was isolated using the QIAprep Spin Miniprep Kit.

The plasmid pcDNA3.1-RasV12C40 was kindly provided by K. Krause (Leipzig, Germany). Mutagenesis and cloning, to receive the overexpressing construct pcDNA3.1-RASV12, was already described in chapter 2 (see 2.2.4).

2.2.4 Transfection of FTC-133 cells

For transient transfection, FTC-133 cells were seeded onto poly-L-Lysine, collagen or non coated 16 or 35 mm dishes and grown to 80 % confluence for 48 h. For each reaction in 35 mm dishes, a transfection mixture containing 4 µg DNA and 250 µl OptiMem as well as 10 µl Lipofectamine 2000® and 250 µl OptiMem were prepared at RT. Afterwards, the transfection mixture was added to the cells and cells were

incubated for 16 h at 5 % CO_2 and 37 °C. The medium was replaced by normal growth medium and cells were assayed 24-48 h post-transfection. For 16 mm dishes the adapted volume of transfection mixture was used.

2.2.5 siRNA transfection

FTC-133 cells were plated in antibiotic-free normal growth medium on poly-l-lysine, collagen or non-coated 16 or 35 mm dishes and cultured until 70-80 % of confluence for 48 h. Solution mixes of claudin-1 siRNA (10 mM) or nontargeting control siRNA (10 mM) with siRNA transfection medium and siRNA transfection reagent were prepared by following the procedure recommended by the manufacturers. Transfection cocktail was incubated at room temperature for 30 min. Cells were washed once with siRNA transfection medium and incubated afterwards with transfection mixture for 6 h at 37 °C and 5% CO2. Normal growth medium containing 2x FBS was added and cells were incubated for 18 h at 37 °C and 5% CO_2. The medium was aspirated and replaced by fresh normal growth medium and cells were incubated for 24 h at 37 °C and 5% CO_2 before assayed.

2.2.6 PKC activation by phorbol-12-myristate-13-acetate

For PKC activation, cells were seeded in 35 mm dishes and cultured to confluent monolayers. Phorbol-12-myristate-13-acetate (PMA) was dissolved in DMSO and the corresponding medium to a concentration of 200 nM. Then cells were incubated in either the presence of PMA or equivalent amounts of DMSO (<0.02 %) for 6 h at 37 °C and 5 % CO_2.

2.2.7 PKC inhibition by Gö6983

For PKC inhibition cells were seeded in 35 mm dishes and cultured to confluent monolayers. Gö6983 was dissolved in DMSO and the corresponding medium to a concentration of 100 nM. Then cells were incubated in either the presence of Gö6983 or equivalent amounts of DMSO (<0.02 %) for 6 h at 37 °C and 5 % CO_2.

2.2.8 Immunoblot

The following antibodies were used: anti-claudin-1 (1:250), anti-β-Actin (1:2000), anti-RasV12 (1:200), anti-PKC (1:500), anti-phospho-PKC (1:250), anti-phospho-p44/42 MAPK (1:1000), anti-phospho-Akt (1:1000) and anti-mouse/rabbit-IgG (1:2000). Whole protein lysates were extracted by RIPA buffrer and quantified like described by BCA protein assay. Aliquots of proteins (10-20 µg) were fractionated on Any kD Criterion TGX SDS polyacrylamide gels and blotted by the Trans-Blot Turbo Transfer System onto PVDF membranes. Unspecific binding sides were blocked with 5 % non-fat milk for 1 h at RT. Primary antibodies were incubated overnight at 4 °C in 5 % non-fat milk. β-Actin was used as a protein loading control. Incubation of the secondary antibody was performed for 2 h at RT in 2.5 % non-fat milk. The visualization of the proteins was done by luminescence using the Immun-Star™ WesternC™ Kit or by fluorescence dependent on the secondary antibody. Differences in protein expression levels were quantified by densitometry using the ImageLab™ Software. Relative values of either the loading control β-Actin or total PKC were calculated. The target protein values were divided by the calculated relative values of the respective control. The adjusted values were used to calculate geometric mean of the controls and target protein followed by calculation of the percent of protein level alteration.

2.2.9 Immunofluorescence

Cells were seeded on poly-L-Lysin coated 16 mm cover slides and incubated at 5 % CO_2 and 37 °C. Cells were washed twice with phosphate buffer saline (PBS) for 5 min and then fixed with 4 % paraformaldehyde (PFA) for 15 min at RT and permeabilized using 0.1 % Triton X-100 in PBS for 10 min at RT. PFA was aspirated, cells were washed three times with PBS. Blocking was performed by using 3 % BSA in PBS for 30 min at RT. Cells were washed three times with 0.1 % BSA/ PBS and a specific primary antibody against claudin-1 (1:1000) was diluted in 0.1% BSA/ PBS. After incubation with the primary antibody (4°C, overnight) cells were washed six times with 0.1 % BSA/ PBS. Then, cells were incubated with the secondary antibody AlexaFluor® 488 (1:200) for 1 h at RT in 0.1 % BSA/ PBS. Cells were washed again six times with

0.1 % BSA/ PBS for 5 min and detection of the cytoskeleton was performed by incubation with Phalloidin® 555 (1:40) in 0.1% BSA/ PBS for 20 min at RT. Visualizing of the nuclei was performed with Hoechst 33342 (1:1000) for 5 min at RT. Cover slides were embedded in ImmuMount and viewed on the confocal microscope Nikon Eclipse T_i.

2.2.10 Scratch assay (wound healing)

Cells were seeded onto collagen-I coated 16 mm dishes and grown to confluence for 48 h. Transfection was performed as described. Medium was replaced by serum-low medium and cells were incubated 24 h before the scratch was performed by cross-scraping the monolayer with a pipette tip. Scratch assay and analysis was performed as described for DJ-1 in chapter 2 (see 2.2.7).

2.2.11 Trans-well migration assay

Cell culture inserts were placed onto 16 mm dishes. Cells were seeded (35.000 cells/ml) on the membrane of the insert in 200 µl serum-low medium. Each well was filled with 700 µl of normal growth medium. Trans-well migration was performed at 5 % CO_2 and 37 °C for 24 h. Medium was aspirated and the non-migrated cells were removed from the filter by using a cotton bud. Migrated cells were fixed with 100 % methanol for 2 min at RT and stained by 0.05 % toluidine blue in aqua bidest for 2 min at RT. After washing six times with aqua bidest, trans-well filters were cut out and mounted in immersion oil. Analysis was performed by a light microscope with camera system (Olympus CK40 with Olympus C5060 camera) and a percentage of migrated cells per well normalized to the respective control was determined.

2.2.12 Trans-well invasion assay

Cell culture inserts were placed onto 16 mm dishes. Small amounts of matrigel (25 µl, 200-300 µg/ml) were diluted with 975 µl coating buffer, 75 µl of this solution were placed on the membrane of the cell culture insert and incubated for 2 h at 37 °C. Then

cells (40.000 cells/ml) were seeded onto the matrigel in 200 µl of serum-low medium. Each well was filled with 700 µl of normal growth medium. The invasion was performed at 5 % CO_2 and 37 °C for 24 h. Medium was aspirated and matrigel as well as the non-migrated cells were removed from the inserts by using a cotton bud. The same protocol as described for the trans-well migration assay was used. The percentage of invaded cells/well normalized to the respective control was determined.

2.2.13 Proliferation assay

For assessment of proliferation, cells (10.000 cells/ml) were seeded onto 6 mm dishes and cultured for 24 h at 37 °C and 5 % CO_2. 5-Bromo-2'-Deoxyuridine (BrdU, 10µM) labeling solution was incubated for 2 h at 37 °C and 5 % CO_2. Then cells were washed once with 10 x PBS, fixed with 70 % ethanol/ 0.5M HCl for 30 min at RT, washed three times with PBS/ 10% FBS and nucleases were added for 30 min at 37 °C. Cells were washed three times, incubated with anti-BrdU-POD solution (200 mU/ml) for 30 min at 37 °C, washed again three times and incubated with a peroxidase substrate for 2-30 min at RT. Cells were assayed by an ELISA reader at 405 nm and a reference wavelength of 490 nm. The percentage of proliferating cells normalized to the respective control was determined.

2.2.14 Statistical analysis

For immunohistochemistry, the median H-Score was calculated. Cell culture experiments were performed in triplicates and repeated at least in n=3-6 independent experiments. Results are shown as mean ± S.E.M. Values obtained significant by unpaired t-test. Differences were considered significant if *$p<0.05$, **$p<0.01$, ***$p<0.001$.

3 Results

3.1 Cytoplasmic and nuclear claudin-1 localization in human follicular thyroid carcinoma tissues

Claudin-1 expression and localization was investigated in normal thyroid tissues, follicular adenomas, follicular thyroid carcinomas (FTC) and their metastases. In normal thyroid tissue, claudin-1 was expressed in the plasma membrane and cytoplasm. In follicular adenoma and primary FTC, claudin-1 staining was found in the plasma membrane and cytoplasm with few nuclear staining areas. In FTC metastases absent plasma membrane and increased nuclear claudin-1 expression was found (Fig. 24).

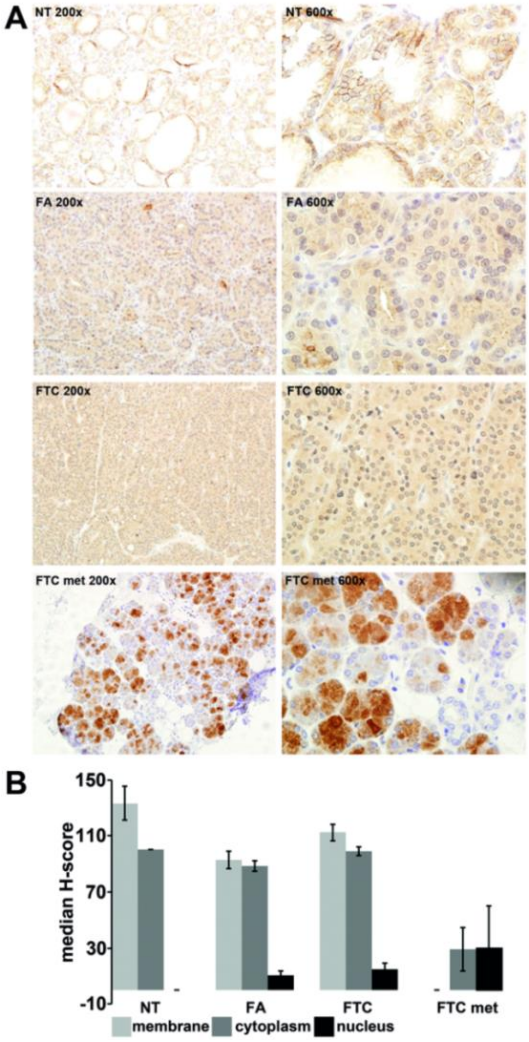

Figure 24: Immunohistochemical analysis of claudin-1 localization and expression. Immunohistochemical analysis of claudin-1 localization in normal thyroid tissues, follicular thyroid tumours and metastases of follicular thyroid cancer. (A) Normal thyroid tissue (NT) shows claudin-1 staining in the plasma membrane and cytoplasm. Decreased membrane claudin-1 expression was observed in follicular adenoma (FA) and follicular thyroid

carcinoma (FTC). Soft tissue metastasis of FTC (FTC met) showing absent membrane and exclusive nuclear and cytoplasmic claudin-1 staining. Olympus BX51 upright microscope with a magnification of either 200x or 600x. Representative examples are shown. (B) Semi-quantitative analysis of claudin-1 immuno-staining was performed for membrane, cytoplasm and nucleus localization by determining the median H-score in normal thyroid tissues, 40 FA, 44 FTC and six FTC metastases. The median H-Score shows a trend for lower claudin-1 membrane immuno-reactivity in follicular tumours (FA and FTC) as well as absent membrane and increased nuclear claudin-1 expression in FTC metastases.

3.2 Claudin-1 expression is increased in FTC cells and correlates with metastatic potential

The functional relevance of altered claudin-1 expression in follicular thyroid cancer was subsequently investigated in vitro. First, claudin-1 expression and localization was analysed by western blot and immunofluorescence in two follicular thyroid carcinoma cell lines FTC-133 and FTC-238, which represent distinct metastatic levels of the same primary FTC (Fig. 25A, B). Claudin-1 was expressed in both cell lines but a 67 % higher protein expression was seen in FTC-238, derived from a lung metastasis compared to FTC-133 cells, derived from a lymph node metastasis in proximity to the primary FTC (Fig. 25A). Both FTC-133 and FTC-238 cells exhibited claudin-1 expression mainly in the cell nucleus (Fig. 25B). On functional characterization, FTC-133 cells showed a slower cell migration, cell invasion and cell proliferation compared to FTC-238 cells (Fig. 25C, D). Likewise, in the scratch assay, FTC-133 cells showed a slower reconstitution of an intact cell monolayer compared to FTC claudin-1 expression in FTC-133 cells after scratching the cell monolayer (Fig. 25A). Interestingly, in immunofluorescence analysis, cells located close to the scratch showed higher claudin-1 fluorescence signals mainly in the nuclei as compared to cells in other areas of the cell monolayer (Fig. 25B). This applied for both FTC cell lines.

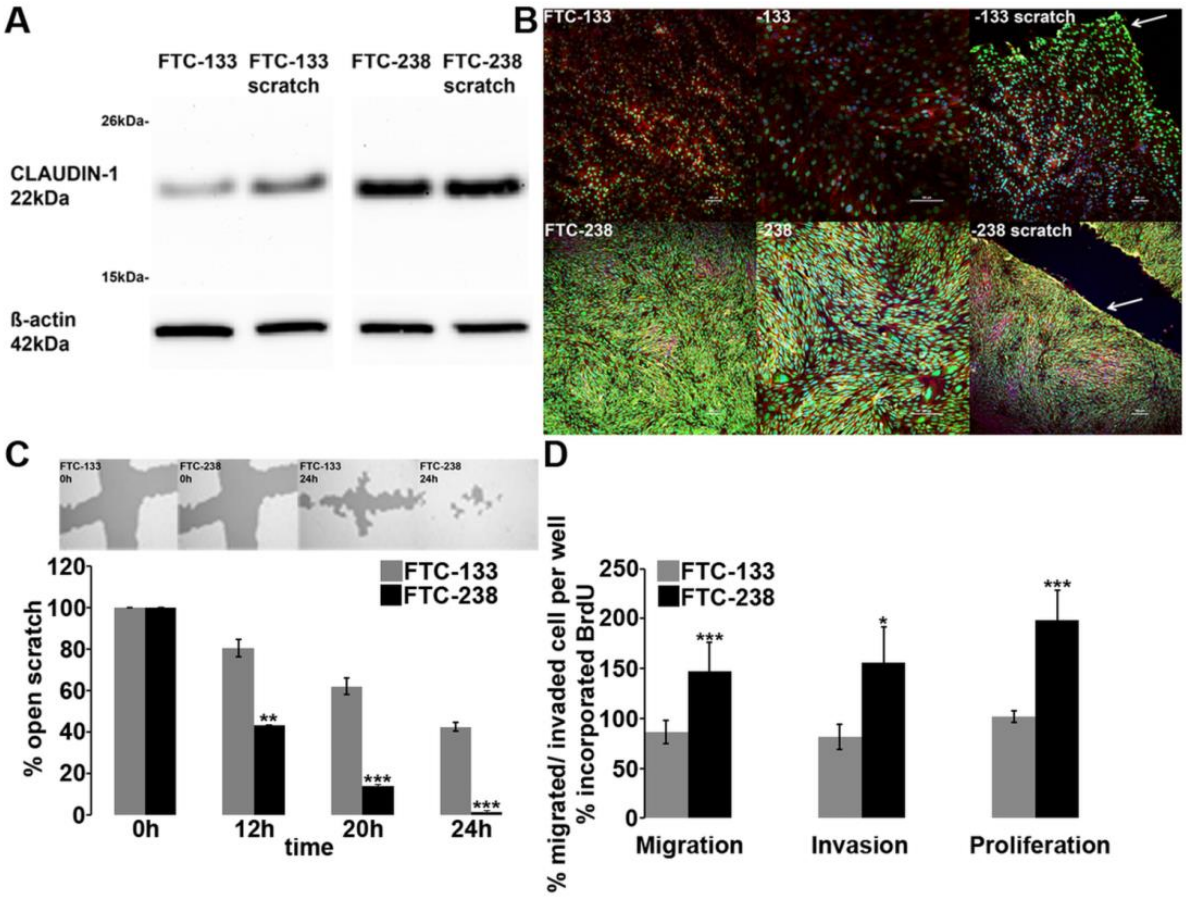

Figure 25: Claudin-1 expression is increased in metastatic follicular thyroid carcinoma cells. (A) Protein expression of claudin-1 (22 kDa) in FTC-133 and FTC-238 cells with and without scratch induction (6 h post-scratch induction). Higher claudin-1 expression in FTC-238 as compared to FTC-133 cells. Increase of claudin-1 expression during scratch closing process (6 h post-scratch induction). β-actin (42 kDa) was used as a loading control. (B) FTC cells with claudin-1 (green) protein expression in the cell nucleus and enhanced claudin-1 expression in FTC-238 as compared to FTC-133 cells. FTC-133 and FTC-238 cells 6 h post-scratch induction with increased claudin-1 fluorescence signals around the scratch (arrow). F-actin cytoskeleton was stained by AlexaFluor 555 Phalloidin (red). Nuclei were stained by Hoechst33342 (cyan). Scale bar: 100 mm. Confocal microscope Nikon Eclipse Ti. Representative examples are shown (n=3). (C) Faster closing of the scratch in FTC-238 than FTC-133 cells. Analysis was performed by TScratch Software. The percentage of the open scratch at the distinct time intervals normalized to the respective control (time point at 0 h) is shown. (D) Transwell migration, transwell invasion and cell proliferation rate of FTC cells. FTC-238 cells show a higher migration and invasion as well as proliferation rate as compared to FTC-133 cells. The percentage of migration, invasion or proliferation of cells/well normalized to the respective control is shown. Data are represented as mean±S.E.M., n=3–6, t-test, *P<0.05, **P<0.01 and ***P<0.001.

Based on these findings, FTC-133 and FTC-238 cells were selected as suitable in vitro models to further study the impact of claudin-1 in FTC aggressiveness. To investigate if an increase of the pathogenic character of FTC-133 cells influences claudin-1 expression, a RASV12 mutation was introduced by transient transfection. EV transfected FTC-133 cells were used as a negative control. In FTC-133+EV cells, no endogenous RASV12 expression was detected (Fig. 26A). In Western blot analysis, FTC-133+RASV12 cells showed a 35 % higher claudin-1 expression as compared to

FTC-133-EV cells (Fig. 26A). In the scratch assay, FTC-133+RASV12 cells revealed a faster closing of the scratch than the control (Fig. 26B). A higher cell migration rate of FTC-133+RASV12 as compared to controls could also be demonstrated in the transwell migration assay (Fig. 26C). Furthermore, in the transwell invasion assay the FTC-133+RASV12 cells were more invasive than control cells (Fig. 26D) and a higher percentage of cells incorporating BrdU was found in line with the induction of cell proliferation (Fig. 26E).

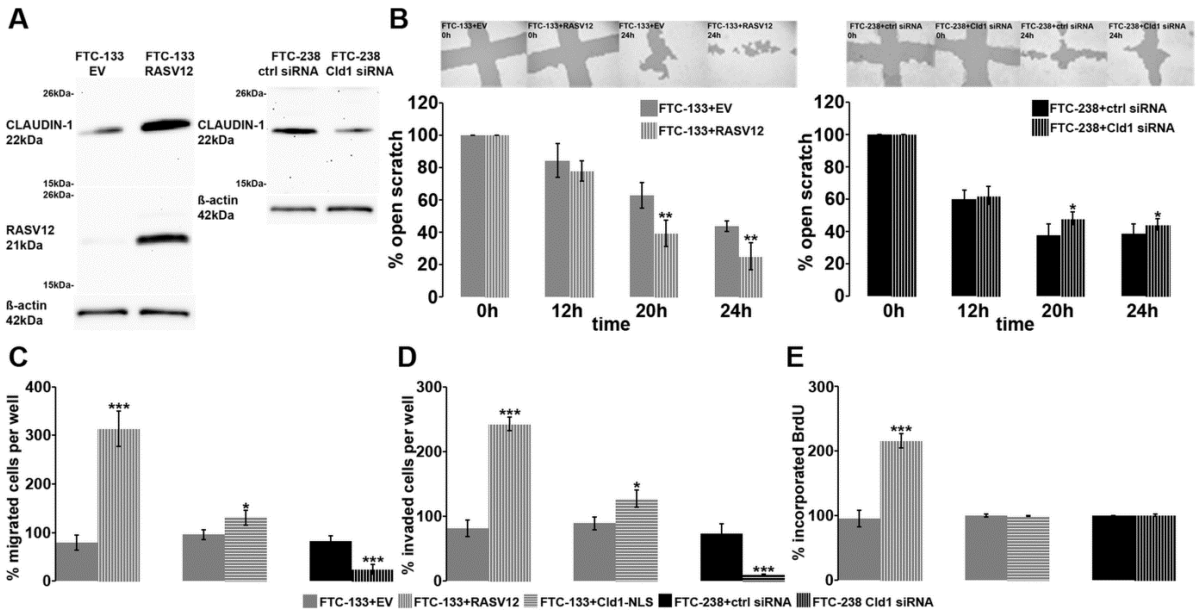

Figure 26: Modulation of claudin-1 expression alters the aggressiveness of follicular thyroid carcinoma cells. (A) Upregulation of claudin-1 by transient transfection of FTC-133 cells with RASV12 and downregulation of claudin-1 by Cld1 siRNA treatment of FTC-238 cells. EV transfected FTC-133 cells and control (ctrl) siRNA-treated FTC-238 cells were used as controls. No endogenous RASV12 expression in EV transfected FTC-133 cells. Successful transfection was determined by RASV12 (21 kDa) protein expression. β-actin (42 kDa) was used as a loading control. (B) FTC-133+RASV12 cells show a significantly faster reconstitution of an intact cell monolayer as compared to controls. In contrast, FTC-238+Cld1 siRNA cells show a significantly decreased scratch closing rate compared to FTC-238C ctrl siRNA cells. Non-targeting siRNA per se also slightly decreases the scratch closing capacity of FTC-238 cells. Analysis was performed by TScratch. The percentage of the open scratch at the distinct time intervals normalized to the respective control (at start of experiment, 0 h) is shown. (C, D) FTC-133+RASV12 and Cld1-NLS transfected FTC-133 cells show a faster cell migration and invasion than the respective controls. In contrast, FTC-238+Cld1 siRNA cells reveal a slower cell migration and invasion as compared to controls. The percentage of migrated or invaded cells/well normalized to the respective control is shown. (E) RASV12 transfected FTC-133 cells show increased BrdU incorporation, but direct claudin-1 modulation by siRNA or Cld1-NLS transfection shows no effect on BrdU incorporation, suggesting that the RASV12 effect is mediated by other signalling pathways than claudin-1. The percentage of cells with BrDU incorporation normalized to the respective control is shown. Data are represented as mean±S.E.M., n=3–6, t-test, *P<0.05, **P<0.01 and ***P<0.001.

3.3 Nuclear claudin-1 modulation alters the aggressiveness of follicular thyroid carcinoma cells

Next we asked if the modulation of nuclear claudin-1 expression in FTC cell lines alters their functional behaviour. Therefore, FTC-133 cells were transiently transfected with Cld1-NLS to over-express nuclear claudin-1, whereas in FTC-238 cells claudin-1 was downregulated by siRNA transfection. An EV or a non-targeting siRNA was used as negative controls. Positive transfection of Cld1-NLS was determined by fluorescence microscopy. Successful siRNA transfection of FTC-238 cells showing 44 % downregulation of claudin-1 expression was determined by western blot analysis (Fig. 26A). In the scratch assay, a slower reconstitution of an intact cell monolayer was found for claudin-1 siRNA transfected FTC-238 cells as compared to the control (Fig. 26B). In fact, non-targeting control siRNA led to a slight decrease of scratch closing capacity in FTC-238 cells. In addition, a slower cell migration rate was found for claudin-1 siRNA transfected FTC-238 cells compared to the control in the transwell migration assay (Fig. 26C). Because of equal results obtained by scratch assay and transwell migration, only transwell migration was investigated in the subsequent studies. Thus, faster cell migration was found for Cld1-NLS transfected FTC-133 cells compared to the control in the transwell migration assay (Fig. 26C). Furthermore, in the transwell invasion assay the FTC-133+Cld1-NLS cells were more invasive, whereas claudin-1 siRNA transfected FTC-238 cells were less invasive than the respective control (Fig. 26D). Interestingly, BrdU incorporation was not different in either the Cld1-NLS transfected FTC-133 cells or the claudin-1 siRNA transfected FTC-238 cells as compared to the respective controls (Fig. 26E).

3.4 Positive correlation of claudin-1 and phosphoprotein kinase C expression in follicular thyroid carcinoma cells

To investigate which molecular mechanism or signal transduction pathways could be involved in claudin-1 regulation in human follicular thyroid carcinoma, protein expression patterns of phospho-Akt (pAkt), phospho-Erk1/2 (pErk1/2), phosphoPKC (pPKC) and total PKC were determined in claudin-1 knock-down FTC-238 cells and compared to protein expression of FTC-238 cells transfected with non-targeting control

siRNA by western blot analysis. Neither protein expression of pAkt nor protein expression of pErk1/2 was altered between claudin-1 knock-down FTC-238 cells and the control (Fig. 27A). However, western blot analysis revealed a 25–32 % decreased pPKC expression in claudin-1 siRNA transfected FTC-238 cells as compared to the control either normalized to total PKC expression or the respective
loading control (Fig. 27A). The PKC antibodies for total PKC and pPKC used in this study detect several PKC isoforms. As a next step, endogenous pPKC expression was investigated by western blot in the two follicular thyroid carcinoma cell lines (Fig. 27B). We found a 55 % higher pPKC protein expression in FTC-238 as compared to FTC-133 cells. To determine if PKC activation or inhibition influences claudin-1 expression, FTC-133 and FTC-238 cells were either treated with the PKC activator PMA or the PKC inhibitor Gö6983. Successful PKC activation and inhibition were demonstrated by 45 % increased and 38 % decreased pPKC protein levels, respectively (Fig. 27B). PKC activation of FTC-133 cells resulted in 45 % increased claudin-1 expression, whereas inhibition of PKC showed a 30 % decreased claudin-1 expression as compared to the respective control (Fig. 27B). FTC-133+PMA cells revealed a faster cell migration, whereas FTC-238+Gö6983 cells showed a slower cell migration than the respective control (Fig. 27C). In addition, in the transwell invasion assay, pharmacological PKC activation in FTC-133 cells resulted in a higher invasion rate and PKC inhibition in FTC-238 cells diminished the transwell invasion rate (Fig. 27D). In the same manner, cell proliferation was increased by PMA treatment of FTC-133 and decreased by Gö6983 treatment of FTC-238 cells resulting in a higher or lower percentage of cells incorporating BrdU compared to the control (Fig. 27E).

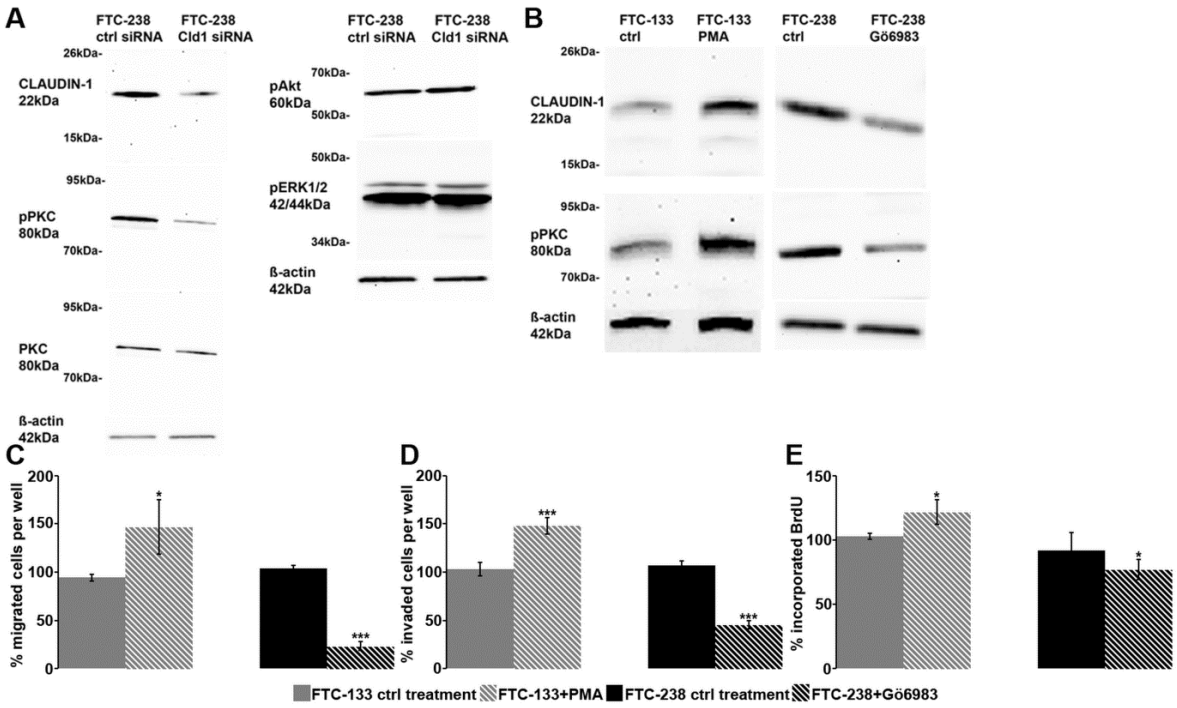

Figure 27: Claudin-1 and phosphoprotein kinase C expression are correlated in follicular thyroid carcinoma cells. (A) Protein expression of phosphoprotein kinase C (pPKC), total PKC, phospho-Akt (pAkt) and phospho-Erk1/2 (pErk1/2) in claudin-1 (Cld1) siRNA and control (ctrl) siRNA transfected FTC-238 cells. Diminished pPKC (80 kDa) expression in FTC-238+Cld1 siRNA cells as compared to FTC-238Cctrl siRNA cells. No change in protein expression between ctrl siRNA and Cld1 siRNA transfected FTC-238 cells for pAkt (60 kDa) and pErk1/2 (42/44 kDa). (B) Successful pPKC modulation by phorbol-12-myristate-13-acetate (PMA) and Gö6983. PKC activation increases claudin-1 (22 kDa) protein expression in FTC-133 cells, whereas PKC inhibition decreases claudin-1 protein expression in FTC-238 cells to the respective control. β-actin (42 kDa) was used as a loading control. (C–D) FTC-133+PMA cells show faster cell migration and invasion as compared to the control. FTC-238+Gö6983 cells reveal a slower cell migration and invasion as compared to the control. The percentage of migrated or invaded cells/well normalized to the respective control is shown. (E) FTC-133+PMA cells show a faster proliferation rate, whereas FTC-238+Gö6983 cells reveal a reduced cell proliferation compared to controls. The percentage of cell proliferation normalized to the respective control is shown. Data are represented as mean±S.E.M., n=3–4, t-test, *P<0.05 and ***P<0.001.

4 Discussion

Claudin-1 expression is altered in several human malignancies (Resnick *et al.*, 2005; Tokés *et al.*, 2005; Chao *et al.*, 2009) and subcellular expression of claudin-1 has been linked with tumour invasiveness and an advanced tumour stage (Dhawan *et al.*, 2005; Kinugasa *et al.*, 2012; Eftang *et al.*, 2013). We asked whether claudin-1 is relevant for the biological behaviour of human follicular thyroid cancer.

Our study confirms claudin-1 expression in human thyroid tissues and shows a shift to subcellular claudin-1 localization in follicular thyroid cancers and nuclear claudin-1 expression in FTC metastases. These findings are in contrast to two previous reports on claudin-1 in thyroid cancer. Very low or nearly absent claudin-1 expression was found in human follicular tumours by immunohistochemistry in one study, while another study found weak claudin-1 expression in human FA and FTC tissues (Németh *et al.*, 2010) and postulated that low claudin-1 expression correlates with tumour de-differentiation (Tzelepi *et al.*, 2008).

Technical or experimental differences as well as different selections of patients account for these discrepant findings. One shortcoming of our study is that data on clinical courses of our FA and FTC patients are lacking. On the other hand, we clearly show a shift of claudin-1 expression with a more pronounced nuclear claudin-1 localization in FTC metastases.

To explore these first findings on immunohistochemistry, we employed two FTC cell lines as *in vitro* models of follicular thyroid cancer. In cell culture, we could confirm the more aggressive behaviour of FTC-238 cells by a faster scratch repair, higher migration and invasion rates and a higher proliferation rate as compared to FTC-133 cells. Both cell lines, FTC-133 and FTC-238, were found to express nuclear localized claudin-1, yet a higher protein expression was demonstrated in the more aggressive FTC-238 cells. Translocation of claudin-1 from the cell membrane to subcellular compartments has been described in different human tumours and has been associated with the tumourigenicity of cancer cells (Miwa *et al.*, 2001). In addition, loss of membranous tight junction proteins could negatively influence cell cohesion and/or cell differentiation (Ding *et al.*, 2013). Moreover, in colon cancer, nuclear claudin-1 localization has been linked to cellular and metastatic behaviour (Dhawan *et al.*, 2005).

The molecular mechanism involved in the internalization of claudin-1 into subcellular or nuclear compartments is hypothesized to be regulated by post-translational modifications like phosphorylation (D'Souza *et al.*, 2005), mutations (Dhawan *et al.*, 2005), and/or promotor gene hypermethylation (Boireau *et al.*, 2007). The increase in nuclear claudin-1 expression during scratch induction could reflect enhanced migration in close proximity of the scratch, because it has been suggested that claudin proteins translocate from the cell surface to intracellular compartments at the site where cell migration occurs (Takehara *et al.*, 2009). In our cell models, claudin-1 is already localized in the cell nucleus and only shows an enriched nuclear expression around the scratch in FTC cell lines.

Furthermore, we observed that claudin-1 expression is increased in FTC-133 cells by transient transfection of *H-RASV12*. Mutations in one of the three *RAS* genes are frequently observed in human carcinomas (Takashima and Faller, 2013). In addition, the *RASV12* mutation is a well known molecular alteration in FTC leading to constitutive activation of *RAS*-mediated signaling pathways (Theoharis *et al.*, 2012). It can thus be suggested that the elevated pathogenic character of *RASV12* transfected FTC-133 cells involves the increase claudin-1 protein expression. This increase in claudin-1 expression after *RASV12* transfection was also observed in normal renal epithelial cells, whereby in these normal cells claudin-1 was localized in the cell membrane (Mullin *et al.*, 2005). As a side note, we tried claudin-1 downregulation by claudin-1 siRNA transfection of RASV12 transfected FTC-133 cells, which resulted in cell death within few hours, potentially due to the augumented stress of the cells, and irrespective if cells were transfected either with ctrl. siRNA or claudin-1 siRNA transfection mixture. However, RASV12 transfection in FTC-133 cells not only resulted in an increased claudin-1 expression but also showed faster migration, invasion and proliferation rates. This indirectly suggests a regulatory function of subcellular claudin-1 expression in the biological behaviour of FTC cells. As a proof of the relevance of nuclear claudin-1 in the biological behaviour of FTC cell lines, the nuclear claudin-1 protein amount was modulated, i.e., elevated by *claudin-1-NLS* transfection of FTC-133 cells or reduced by *claudin-1* siRNA transfection in FTC-238 cells. Increased nuclear claudin-1 expression in FTC-133 cells augumented cell migration and invasion. However, effects were less pronounced than in FTC-133+RASV12 cells. These

differences could be, on the one hand, explained by the high oncogenic potential of RASV12 (Saavedra *et al.*, 2000). On the other hand, claudin-1 could be predominantly associated with FTC motility leading to a promotion of metastases. Interestingly, cell proliferation of FTC-133 cells is not altered by *claudin-1-NLS* transfection. claudin-1 knockdown in FTC-238 cells by claudin-1 siRNA leads to opposite results with lower migration and invasion rates as compared to non-trageting siRNA transfection. The slight decrease in the scratch repair capacity of FTC-238 cells by transfection of non-trageting siRNA could be explained by non-specific influences of the scrambled sequence within the cellular mRNA of FTC-238 cells and re-emphasizes the necessity for adequate controls. Similary to *claudin-1-NLS* transfected FTC-133 cells, cell proliferation is not influenced in *claudin-1* knockdown cells. In melanoma cells, an increase of nuclear claudin-1 by transfection of *claudin-1-NLS* also showed no changes in cell proliferation to EV control cells (French *et al.*, 2009). Therefore, it could be speculated that claudin-1 influences the tumourigenic behaviour of FTC cells but does not affect proliferative activity.

The role of PKC has previously been studied in relation to thyroid tumourigenesis and thyroid cancer (Hoelting *et al.*, 1997; Knauf *et al.*, 2002; Molè *et al.*, 2012). In FTC-133 cells, PKC activation by PMA increased cell invasion (Hoelting *et al.*, 1997). Others, however, have found a negative correlation between PKC activation and cell proliferation in human thyroid cancer cells (Koike *et al.*, 2006; Afrasiabi *et al.*, 2008). In our study we found a higher pPKC protein expression in FTC-238 cells compared to FTC-133 cells. In addition, claudin-1 knockdown resulted in a decrease in pPKC expression in FTC-238 cells. In melanoma, a claudin-1 dependent increase of cell motility has previously been described and was linked to PKC activation (Leotlela *et al*., 2007). Whether PKC activity also influences claudin-1 expression in FTC cell lines was further investigated by treatment of FTC cells with either the PKC activator PMA or the PKC inhibitor Gö6983. In this setting we could confirm the study of Hoelting *et al.* (1997), showing a positive correlation between PKC activity and cell migration and invasion as well as proliferation. Moreover, PKC activation by PMA increased claudin-1 protein expression in FTC-133 cells, whereas PKC inhibition by Gö6983 diminished claudin-1 protein expression in FTC-238 cells. These results are in line with previous studies of PKC, claudin-1 interaction in human melanoma cells (Leotlela *et al.*, 2007).

The question, which PKC isoform could be involved in claudin-1 regulation in FTC cell lines, arises. Previous studies in human liver cells showed a correlation between claudin-1 and PKC delta expression (Yoon *et al.*, 2010). In melanoma cells, an involvement of several PKC isoforms (α, β and δ) in claudin-1 regulation has been reported (Leotlela *et al.*, 2007), and furthermore, it was shown that PKC-induced upregulation of claudin-1 results in the upregulation of the MMP-2 (Leotlela *et al.*, 2007). Interestingly, MMP-2 expression has also been reported in human FTC tissues (Cho Mar *et al.*, 2006) and, more recently, it was shown that the cellular growth capacity of FTC-133 cells is influenced by MMP-2 activity (Mitmaker *et al.*, 2011). We therefore speculate that MMP-2 could be regulated by claudin-1 via PKC and FTC. The PKC modulators PMA and Gö6983 used in this study are directed against PKC isoforms α, β, γ, δ and ε (Ryves *et al.*, 1991; Leotlela *et al.*, 2007). It has been shown that FTC-133 cells express PKC isoforms beta II and delta on the protein level, which may suggest that these isoforms are relevant for claudin-1 regulation in follicular thyroid cancer. However, further studies need to be conducted to clarify which isoforms of PKC are involved and to which extent PKC, claudin-1 and MMPs interact. To this end a strategy could involve the use of isoform-selective PKC inhibitors, PKC specific agonist and antagonist peptides (Chang and Tepperman, 2003) and MMP specific inhibitors either alone or in combination with claudin-1 modulation in FTC cell lines.

In conclusion, claudin-1 expression and localization is altered in follicular thyroid carcinoma and FTC metastases. In cell culture experiments modulation of claudin-1 expression influences the functional behaviour of follicular thyroid carcinoma cells. Furthermore, we provide the first evidence for a role of PKC signaling in regulation of claudin-1 expression and FTC aggressiveness opening new potential avenues for thyroid cancer targeting.

5 References

Afrasiabi E, Ahlgren J, Bergelin N, Törnquist K 2008 Phorbol 12-myristate 13-acetate inhibits FRO anaplastic human thyroid cancer cell proliferation by inducing cell cycle arrest in G1/S phase: evidence for an effect mediated by PKCdelta. *Molecular and cellular endocrinology* **292** 26–35.

Anderson JM, Van Itallie Christina M 2009 Physiology and function of the tight junction. *Cold Spring Harbor perspectives in biology* **1** a002584.

Boireau S, Buchert M, Samuel MS, Pannequin J, Ryan JL, Choquet A, Chapuis H, Rebillard X, Avancès C, Ernst M, Joubert D, Mottet N, Hollande F 2007 DNA-methylation-dependent alterations of claudin-4 expression in human bladder carcinoma. *Carcinogenesis* **28**, 246–258.

Chang Q, Tepperman BL 2003 Effect of selective PKC isoform activation and inhibition on TNF-alpha-induced injury and apoptosis in human intestinal epithelial cells. *British journal of pharmacology* **140** 41–52.

Chao YC, Pan SH, Yang SC, Yu SL, Che TF, Lin CW, Tsai MS, Chang GC, Wu CH, Wu YY, Lee YC, Hong TM, Yang PC 2009 Claudin-1 is a metastasis suppressor and correlates with clinical outcome in lung adenocarcinoma. *American journal of respiratory and critical care medicine* **179** 123–133.

Cho Mar K, Eimoto T, Tateyama H, Arai Y, Fujiyoshi Y, Hamaguchi M 2006 Expression of matrix metalloproteinases in benign and malignant follicular thyroid lesions. *Histopathology* **48** 286–294.

Dhawan P, Singh AB, Deane NG, No Y, Shiou SR, Schmidt C, Neff J, Washington MK, Beauchamp RD 2005 Claudin-1 regulates cellular transformation and metastatic behavior in colon cancer. *The Journal of clinical investigation* **115** 1765–1776.

Ding L, Lu Z, Lu Q, Chen YH 2013 The claudin family of proteins in human malignancy: a clinical perspective. *Cancer management and research* **5** 367–375.

D'Souza T, Agarwal R, Morin PJ 2005 Phosphorylation of claudin-3 at threonine 192 by cAMP-dependent protein kinase regulates tight junction barrier function in ovarian cancer cells. *The Journal of biological chemistry* **280** 26233–26240.

Eftang LL, Esbensen Y, Tannæs TM, Blom GP, Bukholm Ida RK, Bukholm G 2013 Up-regulation of CLDN1 in gastric cancer is correlated with reduced survival. *BMC cancer* **13**, 586.

Feigin ME & Muthuswamy SK 2009 Polarity proteins regulate mammalian cell-cell junctions and cancer pathogenesis. *Current opinion in cell biology* **21** 694–700.

French AD, Fiori JL, Camilli TC, Leotlela PD, O'Connell MP, Frank BP, Subaran S, Indig FE, Taub DD, Weeraratna AT 2009 PKC and PKA phosphorylation affect the subcellular localization of claudin-1 in melanoma cells. *International journal of medical sciences* **6** 93–101.

González-Mariscal L, Betanzos A, Nava P, Jaramillo BE 2003 Tight junction proteins. *Progress in biophysics and molecular biology* **81** 1–44.

Hoelting T, Duh QY, Clark OH, Herfarth C 1997 Invasion of metastatic human follicular thyroid cancer is inhibited via antagonism of protein kinase C. *Cancer letters* **119** 1–5.

Kinugasa T, Akagi Y, Ochi T, Tanaka N, Kawahara A, Ishibashi Y, Gotanda Y, Yamaguchi K, Shiratuchi I, Oka Y, Kage M, Shirouzu K 2012 Increased claudin-1 protein expression in hepatic metastatic lesions of colorectal cancer. *Anticancer researc*h **32** 2309–2314.

Knauf JA, Ward LS, Nikiforov YE, Nikiforova M, Puxeddu E, Medvedovic M, Liron T, Mochly-Rosen D, Fagin JA 2002 Isozyme-specific abnormalities of PKC in thyroid cancer: evidence for post-transcriptional changes in PKC epsilon. *The Journal of clinical endocrinology and metabolism* **87** 2150–2159.

Koike K, Fujii T, Nakamura AM, Yokoyama G, Yamana H, Kuwano M, Shirouzu K 2006 Activation of protein kinase C delta induces growth arrest in NPA thyroid cancer cells through extracellular signal-regulated kinase mitogen-activated protein kinase. *Thyroid : official journal of the American Thyroid Association* **16** 333–341.

Krause G, Winkler L, Mueller SL, Haseloff RF, Piontek J, Blasig IE 2008 Structure and function of claudins. *Biochimica et biophysica acta* **1778** 631–645.

Leotlela PD, Wade MS, Duray PH, Rhode MJ, Brown HF, Rosenthal DT, Dissanayake SK, Earley R, Indig FE, Nickoloff BJ, Taub DD, Kallioniemi OP, Meltzer P, Morin PJ, Weeraratna AT 2007 Claudin-1 overexpression in melanoma is regulated by PKC and contributes to melanoma cell motility. *Oncogene* **26** 3846–3856.

Madara JL, Parkos C, Colgan S, Nusrat A, Atisook K, Kaoutzani P 1992 The movement of solutes and cells across tight junctions. *Annals of the New York Academy of Sciences* **664** 47–60.

McCartney MD & Cantu-Crouch D 1992 Rabbit corneal epithelial wound repair: tight junction reformation. *Current eye research* **11** 15–24.

Mitmaker EJ, Griff NJ, Grogan RH, Sarkar R, Kebebew E, Duh QY, Clark OH, Shen WT 2011 Modulation of matrix metalloproteinase activity in human thyroid cancer cell lines using demethylating agents and histone deacetylase inhibitors. *Surgery* **149** 504–511.

Miwa N, Furuse M, Tsukita S, Niikawa N, Nakamura Y, Furukawa Y 2001 Involvement of claudin-1 in the beta-catenin/Tcf signaling pathway and its frequent upregulation in human colorectal cancers. *Oncology research* **12** 469–476.

Molè D, Gentilin E, Gagliano T, Tagliati F, Bondanelli M, Pelizzo MR, Rossi M, Filieri C, Pansini G, degli Uberti Ettore C, Zatelli MC 2012 Protein kinase C: a putative new target for the control of human medullary thyroid carcinoma cell proliferation in vitro. *Endocrinology* **153** 2088–2098.

Mullin JM, Leatherman JM, Valenzano MC, Huerta ER, Verrechio J, Smith DM, Snetselaar K, Liu M, Francis MK, Sell C 2005 Ras mutation impairs epithelial barrier function to a wide range of nonelectrolytes. *Molecular biology of the cell* **16** 5538–5550.

Németh J, Németh Z, Tátrai P, Péter I, Somorácz A, Szász AM, Kiss A, Schaff Z 2010 High expression of claudin-1 protein in papillary thyroid tumor and its regional lymph node metastasis. *Pathology oncology research : POR* **16** 19–27.

Resnick MB, Konkin T, Routhier J, Sabo E, Pricolo VE 2005 Claudin-1 is a strong prognostic indicator in stage II colonic cancer: a tissue microarray study*. Modern pathology : an official journal of the United States and Canadian Academy of Pathology*, *Inc* **18** 511–518.

Riehl TE & Stenson WF 1994 Mechanisms of transit of lipid mediators of inflammation and bacterial peptides across intestinal epithelia. *The American journal of physiology* **267** G687-95.

Ryves WJ, Evans AT, Olivier AR, Parker PJ, Evans FJ 1991 Activation of the PKC-isotypes alpha, beta 1, gamma, delta and epsilon by phorbol esters of different biological activities. *FEBS letters* **288** 5–9.

Saavedra HI, Knauf JA, Shirokawa JM, Wang J, Ouyang B, Elisei R, Stambrook PJ, Fagin JA 2000 The RAS oncogene induces genomic instability in thyroid PCCL3 cells via the MAPK pathway. *Oncogene* **19** 3948–3954.

Takashima A & Faller DV 2013 Targeting the RAS oncogene. *Expert opinion on therapeutic targets* **17** 507–531.

Takehara M, Nishimura T, Mima S, Hoshino T, Mizushima T 2009 Effect of claudin expression on paracellular permeability, migration and invasion of colonic cancer cells. *Biological & pharmaceutical bulletin* **32** 825–831.

Theoharis C, Roman S, Sosa JA 2012 The molecular diagnosis and management of thyroid neoplasms. *Current opinion in oncology* **24** 35–41.

Ting S, Mairinger FD, Hager T, Welter S, Eberhardt WE, Wohlschlaeger J, Schmid KW, Christoph DC 2013 ERCC1, MLH1, MSH2, MSH6, and βIII-tubulin: resistance proteins associated with response and outcome to platinum-based chemotherapy in malignant pleural mesothelioma. *Clinical lung cancer* **14** 558-567.

Tokés AM, Kulka J, Paku S, Szik A, Páska C, Novák PK, Szilák L, Kiss A, Bögi K, Schaff Z 2005 Claudin-1, -3 and -4 proteins and mRNA expression in benign and malignant breast lesions: a research study. *Breast cancer research : BCR* **7** R296-305.

Tzelepi VN, Tsamandas AC, Vlotinou HD, Vagianos CE, Scopa CD 2008 Tight junctions in thyroid carcinogenesis: diverse expression of claudin-1, claudin-4, claudin-7 and occludin in thyroid neoplasms. *Modern pathology : an official journal of the United States and Canadian Academy of Pathology, Inc* **21** 22–30.

Yoon CH, Kim MJ, Park MJ, Park IC, Hwang SG, An S, Choi YH, Yoon G, Lee SJ 2010 Claudin-1 acts through c-Abl-protein kinase Cdelta (PKCdelta) signaling and has a causal role in the acquisition of invasive capacity in human liver cells. *The Journal of biological chemistry* **285** 226–233.

Chapter 4: Differential regulation of monocarboxylate transporter 8 expression in thyroid cancer and hyperthyroidism

1 Introduction

1.1 Thyroid hormone transporters – an overview

The influx-and efflux of TH into organs/cells is facilitated by thyroid hormone transporters. Known transporters which guide TH entry into the target cells belong to the monocarboxylate transporter family (Mct), to the L-type amino acid transporter family and to the organic anion-transporting polypeptide gene family (Oatp).

So far, the most specific transporter for the thyroid hormones T3, T4, reverse T3 and 3,5-diiodo-L-thyronine (T2) is the monocarboxylate transporter 8 (MCT8) (Friesema, Edith CH *et al*., 2003; Di Cosmo *et al*., 2010), which belongs to the major facilitator superfamily (Friesema, Edith CH *et al*., 2006). This TH transporter is encoded by the *SLC16A2* gene and is located on chromosome Xq13.2. It is a 12-transmembrane spanning protein with its N- and C-termini located in the cytoplasm (Visser *et al*., 2008). The transporter is expressed in brain, heart, kidney, liver, skeletal muscle, placenta, testis and the basolateral plasma membrane of thyroid epithelial cells consistent with its role in thyroxine export from thyroid follicles (Friesema, Edith CH *et al*., 2003; Chan *et al*., 2006; Kinne *et al*., 2011; Weber et al., 2017). The human *MCT8* gene consists of 613 amino acids (aa) and encodes a 65 kDa protein (Friesema, Edith CH *et al*., 2006). Mutations in *SLC16A2* cause the Allan-Herndon-Dudley syndrome (AHDS), which is characterized by X-linked mental retardation (Friesema *et al*., 2004). The phenotype involves hypotonia, spasticity, limited mobility and lack of cognitive function. AHDS patients show high TSH and elevated T3 levels but low T4. *Mct8* knockout mice share the same highly elevated T3 and T4 levels with human patients. Additionally, enlarged follicles inside the thyroid were detected in these mice.

Secondary TH transporters like the large neutral amino acid transporters LAT2, LAT3 and LAT4 (Wagner *et al*., 2001) facilitate in- and efflux of TH and other substrates e.g. amino acids. Thus, while the preferred TH substrate of LAT2 is 3,3'-T2, LAT2 also transports large neutral amino acids, amino-acid related compounds and small amino

acids (Wagner *et al*., 2001). LAT2 is expressed in many tissues including the thyroid gland (Kinne *et al*., 2011).

LAT4 is a sodium, chloride and pH independent transporter and is detected in kidney, placenta, peripheral blood leukocytes and spleen (Bodoy *et al*., 2005). Recent studies suggest that LAT4 is not involved in T3 and T4 transport but facilitates T2 efflux (Zevenbergen *et a*l., 2015). Thus, known TH transporters differ in terms of substrate preferences, direction of TH transport (influx and efflux) and tissue expression pattern.

TH transporter expression in the thyroid gland was first demonstrated by Di Cosmo *et al*. in an elegant Mct8 mouse knock-out study (Di Cosmo *et al*., 2010). Mct8 expression was found at the basolateral membrane of thyrocytes, strongly suggesting that Mct8 plays a role in TH release. Subsequent studies in mice have shown that Lat2 is also expressed in the thyroid gland (Di Cosmo *et al*., 2010) with a cytoplasmic localization.

1.2 Aims & working hypothesis

Whether alterations of thyroid differentiation or thyroid function may have an impact on TH transporter expression in the thyroid is currently unknown. Here we asked whether expression and/ or localization of MCT8 and secondary TH transporters differ between benign and malignant thyroid tumours and in hyperfunctioning vs normal thyroid tissues (NTs). Based on our findings we suggest that MCT8 is a suitable marker for thyroid differentiation and that MCT8 upregulation occurs in hyperfunctioning thyroid tissue consistent with its role in TH export.

2 Material and Methods

2.1 Material

All compositions of buffers, used substances and manufactures of used products can be found in detail in Appendix C (Material).

2.2 Methods

2.2.1 Immunohistochemistry

Thyroid tissue samples from 238 patients were investigated. Histological classification of tissue specimen according to WHO criteria was obtained by certified pathologists. TH transporter expression was investigated on paraffin-embedded tissues of 19 normal thyroid tissues (NT), 44 follicular adenomas (FA), 45 follicular thyroid carcinomas (FTC), 40 papillary thyroid carcinomas (PTC), 40 anaplastic thyroid carcinomas (ATC), and 50 Graves' disease (GD) thyroid specimen.

For immunohistochemical analysis the following antibodies were used: anti-MCT8/SLC16A2 (1:150), anti-LAT2 (1:200), anti-LAT3/SLC43A1 (1:50) and anti-LAT4/SLC43A2 (1:10). All tissue sections were deparaffinized and rehydrated through graded series of alcohols (70%-/96%-100% v/v ethanol). Pretreatment was performed for 20 min in citrate buffer (pH 6.0) at 95 °C. Tissue sections were blocked in an aqueous hydrogen peroxide solution (3 % v/v H_2O_2). Primary antibodies were incubated for 30 min at RT. Immunoreactivity was demonstrated using a classical polymer system. Cell nuclei were stained with haematoxylin (1:8) for 5 min and sections were mounted in Entellan. All steps were performed in a semi-automated fashion using the Dako Autostainer. Paraffin-embedded human kidney tissue sections were used as positive controls for LAT3 and LAT4. Negative controls (no primary antibody) were included in the experimental set-up. The Olympus BX51 upright microscope was used for light microscopy. Tumour staining intensities were evaluated by calculating the 'hybrid' (H) score as previously described (see 2.2.1).

2.2.2 Cell culture

For cell culture experiments the rat follicular thyroid cell line PCCL3 (Fusco *et al*., 1987) was used. Cells were cultured in Ham's F12 medium with 5 % w/v fetal bovine serum, 5 µg/ml Transferrin, 10 µg/ml insulin, 10 ng/ml Somatostatin, 1 mU/ml TSH and 10 nM Hydrocortison. PCCL3 cells were used between passages 5 and 15. Cells were grown at 37 °C and 5 % CO_2. PCCL3 cell line was re-authenticated by mRNA expression profile of thyroid hormone markers (rTg, rTpo, rNis and rThox1).

2.2.3 Three-dimensional cultivation of PCCL3 cells

For cultivation of PCCL3 cells in a hanging drop culture, methocel medium containing Ham's F12 and methylcellulose powder was prepared. The powder (0.012g/ml) was dissolved in warm medium (50 °C) and swirled for three days at RT. Subsequently 2 ml of the methocel medium were mixed with 8 ml of normal PCCL3 medium and 400.000 PCCL3 cells. Then droplets with a total volume of 25 µl were placed on a cell culture dish and incubated upside down for 48-72 h at 37 °C and 5 % CO2. The formed spheroids in the droplets were harvested and centrifuged for 7 min at 800 rpm. After supernatant was removed, spheroids were suspended in 200 µl of warm Histogel® and placed in a Cryomold on ice. After curing, cells were fixed with Histofix® for 24 h. Subsequently cells were paraffin-embedded and analyzed by immunohistochemistry.

2.2.4 Stimulation of PCCL3 cells

For stimulation experiments, PCCL3 cells (50.000 cells/ml) were seeded in 6-well plates and were cultured for three days until they reached 70-80 % confluence. Prior to stimulation cells were starved for 72 h with medium containing Ham's F12 without serum and hormones (starvation medium). Then cells were incubated in presence of either 10 mU/ml TSH for 8 h.

2.2.5 Immunoblot

The following antibodies were used: anti-MCT8/SLC16A2 (1:1000), anti-LAT4/SLC43A2 (1:1000), anti-alpha 1 Sodium Potassium ATPase (1:1000), anti-β-Actin (1:1000), anti-Gapdh (1:1000), anti-rabbit IgG HRP-linked antibody (1:200) and anti-rabbit IgG DyLight 488 (1:5000). Whole protein lysates were extracted by RIPA-buffer. In addition, a phosphatase and protease inhibitor cocktail were added to the buffer. Lysed cells were incubated on ice for 20 min an and then centrifuged for 20 min at 4 °C and 13300 rpm. Extraced proteins were quantified by BCA protein assay. Protein fractionation was performed by using the subcellular protein fractionation kit for cultured cells. Aliquots of proteins (20 µg) were separated on an 8 % SDS-gel, blotted onto a PVDF membrane using the wet-blot technique at 4 °C overnight. Unspecific binding sides were blocked with 5 % non-fat milk or 5 % BSA for 1 h at RT. Primary antibodies were incubated overnight at 4 °C in 5 % BSA/ T-BST. Incubation of the secondary antibody was performed for 2 h at RT in 2.5 % non-fat milk/ T-BST. The visualization of the proteins was done by luminescence using the Immun-Star™ WesternC™ Kit or by fluorescence dependent on the secondary antibody. Differences in protein expression levels were quantified by densitometry using the ImageLabTM Software. Relative values of either the loading control β-Actin or Gapdh as well as Mct8 or Lat4 were calculated. The target protein values were divided by the calculated relative values of the respective control. The adjusted values were used to calculate geometric mean of the controls and target protein followed by calculation of the percent of protein level alteration.

2.2.6 Immunofluorescence

PCCL3 cells (50 000 cells/ml) were seeded on cover slides and incubated at 5 % CO_2 and 37 °C for 48 h. Cells were washed twice with phosphate buffer saline (PBS) for 5 min and then fixed with 4 % paraformaldehyde (PFA) for 15 min at RT. PFA was aspirated, cells were washed three times with PBS and were permeabilized with 0.1 % TritonTM X-10 in PBS for 10 min at RT. Blocking was performed by using 3 % BSA in PBS for 1 h at RT. Cells were washed three times with 0.1 % BSA/ PBS and a specific primary antibody against MCT8/SLC16A2 (1:1000) was diluted in 0.1% BSA/ PBS.

After incubation with the primary antibody (4°C, overnight) cells were washed six times with 0.1 % BSA/ PBS. Then, cells were incubated with the secondary antibody AlexaFluor® 488 goat anti rabbit (1:250) for 1 h at RT in 0.1 % BSA/ PBS. Cells were washed again six times with 0.1 % BSA/ PBS for 5 min and detection of the cytoskeleton was performed by incubation with Phalloidin® 555 (1:60) in 0.1% BSA/ PBS for 20 min at RT. Visualizing of the nuclei was performed with Draq5TM (1:500) for 1 h at RT. Cover slides were embedded in ImmuMount and viewed with an LSM 510 Meta confocal microscope.

2.2.7 Statistical analysis

Results of the H-Score analysis are shown as mean ± standard error of the mean (SEM). Analysis was performed by One-way ANOVA with Bonferroni's multiple comparison post-hoc test using GraphPad Prism 5 software. Expression in thyroid carcinoma samples was compared to follicular adenoma and normal thyroid tissues. Expression in Graves' disease tissues was compared to normal thyroid tissues. For immunoblot analysis Student's *t*-test was performed. Differences were considered significant if p values were: *$p<0.05$, **$p<0.01$ and ***$p<0.001$.

3 Results

3.1 TH transporter expression differs significantly between benign and malignant thyroid tumours

TH transporter expression was investigated in FA, FTC, PTC, ATC and normal thyroid tissues respectively. Plasma membrane staining was found for MCT8 and LAT4 while LAT2 showed mainly cytoplasmic localization (Fig. 28).

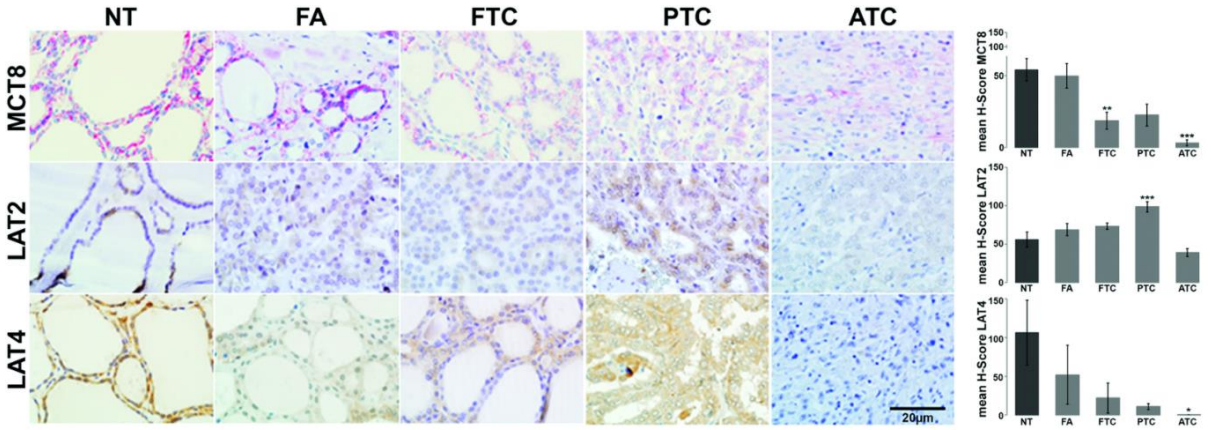

Figure 28: TH transporter expression differs significantly between benign and malignant thyroid tissue. Immunohistochemical analysis of TH transporters in normal thyroid tissue (NT), follicular adenoma (FA), follicular thyroid carcinoma (FTC), papillary thyroid carcinoma (PTC) and anaplastic thyroid carcinoma (ATC). Monocarboxylate transporter 8 (MCT8) is localized at the basolateral plasma membrane. Downregulation of MCT8 is found in thyroid carcinoma as compared to NT. L-type amino acid transporter type 2 (LAT2) is localized in the cytoplasm. LAT2 is significantly upregulated in PTC as compared to NT. LAT4 is localized in the plasma membrane and LAT4 downregulation was found in ATC as compared to NT. Immunostaining in thyroid tumours was normalized to NT. Data are presented as mean H-Scores, mean±SEM. NT: n=5 (LAT4) or n=19 (MCT8, LAT2). FA: n=5 (LAT4) or n=19 (LAT2) an n=44 (MCT8). FTC: n=5 (LAT4) or n=45 (LAT2, MCT8). PTC: n=5 (LAT4) or n=40 (LAT2, MCT8). ATC: n=5 (LAT4) or n=40 (LAT2, MCT8). Results were considered significant if **p<0.01 and ***p<0.001. One-way ANOVA with Bonferroni's multiple comparison post-hoc test was used for statistical analysis. Olympus BX51 upright microscope (scale bar: 20µm, Olympus). Representative examples are shown.

The mean H-Score of MCT8, LAT2, LAT3 and LAT4 differed between thyroid tumour entities. MCT8 was significantly downregulated in malignant thyroid tumours as compared to normal thyroid tissue. LAT2 was significantly upregulated in PTC as compared to NT. No differences in LAT2 expression were observed between FA and NT. Significant upregulation of LAT2 was found in PTC compared to NT and FA. A non-significant increase in LAT3 staining intensity was observed in FTC as compared to FA and NT. LAT4 was significantly downregulated in ATC as compared to NT, whereas LAT4 staining in other tumours revealed a more heterogenous expression pattern (Fig. 28, Table 4).

Table 4: Immunohistochemical analysis of TH transporters in normal thyroid tissues, thyroid follicular adenoma and thyroid cancers (PTC, FTC and ATC)

TH transporter	Thyroid entity	Number	Mean H-Score ± SEM
MCT8	NT	19	53.9 ± 7.8
	FA	44	49.6 ± 8.5
	FTC	45	18.6 ± 5.8
	PTC	40	22.6 ± 7.5
	ATC	40	3.3 ± 2.0
LAT2	NT	19	55.8 ± 9.7
	FA	19	68.7 ± 7.8
	FTC	45	73.3 ± 4.3
	PTC	40	98.6 ± 6.7
	ATC	40	39.1 ± 5.4
LAT4	NT	5	106.3 ± 41.6
	FA	5	52.0 ± 38.1
	FTC	5	22.0 ± 19.5
	PTC	5	11.0 ± 3.7
	ATC	5	0 ± 0

3.2 TH transporter expression is increased in hyperfunctional Graves' disease tissues

To address whether expression of TH transporters is altered in hyperfunctional thyroid tissues, immunohistochemical analysis of MCT8, LAT2, LAT3 and LAT4 was performed in Graves' disease tissues and was compared to NTs. Significantly enhanced staining was observed for MCT8, LAT2 and LAT4 in Graves' tissues. Membrane localization was confirmed for MCT8 and LAT4 while LAT2 and LAT3 were

localized in the cytoplasm (Fig. 29, Table 5).

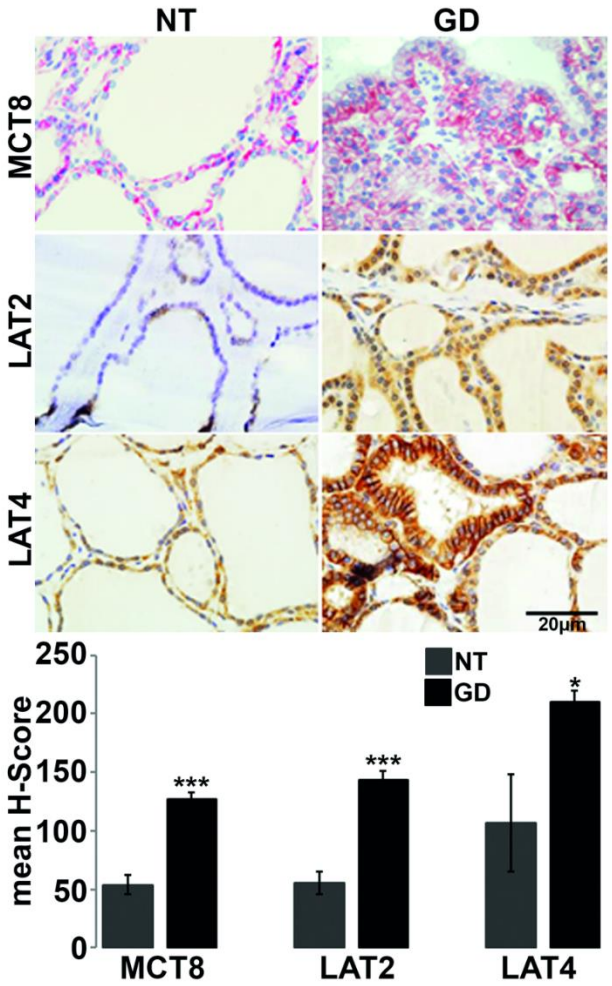

Figure 29: TH transporter expression is elevated in hyperfunctional Graves' disease tissues. Immunohistochemical analysis of TH transporter expression in normal thyroid tissues (NT) and Graves' disease (GD). SignificantUpregulation of monocarboxylate transporter 8 (MCT8), L-type amino acid transporter 2 (LAT2) and LAT4 was found in Graves disease (GD) as compared to NT. MCT8 and LAT4 show membrane localization. Expression levels in GD were normalized to NT. Data are presented as mean H-Scores, mean±SEM. NT: n=5 (LAT4) or n=19 (LAT2, MCT8). GD: n=5 (LAT4) or n=50 (LAT2, MCT8). Results were considered significant if *p<0.05, ***p<0.001. One-way ANOVA with Bonferroni's multiple comparison post-hoc test was used for statistical analysis. Olympus BX51 upright microscope (Scale bar: 20µm, Olympus). Representative samples are shown.

Table 5: Immunohistochemical analysis of TH transporter expression in Graves' disease tissues

TH transporter	Thyroid entity	Number	Mean H-Score ± SEM
MCT8	NT	19	53.9 ± 7.8
	GD	50	126.6 ± 6.5
LAT2	NT	19	55.8 ± 9.7
	GD	50	143.5 ± 7.7
LAT4	NT	5	106.3 ± 41.6
	GD	5	210.0 ± 10.0

3.3 MCT8 expression in rat thyroid cells is upregulated by TSH stimulation

To investigate which pathways may contribute to TH transporter expression, we performed in vitro experiments in rat thyroid PCCL3 cells and focused on MCT8, LAT2 and LAT4 because these TH transporters showed distinct expression patterns for hyperfunctional thyroid tissues and/ or malignant thyroid tumours. MCT8 expression and localization was determined in PCCL3 cells using western blot analysis, immunofluorescence and immunocytochemistry. Western blot analysis showed MCT8 expression at the plasma membrane (Fig. 30).

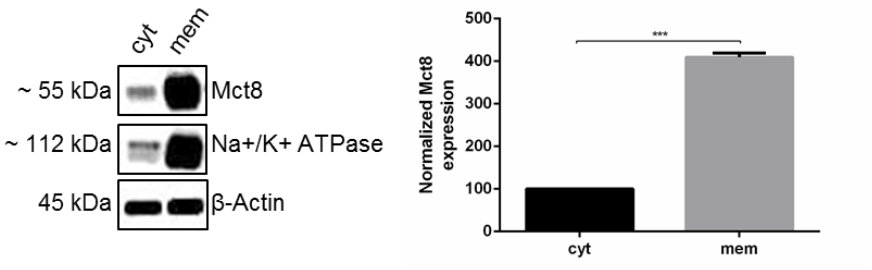

Figure 30: MCT8 is mainly located at the plasma membrane after protein fractionation. Western blot analysis showed predominant localization of MCT8 at the plasma membrane.Na+/K+ ATPase war used as control for the membrane fraction. β-actin was used as loading control.

By immunofluorescence, MCT8 was mainly located at the plasma membrane (Fig. 31A). Immunohistochemistry of a hanging drop culture of PCCL3 cells revealed exclusive membrane staining of MCT8 in PCCL3 cells (Fig. 31B).

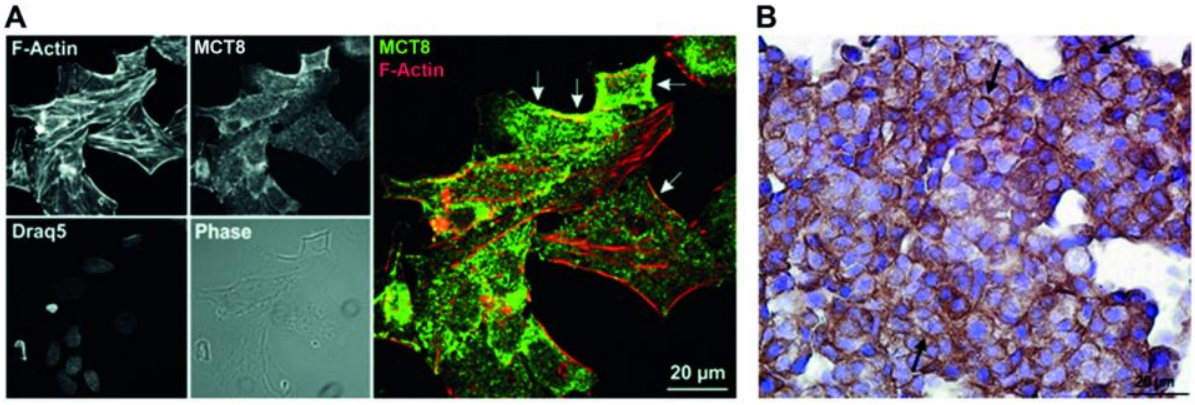

Figure 31: MCT8 is predominantly located at the plasma membrane of PCCL3 cells. A) PCCL3 cells with predominant monocarboxylate transporter 8 (MCT8, green) localization at the plasma membrane (highlighted by arrows) by immuno-fluorescence. Detection of nuclear DNA was performed with Draq5 (blue), while the F-Actin cytoskeleton was visualized by Alexa 555-coupled Phalloidin staining (red). Microscopy was performed with confocal microscopy using the LSM510 (Zeiss, Germany). B) Immunocytochemical analysis of Mct8 in PCCL3 cells. MCT8 is located in the plasma membrane of the PCCL3 cells. Olympus BX51 upright microscope (60x, Olympus, Germany). Scale bar: 20 µm, n=3. Representative samples are shown.

Since hyperthyroidism, i.e. due to Graves' disease, involves augmentation of cyclic adenosine monophosphate (cAMP) signaling, we asked whether TSH stimulation impacts TH transporter expression in PCCL3 cells. MCT8 protein expression was significantly upregulated after 8 hours of TSH stimulation (Fig. 32A). Notably investigation of LAT2 and LAT4 expression in PCCL3 cells under TSH stimulation demonstrated that neither LAT2 nor LAT4 expression levels were altered by TSH stimulation of PCCL3 cells. These in vitro data suggest TSH-dependent regulation of MCT8 but not other investigated transporters in thyroid tissues (Fig. 32B,C).

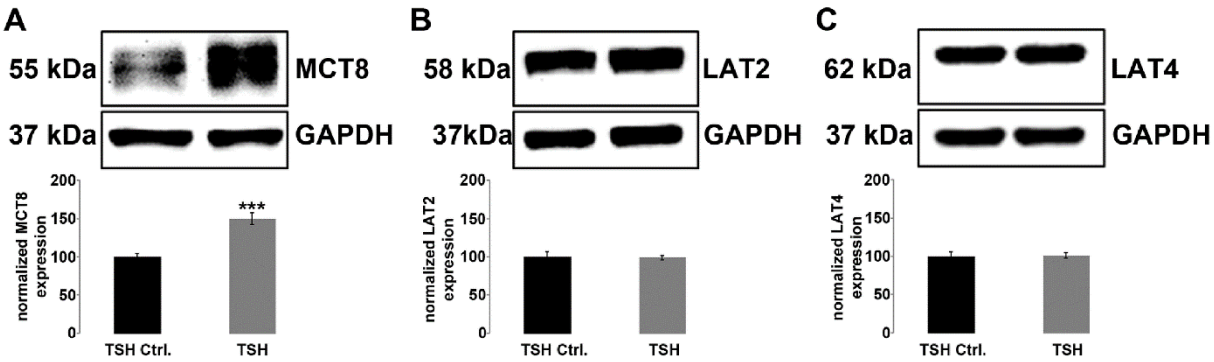

Figure 32: MCT8 expression is regulated by TSH stimulation in PCCL3 cells. Immunoblot analysis of PCCL3 cells after stimulation with thyroid stimulating hormone (TSH, 1mU/ml) for 8 h at 37 °C. A) Significant upregulation of monocarboxylate transporter 8 (MCT8) after TSH stimulation. B) No differences in L-type amino acid transporter type 2 (LAT2) expression by TSH stimulation of PCCl3 cells. C) No differences in LAT4 expression by TSH stimulation of PCCL3 cells. Representative samples are shown. Data are represented as mean ± SEM of three independent experiments, Student's t-test, ***p<0.001.

4 Discussion

Here, we asked whether TH transporter expression in human thyroid tissues is linked to morphology and functional tissue status, which to our knowledge has not been investigated in detail so far. For immunohistochemistry analysis we employed a large series of 238 thyroid tissues, comprising NTs, FA, FTC, PTC ATC and Graves' disease tissues and used a semi-quantitative scoring system to covert expert, but still subjective perception of protein expression into quantitative data which can be used for statistical analysis. The H-Score scoring system is a reproducible scoring system which is applied by pathologists for routine immuno-analysis of human tissue specimen (Detre *et al*., 1995; Potts *et al*., 2012; Mazières *et al*., 2013; Ting *et al*., 2013).

First, we addressed MCT8 since it is the most specific and best investigated thyroid hormone transporter. By immunohistochemistry, we found moderate plasma membrane staining for MCT8 in human thyroid tissue samples. Furthermore, we observed downregulation of MCT8 in thyroid cancers (FTC, PTC and ATC) compared to normal thyroid tissue. Our results on the mRNA expression profile of MCT8 could confirm these results showing also a significant downregulation of MCT8 in FTC and PTC as compared to FA. Since MCT8 has been shown to play a role in TH export from thyroid follicles, this is in line with decrease in efficient TH synthesis as known for thyroid cancers (Krause *et al*., 2007) and thyroid cancers. Hence MCT8 could represent a suitable marker of thyroid differentiation. A potential role for MCT8 and alteration of TH intra-thyroidial tissue states has been discussed on the basis of a case report of papillary thyroid cancer diagnosed in a patient with MCT8 deficiency and the finding of papillary thyroid structures in the *Mct8* knock-out mouse model at 600 d of age (Wirth *et al*., 2011). Studies using mice with a global deficiency in MCT8, and those doubly deficient in MCT8 and related MCT10, revealed a molecular mechanistic explanation for such auto-thyrotoxic states (Weber *et al*., 2017). Thus altered TH transport capabilities of thyrocytes due to lacking MCT8 and/or MCT10, thyroglobulin storage affects and may enhance utilization of thyroglobulin for TH liberation (Weber *et al*., 2017), thereby resulting in increased intra-thyroidal TH levels (Muller and Heuer, 2014). The pivotal role of MCT8 in thyroid hormone synthesis and release is also illustrated in our analysis of Graves' tissues showing markedly increased MCT8 transporter expression, consistent with a functional role of MCT8 in augumented TH

release in hyperthyroidism. Furthermore, MCT8 expression is upregulated by TSH stimulation shown in our *in vitro* experiments in PCCL3 cells suggesting a cAMP dependent upregulation of MCT8 consistent with other proteins relevant for efficient thyroid hormone synthesis including the sodium iodide symporter (NIS) (Ohno *et al*., 1999). We also addressed the localization pattern of MCT8 in the rat thyroid cell line PCCL3. Results obtained by confocal microscopy of immuno-stained PCCL3 cells are in agreement with immunohistochemically studies of human tissue samples in that TH transporter are localized in cytoplasmic structures and at the cell surface between neighbouring cells, i.e. at the basolateral plasma membrane domain of thyrocytes.

Interestingly, a similar regulation pattern as for MCT8 was found for the thyroid hormone transporter LAT4 *in vitro* and *in vivo*. Although previous studies suggest that LAT4 does not function as a transporter of classical TH T3 and T4 (Zevenbergen *et al*., 2015), LAT4 expression patterns in GD tissues strongly suggest that this TH transporter contributes to adaption of thyroidal TH homeostasis in hyperthyroidism if not exerting a functional role in TH release. In contrast to TSH-dependent upregulation of MCT8 in PCCL3 cells, LAT4 protein level was not altered by TSH. Therefore, LAT4 downregulation in ATC as well as upregulation in GD tissues might hint to other functional roles of this transporter, e.g. amino acid rather than TH transport.

LAT2 immunostaining of human thyroid specimen revealed a heterogenous expression pattern. Thus, for LAT2 we found moderate staining mainly in the cytoplasm. Normally, plasma membrane localization would be expected for TH transporters exporting TH from thyrocytes (McInnes et al., 2013; Weber et al., 2013). However, in our series LAT2 was mainly located in cytoplasmic structures, presumably in vesicles of the endocytic pathway, which might be linked to the hypothesis of an endo-lysosomal functioning property of LAT2 in the thyroid (K. Brix, personal communication). Quantification of immunohistochemical analysis showed a significant upregulation of LAT2 in PTC as compared to NT. Likewise, in Graves' disease, we found significant upregulation for LAT2. Thus, expression pattern of LAT2 observed in the different tissues are more likely reflecting other transporter properties of LAT2. In accordance, TSH stimulation of PCCL3 cells did not affect LAT2 expression.

In summary, we observed a gradual downregulation of MCT8 in FA and thyroid carcinomas (FTC, PTC, ATC) which would be in agreement with the activation of other signaling pathways over cAMP dependent maintenance of thyroid cell differentiation during thyroid carcinogenesis. Additionally, upregulation of TH transporter MCT8 in hyperfunctioning Graves' disease tissues is TSH-dependent and consistent with its proposed role in TH release.

In conclusion, MCT8 represents as a novel thyroid differentiation marker and could be involved in excessive TH supply in states of hyperthyroidism, thereby contributing to disease manifestation.

5 References

Babu E, Kanai Y, Chairoungdua A, Kim DK, Iribe Y, Tangtrongsup S, Jutabha P, Li Y, Ahmed N, Sakamoto S, Anzai N, Nagamori S, Endou H 2003 Identification of a novel system L amino acid transporter structurally distinct from heterodimeric amino acid transporters. *The Journal of biological chemistry* **278** 43838–43845.

Bodoy S, Martín L, Zorzano A, Palacín M, Estévez R, Bertran J 2005 Identification of LAT4, a novel amino acid transporter with system L activity. *The Journal of biological chemistry* **280** 12002–12011.

Chan SY, Franklyn JA, Pemberton HN, Bulmer JN, Visser TJ, McCabe CJ, Kilby MD 2006 Monocarboxylate transporter 8 expression in the human placenta: the effects of severe intrauterine growth restriction. *The Journal of endocrinology* **189** 465–471.

Detre S, Saclani Jotti G, Dowsett M 1995 A "quickscore" method for immunohistochemical semiquantitation: validation for oestrogen receptor in breast carcinomas. *Journal of clinical pathology* **48** 876–878.

Di Cosmo C, Liao XH, Dumitrescu AM, Philp NJ, Weiss RE, Refetoff S 2010 Mice deficient in MCT8 reveal a mechanism regulating thyroid hormone secretion. *The Journal of clinical investigation* **120** 3377–3388.

Friesema Edith CH, Ganguly S, Abdalla A, Manning Fox Jocelyn E, Halestrap AP, Visser TJ 2003 Identification of monocarboxylate transporter 8 as a specific thyroid hormone transporter. *The Journal of biological chemistry* **278** 40128–40135.

Friesema Edith CH, Kuiper George GJM, Jansen J, Visser TJ, Kester Monique HA 2006 Thyroid hormone transport by the human monocarboxylate transporter 8 and its rate-limiting role in intracellular metabolism. *Molecular endocrinology (Baltimore, Md.)* **20** 2761–2772.

Fusco A, Berlingieri MT, Di Fiore PP, Portella G, Grieco M, Vecchio G 1987 One- and two-step transformations of rat thyroid epithelial cells by retroviral oncogenes. *Molecular and cellular biology* **7** 3365–3370.

Haase C, Bergmann R, Fuechtner F, Hoepping A, Pietzsch J 2007 L-type amino acid transporters LAT1 and LAT4 in cancer: uptake of 3-O-methyl-6-18F-fluoro-L-dopa in human adenocarcinoma and squamous cell carcinoma in vitro and in vivo.

Journal of nuclear medicine : official publication, Society of Nuclear Medicine **48** 2063–2071.

Kinne A, Kleinau G, Hoefig CS, Grüters A, Köhrle J, Krause G, Schweizer U 2010 Essential molecular determinants for thyroid hormone transport and first structural implications for monocarboxylate transporter 8. *The Journal of biological chemistry* **285** 28054–28063.

Kinne A, Schülein R, Krause G 2011 Primary and secondary thyroid hormone transporters. *Thyroid research* **4** 7.

Krause K, Karger S, Schierhorn A, Poncin S, Many M-C, Fuhrer D 2007 Proteomic profiling of cold thyroid nodules. *Endocrinology* **148** 1754–63.

Mazières J, Brugger W, Cappuzzo F, Middel P, Frosch A, Bara I, Klingelschmitt G, Klughammer B 2013 Evaluation of EGFR protein expression by immunohistochemistry using H-score and the magnification rule: re-analysis of the SATURN study. *Lung cancer (Amsterdam, Netherlands)* **82** 231–237.

McInnes J, Weber J, Rehders M, Saftig P, Peters C, Reinheckel T, Schweizer U, Heuer H, Wirth EK and Brix K 2013 Correlation of the expression and localization of thyroid hormone transporters with thyroglobulin processing cathepsins in mouse thyroid epithelial cells. In *37th Annual Meeting of the European Thyroid Association* pp 75-194.

Muller J and Heuer H 2014 Expression pattern of thyroid hormone transporters in the postnatal mouse brain. *Frontiers in Endocrinology* **5** 92.

Ohno M, Zannini M, Levy O, Carrasco N, Di Lauro R 1999 The paired-domain transcription factor Pax8 binds to the upstream enhancer of the rat sodium/iodide symporter gene and participates in both thyroid-specific and cyclic-AMP-dependent transcription. *Molecular and cellular biology* **19** 2051–60.

Potts SJ, Krueger JS, Landis ND, Eberhard DA, Young GD, Schmechel SC, Lange H 2012 Evaluating tumor heterogeneity in immunohistochemistry-stained breast cancer tissue*. Laboratory investigation; a journal of technical methods and pathology* **92** 1342–1357.

Ting S, Mairinger FD, Hager T, Welter S, Eberhardt WE, Wohlschlaeger J, Schmid KW, Christoph DC 2013 ERCC1, MLH1, MSH2, MSH6, and βIII-tubulin: resistance proteins associated with response and outcome to platinum-based

chemotherapy in malignant pleural mesothelioma. *Clinical lung cancer* **14** 558-567.

Visser WE, Friesema Edith CH, Jansen J, Visser TJ 2008 Thyroid hormone transport in and out of cells. *Trends in endocrinology and metabolism: TEM* **19** 50–56.

Wagner CA, Lang F, Bröer S 2001 Function and structure of heterodimeric amino acid transporters. American journal of physiology. *Cell physiology* **281** C1077-93.

Weber J, Rehders M, Saftig P, Verrey F, Schweizer U, Wirth EK, Heuer H and Brix K 2015 Functional analysis of the angio-follicular unit of the mouse gland. *Experimental and Clinical Endocrinology and Diabetes* pp 12-13.

Weber J, McInnes J, Kizilirmak C, Rehders M, Qatato M, Wirth EK, Schweizer U, Verrey F, Heuer H and Brix K 2017 Interdependence of thyroglobulin processing and thyroid hormone export in the mouse thyroid gland. *European Journal of Cell Biology* **96** 440-456.

Wirth EK, Sheu SY, Chiu-Ugalde J, Sapin R, Klein MO, Mossbrugger I, Quintanilla-Martinez L, de Angelis Martin Hrabě, Krude H, Riebel T, Rothe K, Köhrle J, Schmid KW, Schweizer U, Grüters A 2011 Monocarboxylate transporter 8 deficiency: altered thyroid morphology and persistent high triiodothyronine/thyroxine ratio after thyroidectomy. *European journal of endocrinology / European Federation of Endocrine Societies* **165** 555–561.

Zevenbergen C, Meima ME, Lima de Souza Elaine C, Peeters RP, Kinne A, Krause G, Visser WE, Visser TJ 2015 Transport of Iodothyronines by Human L-Type Amino Acid Transporters. *Endocrinology* **156** 4345–4355.

Chapter 5: Conclusion

The present thesis explores potential prognostic markers of thyroid cancers and tried to clarify their impact and association with tumour biology.

We investigated the protein DJ-1 which was described as a putative oncogene and as a novel prognostic marker in breast cancer. Due to this we hypothesized that DJ-1 may play an essential role in tumourigenesis and especially in FTC tumourigenesis.

We found a significantly stronger expression of DJ-1 in FTC as compared to FA. Our findings obtained in human thyroid tumours may help to better distinguish between benign and malignant follicular thyroid tumours using DJ-1. To this, it will be necessary to raise the number of FTC and FA samples and also to reproduce the findings in other cohorts from different countries. Moreover, our data are lacking the clinical course. Due to this we were not able to correlate our obtained data with TNM stage, treatment or clinical outcome. Furthermore, we were not able to investigate DJ-1 expression in FTC metastases for lack of tissue.

Additionally, we investigated the impact of DJ-1 on follicular thyroid carcinogenesis *in vitro*. Therefore, we stably transfected PCCL3 cells as well as FTC-133 cells with EV, DJ-1, RASV12 and PPFP or co-transfected PCCL3 cells or FTC-133 cells with DJ-1-RASV12 and DJ-1-PPFP. We found an additive effect of DJ-1 which was most pronounced with the oncogene RASV12 but not with PPFP.

We investigated the tight junction protein claudin-1 and were able to show that the modulation of claudin-1 influences the behaviour of FTC. Thereby, claudin-1 has an impact on follicular thyroid aggressiveness. So, we presume that claudin-1 might be used as a prognostic marker for the clinical course and outcome of thyroid cancer especially of follicular thyroid cancer as proposed for DJ-1. However, this hypothesis requires confirmation in other cohorts.

To investigate the impact of DJ-1 and claudin-1 on follicular thyroid cancer behaviour we used a mix of 2D (scratch assay, trans-well migration) and 3D (trans-well invasion) *in vitro* assays. 2D-assays lack the architectural and cellular complexity of tumours *in vivo* (Palm *et al*., 2005). The use of 3D-assays may thus provide more insights into the metastatic (aggressive) potential of cells. We used the *in vitro* scratch assay to

investigate migration of our cells. One key limitation of the scratch assay is, that scratching may physically damage the cells adjacent to the wound (Pouliot *et al*., 2013). So, the cell exclusion assay (Ocris™ cell migration assay, Platypus Technologies) which uses silicon stoppers, instead of a physical scratch, would be a method to confirm scratch assay results due to the fact that the removal of the silicon stoppers does not damage the cell surface. A mechanical damage would clarify the discrepant results between trans-well migration and scratch assay performed for DJ-1, RASV12 and PPFP overexpressing as well as DJ-1-RASV12 and DJ-1-PPFP co-transfected PCCL3 cells.

Cell migration is not independent from the environment, so the use of 3D *in vitro* models may better reflect the microenvironment of a tumour. Here, we used the trans-well invasion assay for investigation. We used matrigel as extracellular matrix (ECM) but other matrices e.g. natural basement membrane extracts (human amniotic membranes, chick chorioallantoic membranes) are also possible. Using this kind of invasion assays is a very rapid and low cost alternative to animal experiments. Due to the discrepant results between trans-well migration and trans-well invasion in PCCL3 cells and in parts also in FTC-133 cells, the use of other 3D invasion assays may be of interest. Within this alternative assay cells are layered in between two collagen gels and the quantification will be performed by microscopy simply by measuring the distance of migration from the center line into the gels. This technique has especially the advantage that the cells can be visualized in a 3D matrix without the need to cross the porous membrane like in our trans-well invasion assay (Brekhman *et al*., 2009). However, 2D *in vitro* models remain the preferred option for high throughput drug screening. Thus, one could use such high throughput 2D migration assays to test the effect of different tyrosine kinase inhibitors or anti-thyroid agents on cell migration of DJ-1 or claudin-1 overexpressing cells.

Moreover, to transfer our *in vitro* data to the human system it is necessary to investigate the metastatic potential of DJ-1 as well as claudin-1 also in *in vivo* experiments. To this aim, a mouse model can be used (Reeb et al., 2016).

Next, we asked whether the expression of thyroid hormone transporters is changed with dedifferentiation and alteration of thyroid function. Therefore, we investigated a

large series of thyroid tumours (N=238) and found a significant downregulation of MCT8 protein expression in thyroid cancers allocating MCT8 a role as a thyroid differentiation marker.

We were glad to investigate such a large series of thyroid tumours and to obtain interesting results. However, data on clinical outcome were lacking. It would have been interesting to investigate the correlation between thyroid hormone transporter expression and TNM stage, age and sex. Moreover, other TH transporter are known, which however are difficult to investigate due to lack of specific antibodies.

Furthermore, we investigated the expression pattern of thyroid hormone transporters in hyperfunctioning Graves' disease tissue and found significantly increased protein expression of TH transporters MCT8, LAT2 and LAT4. *In vitro* we were able to confirm the elevated protein expression levels of Mct8 after TSH stimulation also indicating a cAMP dependent regulation of Mct8. It will be interesting to perform other stimulation experiments e.g. epidermal growth factor (EGF) or other substances which trigger tumour growth, to observe how Mct8 expression is altered and to transfer *in vitro* data to the human thyroid tumours.

Taken together we demonstrated that DJ-1 and claudin-1 influence tumour biology in FTC and that the specific TH transporter MCT8 qualifies as a new thyroid differentiation marker.

References

Brekhman, Vera; Neufeld, Gera 2009 A novel asymmetric 3D in-vitro assay for the study of tumor cell invasion. *BMC Cancer* **9** 415-427.

Palm D, Lang K, Brandt B, Zaenker KS, Entschladen F 2005 In vitro and in vivo imaging of cell migration: two interdepending methods to unravel metastasis formation. *Seminars in cancer biology* **5** 396-404.

Pouliot N, Pearson HB and Burrows A 2013 Investigating Metastasis Using In Vitro Platforms. *Metastatic Cancer: Clinical and Biological Perspectives.*Madame Curie Bioscience Database. http://www.ncbi.nlm.nih.gov/books/NBK100379/.

Reeb AN, Ziegler A and Lin RY 2016 Characterization of human follicular cancer cell lines in preclinical mouse models. *Endocrine Connections* **5** 47-54.

Appendix

A) Summary

Chapter 1:

The thyroid is an endocrine gland and thyroid hormones play a huge role in metabolism and growth. Thyroid hormones are essential for a lot of processes in the human body and required for normal function of nearly all tissues. The most important thyroid hormones are triiodothyronine (T3) and thyroxine (T4). Thyroid dysfunction is very common and can be characterized by an overactive (hyperthyroidism) or an underactive (hypothyroidism) thyroid. Thyroid carcinomas can be divided into those with a C-cell differentiation (MTC) and those with a follicle cell differentiation (FTC, PTC, PDTC and ATC). Somatic mutations implicated either in the PI3K- or MAPK pathway occur with a high frequency in thyroid carcinomas but it is still unclear which mechanism influences tumour biology. Moreover, we are unable to distinguish between a benign follicular adenoma and a malignant thyroid carcinoma using cytology.

Here we investigated the putative oncogene DJ-1 and the tight junction protein claudin-1 for their role in tumour biology. We analyzed their expression immunohistochemically in different thyroid tumours and performed *in vitro* experiments to learn more about their function in FTC tumour biology. Moreover, we addressed thyroid hormone transporter expression in thyroid tumours as well in hyperfunctioning tissues.

Chapter 2:

Follicular thyroid carcinoma (FTC) is the second most common thyroid malignancy. It is yet unclear, whether FTC evolves sequentially or distinctly from follicular adenoma (FA) and both RAS mutations and PAX8/PPARγ rearrangements have been reported in benign and malignant follicular thyroid tumours. Previously, we reported an increased expression of the protein DJ-1 in FTC. Here, we investigated whether DJ-1 has oncogenic potential due to the PI3K pathway and might thus play a role in FTC tumourigenesis. Gene and protein expression of DJ-1 were determined by qRT-PCR and immunohistochemistry in 116 thyroid specimen including 27 normal thyroid (NT) tissue, 44 FA and 45 FTC. Functional consequences of DJ-1 overexpression were

investigated in human follicular thyroid carcinoma cells (FTC-133) with and without *DJ-1* knockdown and rat follicular thyroid cells (PCCL3) as well as FTC-133 cells with DJ-1 overexpression or combined expression of DJ-1 with thyroid oncogenes RASV12 and PAX8/PPARγ. Activation of thyroid signaling pathways was investigated by immunoblot. In human FTC tissues, DJ-1 mRNA and protein levels were increased compared to NT and FA. Knockdown of *DJ-1* in FTC-133 cells let to reduced migration and invasion capacity. DJ-1 overexpression in PCCL3 cells resulted in higher proliferation and increased migration rate. DJ-1-RASV12 co-expressing PCCL3 cells showed higher tumourigenicity as compared to DJ-1 PCCL3 cells, while no such effect was seen for DJ-1-PAX8/PPARγ PCCL3 cells. Higher protein expression of pAkt was found in DJ-1 overexpressing PCCL3 cells while expression levels of pAkt and pP70S6K were diminished. DJ-1 overexpression in FTC-133 cells resulted in a higher proliferation rate as compared to the EV and other overexpressing cells. Also migration of DJ-1 overexpressing cells was enhanced as compared to the EV transfected cells. Our data suggest that DJ-1 is an additive factor in follicular carcinogenesis contributing to tumour aggressiveness.

Chapter 3:

Claudin-1 belongs to the family of transmembrane tight junction proteins tightening the paracellular cleft of epithelial cells. In human malignancies, claudin-1 is often dysregulated and located in subcellular compartments, particularly in the nucleus where it may influence cellular behaviour. Here, we studied claudin-1 in relation to the biological characteristics of follicular thyroid carcinoma (FTC). Claudin-1 immuno-staining showed loss of membrane expression and increased nuclear claudin-1 localization in FTC metastases. claudin-1 function was further investigated in two different follicular thyroid carcinoma cell lines: FTC-133 isolated from a regional lymph node metastasis and FTC-238 derived from a lung metastasis. In both cell lines claudin-1 expression was demonstrated in the cell nuclei with a significantly higher protein expression in FTC-238 compared to FTC-133 cells. Interestingly, in vitro scratch assay revealed enriched nuclear claudin-1 expression near the scratch. Furthermore, the increase of the pathogenic character of FTC-133 cells by RASV12 transfection was associated with elevated claudin-1 expression and enhanced cell

migration, invasion and proliferation. Likewise over-expression of nuclear claudin-1 in FTC-133 cells resulted in increased cell migration and invasion. Conversely, claudin-1 downregulation in FTC-238 cells by siRNA resulted in decreased cell migration and invasion and was accompanied by reduced phosphoPKC expression. Moreover, activation and inhibition of PKC resulted in claudin-1 up- and downregulation in FTC cells respectively. These data suggest an impact of claudin-1 on follicular thyroid carcinoma aggressiveness, which could potentially be influenced by PKC activity.

Chapter 4:

Influx and efflux of thyroid hormones (TH) into tissues is facilitated by TH transporters, which are also expressed in the thyroid and may play a role in thyroid hormone release. The physiologically most studied and TH-selective TH transporter is the monocarboxylate transporter 8 (MCT8), whereas the L-type amino acid transporters LAT2 and LAT4 also transport other substances. We asked whether expression of TH transporters is changed with thyroid dedifferentiation and alteration of thyroid function. Protein expression and localization of TH transporters was determined by immunohistochemistry in normal thyroid tissues (NT, n=19), follicular adenoma (FA, n=44), follicular thyroid carcinoma (FTC, n=45), papillary thyroid carcinoma (PTC, n=40), anaplastic thyroid carcinoma (ATC, n=40) and Graves' disease tissues (GD, n=50). Staining intensities were evaluated by calculating the 'hybrid' (H) score. Furthermore, regulation of Mct8 expression and localization was investigated in the rat follicular thyroid cell line PCCL3 under basal and stimulation conditions (TSH). In thyroid tissues MCT8 was localized in the plasma membrane, while LAT transporters showed cytoplasmatic localization. MCT8 expression was downregulated in benign and malignant thyroid cancers as compared to normal thyroid tissue. In contrast, significant upregulation of MCT8, LAT2 and LAT4 was found in hyperfunctioning Graves' tissues. Furthermore, a stronger expression of Mct8 was demonstrated in PCCL3 cells after TSH stimulation. Downregulation of MCT8 in thyroid cancers qualifies MCT8 as a marker of thyroid differentiation. The more variable expression of LATs in distinct thyroid malignancies may be linked with other transporter properties e.g. amino acid transport rather than TH efflux. The consistent strong upregulation of the TH transporters in Graves' disease may functionally be linked to the increased TH-

release in hyperthyroidism, an assumption supported by the in vitro results indicating upregulation of Mct8 through a cAMP dependent signalling pathway.

B) Zusammenfassung

Kapitel 1:

Die Schilddrüse ist eine endokrine Drüse und Schilddrüsenhormone spielen eine sehr wichtige Rolle im Stoffwechsel und beim Wachstum. Schilddrüsenhormone sind für viele Prozesse im menschlichen Körper wichtig und werden von nahezu allen Geweben und Organen benötigt. Die wichtigsten Schilddrüsenhormone sind das Trijodthyronin (T_3) und das Thyroxin (T_4). Fehlfunktionen der Schilddrüse kommen sehr häufig vor und können durch eine Überfunktion (Hyperthyreose) oder Unterfunktion (Hypothyreose) charakterisiert sein. Bösartige Schilddrüsentumore können in Tumore mit einer C-Zell-Differenzierung (MTC) oder in Tumore mit einer Follikel-Zell-Differenzierung (FTC, PTC, PDTC und ATC) unterteilt werden. Somatische Mutationen in SD-Karzinomen finden sich vorallem im PI3K- oder MAPK Signalweg. Allerdings ist immer noch unklar, welche Mechanismen die Tumorbiologie beeinflussen. Außerdem sind wir immer noch nicht in der Lage ein gutartiges follikuläres Adenom von einem bösartigen follikulären Karzinom zytologisch zu unterscheiden.

Wir haben hier das putative Onkogen DJ-1 und das Tight Junction Protein Claudin-1 untersucht, da beide eine Rolle in der Tumorbiologie bei anderen Malignomen spielen. Wir haben ihre Expression mit Hilfe der Immunhistochemie in verschiedenen Schilddrüsentumoren untersucht und *in vitro* Experimente durchgeführt, um mehr über ihre Funktion in der Tumorbiologie zu erfahren. Zudem haben wir uns mit verschiedenen Schilddrüsenhormontransportern befasst und deren Expression in Schilddrüsentumoren und hyperfunktionellem Gewebe (Morbus Basedow) untersucht.

Kapitel 2:

Das follikuläre Schilddrüsenkarzinom (FTC) ist das zweithäufigste SD-Malignom. Es ist jedoch unklar, ob sich ein FTC sequenziell oder direkt aus einem follikulärem Adenom (FA) entwickelt und sowohl RAS-Mutationen als auch PAX8/PPARγ Rearrangements wurde in gutartigen sowie bösartigen follikulären Schilddrüsentumoren beschrieben. Eine erhöhte Expression des Proteins DJ-1 in FTC konnten wir bereits in früheren Untersuchungen zeigen. In dieser Arbeit haben wir untersucht, ob DJ-1 onkogenes Potenzial besitzt und ob DJ-1 eine Rolle in der

Enstehung eines FTC spielt. Die Gen- und Proteinexpressionsanalysen wurden mit Hilfe von qRT-PCR und Immunhistochemie von insgesamt 116 Schilddrüsenproben, darunter 27 normale Schilddrüsen (NT), 44 FA und 45 FTC Proben, untersucht. Die Folgen einer DJ-1 Überexpression wurden in menschlichen follikulären Schilddrüsenkarzinomzellen (FTC-133) mit und ohne DJ-1 Herrunterregulation und in Ratten Schilddrüsenzellen (PCCL3) und humanen Schilddrüsenkarzinomzellen (FTC-133) mit DJ-1 Überexpression oder kombinierte Expression von DJ-1 mit den Onkogenen RASV12 und PAX8/PPARγ untersucht. Die Aktivierung von Schilddrüsensignalwegen wurde mit Hilfe des Immunblots untersucht.
Wir konnten eine deutlich erhöhte Gen- und Proteinexpression von DJ-1 in den FTC Proben, im Vergleich zu FA und NT, finden. Die Herruntergregulation von DJ-1 in FTC-133 Zellen führt zu einer Verminderung des Migrations- und Invasionspotenzials. Eine Überexpression von DJ-1 in PCCL3 Zellen dagegen, führte zu einer erhöhten Proliferations- und Migrationsrate. DJ-1-RASV12 co-exprimierenden PCCL3 Zellen zeigten eine höhere Tumorigenität im Vergleich zu DJ-1 überexprimierenden Zellen, während eine solche Wirkung für DJ-1-PAX8/PPARγ co-exprimierende Zellen nicht bestätigt werden konnte. Unsere Daten deuten demnach darauf hin, dass DJ-1 als zusätzlicher Faktor in der Karzinogenese eines FTC wirkt und außerdem zur Tumoraggressivität beiträgt.

Kapitel 3:
Claudin-1 gehört zur Familie der transmembranen Tight Junction Proteine, welche die parazelluläre Spalte von Epithelzellen abdichten. Bei bösartigen Erkrankungen ist Claudin-1 oft anders reguliert und in subzellulären Kompartimenten angeordnet, insbesondere im Zellkern wo es das zelluläre Verhalten beeinflussen kann. Wir haben Claudin-1 im Bezug auf die biologischen Eigenschaften eines follikulären Schilddrüsenkarzinom (FTC) untersucht.
Immunhistochemische Färbungen von Claudin-1 zeigten den Verlust der Membranexpression und eine gesteigerte Kernexpression in FTC Metastasen. Die Funktion von Claudin-1 wurde in zwei verschiedenen follikulären Schilddrüsenkarzinom Zelllinien untersucht: FTC-133 Zellen welche von einer regionalen Lymphknoten Metastase stammen und FTC-238 Zellen welche aus einer Lungenmetastase isoliert wurden. In beiden Zelllinien wurde Claudin-1 im Zellkern

gefunden, wobei eine signifikant erhöhte claudin-1 Expression in FTC-238 Zellen im Vergleich zu FTC-133 Zellen gezeigt werden konnte. Interessanterweise, konnten wir *in vitro* zeigen, dass Claudin-1 verstärkt im Bereich der Wunde nach dem sogenannten Scratch Assay exprimiert wurde. Außerdem wurde eine Zunahme des pathogenen Charakters von FTC-133 Zellen, transfiziert mit RASV12, in Bezug auf eine gesteigerte Claudin-1 Expression sowie ehöhte Zellmigration, Invasion und Proliferation beobachtet. Auch eine Überexpression von Claudin-1 im Kern von FTC-133 Zellen führte zu einer erhöhten Zellmigration und Invasion. Im Gegensatz dazu zeigte die Transfektion mit Claudin-1 siRNA in FTC-238 Zellen eine verringerten Zellmigration und Invasion und wurde von einer reduzierten phosphoPKC Expression begleitet. Darüberhinaus führte eine Aktivierung der PKC zu einer erhöhten Claudin-1 Expression, während eine Inhibition der PKC zu einer verringerten Expression von Claudin-1 in FTC-133 Zellen führte.
Diese Daten deuten darauf hin, dass Claudin-1 einen Einfluss auf die follikuläre Schilddrüsenkarzinomaggressivität hat, welche potenziell von der PKC Aktivität beeinflusst werden könnte.

Kapitel 4:
Der In- und Efflux von Schilddrüsenhormonen in verschiedene Gewebe wird durch Schilddrüsenhormontransporter erleichtert. Diese werden auch in der Schilddrüse exprimiert und spielen eine Rolle bei der Freisetzung von Schilddrüsenhormonen. Der physiologisch am besten untersuchte und selektivste Transporter ist der Monocarboxylattransporter 8 (MCT8), während die L-Typ Aminosäure Transporter LAT2, LAT3 und LAT4 auch andere Stoffe, wie Aminosäuren, transportieren. Wir haben uns gefragt, ob sich die Expression von Schilddrüsenhormontransportern mit der Schilddrüsendifferenzierung und Veränderung der Schilddrüsenfunktion ändert.
Die Proteinexpression und Lokalisation von Schilddrüsenhormontransportern wurde mit Hilfe von Immunhistochemie in Proben von normalem Schilddrüsengewebe (NT, n = 19), follikulärem Adenom (FA, n = 44), follikulärem Schilddrüsenkarzinom (FTC, n = 45), papillärem Schilddrüsenkarzinom (PTC, n = 40), anaplastischem Schilddrüsenkarzinom (ATC, n = 40) und Schilddrüsen mit Morbus Basedow (GD, n = 50) untersucht. Färbeintensitäten wurden durch die Berechnung des „H-Score“

bewertet. Des Weiteren wurde die Regulation sowie Expression und Lokalisation von MCT8 in einer follikulären Rattenschilddrüsenzelllinie (PCCL3) unter basalen und Stimulationsbedigungen untersucht (TSH).

Der Transporter MCT8 wurde im Schilddrüsengewebe in der Plasmamembran gefunden, während die LAT Transporter im Zytoplasma lokalisiert waren. In bösartigen Schilddrüsentumoren wurde MCT8 geringer exprimiert im Vergleich zu normalem Schilddrüsengewebe. Im Gegensatz dazu war die Expression von MCT8 und LAT4 im Basedow Gewebe signifikant erhöht. Außerdem wurde eine stärkere Expression von MCT8 in PCCL3 Zellen nach TSH Stimulation nachgewiesen.

Die verringerte Expression von MCT8 bei Schilddrüsenkrebs qualifiziert MCT8 als Marker für eine Schilddrüsendifferenzierung. Das variable Expressionsmuster von LAT Transportern in den verschiedenen Schilddrüsentumoren scheint eher mit dem Transport von Aminosäuren als mit dem Efflux von Schilddrüsenhormonen verknüpft zu sein. Die durchgehend stark erhöhte Expression von Schilddrüsenhormontransportern in den Basedow Proben kann funktionell mit der erhöhten Freisetzung von Schilddrüsenhormone während einer Hyperthyreose verknüpft werden. Diese Annahme konnte durch in-vitro Stimulationsexperimente untersützt werden. Außerdem zeigten diese Versuche eine Verknüpfung von MCT8 Expression und dem cAMP abhängigen Signalweg.

C) Material

Laboratory Equipment

Table 6: Laboratory equipment

Name	**Supplier**
Autoclave Systec VX150	Systec GmbH, Linden, Germany
Automated cell counter TC20	BioRad, Hercules, USA
Autostainer for Imnunohostochemistry	Dako, Glostrup, Denmark
Cell counter Coulter counter Z2	Beckman Coulter, Brea, USA
Centrifuge Heraeus FRESCO 17	Thermo Scientific, Waltham, USA
Centrifuge Heraeus™ Megafuge™ 16R	Thermo Scientific, Waltham, USA
CO_2-Incubator Heracell™ 150i	Thermo Scientific, Waltham, USA
Confocal microscope Nikon Eclipse T_i	Nikon, Tokio, Japan
ELYRA PS.1 SIM/PAL-M/STORM/TIRF	Zeiss, Jena, Germany
Freezer – 20 °C	Liebherr, Bulle, Switzerland
Freezer – 80 °C	Thermo Scientific, Waltham, USA
Fridge 4 °C	Liebherr, Bulle, Switzerland
Ice Maker AF100	Scotsman, Vernon Hills, USA
Ikamag Ret Magnetic Stirrer	IKA, Staufen, Germany
Laminar Flow Hood HERASAFE KS	Thermo Scientific, Waltham, USA
Light Cycler 480 II	Roche, Basel, Switzerland
LSM 510 Meta confocal microscope	Zeiss, Jena, Germany
Microscope Olympus BX51 upright	Olympus, Tokio, Japan
Microscope Olympus CK40	Olympus, Tokio, Japan
Microscope Primo Vert	Zeiss, Jena, Germany

Microtome	Jung AG, Germany
Microwave	Daewoo, Seoul, South Korea
Milli-Q® Advantage Water Purification	Merck Millipore, Darmstadt, Germany
Molecular Imager VersaDoc MP4000	BioRad, Hercules, USA
NanoDrop 2000c UV-Vis Spectrophotometer	Thermo Scientific, Waltham, USA
Pipettes	Eppendorf, Hamburg, Germany
S220 SevenCompact™ pH/Ion	Mettler Toledo, Greifensee, Switzerland
Summit-SI Balance SI-114A-DC	Denver Instrument, Bohemia, USA
Thermocycler Tprofessional TRIO	Analytik Jena, Jena, Germany
Trans-Blot Turbo Transfer System	BioRad, Hercules, USA
VersaMax ELISA Microplate Reader	Molecular Devices, USA
Vortex 4 basic	IKA, Staufen, Germany
Waterbath	GFL, Burgwedel, Germany

Chemicals

Table 7: Chemicals for molecular biological, protein biochemical and cell biological applications

Name	**Supplier**
Acetic acid	Sigma Aldrich, St. Louis, USA
Agarose	Sigma Aldrich, St. Louis, USA
Ampicilin	Carl Roth, Karlsruhe, Germany
AnnexinV binding buffer	Becton Dickinson, Franklin Lakes, USA
Aquatex	Merck, Darmstadt, Germany

BD Matrigel™ Basement Membrane Matrix	Becton Dickinson, Franklin Lakes, USA
BlueJuice™ Gel Loading Buffer (10X	Thermo Scientific, Waltham, USA
Bovine serum albumin	Sigma Aldrich, St. Louis, USA
Citrate buffer (pH 6.0)	Zytomed, Berlin, Germany
Clarity Western ECL Substrate	BioRad, Hercules, USA
Collagen I	Sigma Aldrich, St. Louis, USA
cOmplete ULTRA Tablets	Roche, Basel, Switzerland
Crytsal violet	Carl Roth, Karlsruhe, Germany
Dimethyl sulfoxide	Sigma Aldrich, St. Louis, USA
Dithiothreitol	Sigma Aldrich, St. Louis, USA
Entellan	Merck, Darmstadt, Germany
Ethanol 100 %	UK Essen pharmacy, Essen, Germany
Ethanol 70 %	UK Essen pharmacy, Essen, Germany
Ethylenediaminetetraacetic acid	Sigma Aldrich, St. Louis, USA
Etoposide	Sigma Aldrich, St. Louis, USA
Geneticindisulfate	Carl Roth, Karlsruhe, Germany
Glycerol	Sigma Aldrich, St. Louis, USA
Gö6983	Sigma Aldrich, St. Louis, USA
Haematoxyline	Carl Roth, Karlsruhe, Germany
Histofix	Carl Roth, Karlsruhe, Germany
Histogel	Thermo Scientific, Waltham, USA

Hydrogen peroxide	Carl Roth, Karlsruhe, Germany
Hygromycin B	Invitrogen, Carlsbad, USA
Immersion oil	Merck, Darmstadt, Germany
ImmuMount	Thermo Scientific, Waltham, USA
Isopropanol	Sigma Aldrich, St. Louis, USA
Kanamycin	Carl Roth, Karlsruhe, Germany
Laemmli Sample Buffer	BioRad, Hercules, USA
Lipofectamin 2000	Invitrogen, Carlsbad, USA
Magnesium chloride	Sigma Aldrich, St. Louis, USA
Magnesium sulfate	Sigma Aldrich, St. Louis, USA
Methanol	Carl Roth, Karlsruhe, Germany
Methylcellulose	Sigma Aldrich, St. Louis, USA
Milk powder	Carl Roth, Karlsruhe, Germany
Mounting medium	Thermo Scientific, Waltham, USA
Nonidet P40 Substitute	Sigma Aldrich, St. Louis, USA
OptiMem	Invitrogen, Carlsbad, USA
Paraformaldehyd	Sigma Aldrich, St. Louis, USA
Peptone	Carl Roth, Karlsruhe, Germany
Phorbol-12-myristate-13-acetate	Merck, Darmstadt, Germany
PhosSTOP	Roche, Basel, Switzerland
Poly-L-Lysine	Sigma Aldrich, St. Louis, USA
Polymer system	Zytomed, Berlin, Germany
Potassium chloride	Sigma Aldrich, St. Louis, USA

Propidium iodide	Becton Dickinson, Franklin Lakes, USA
Roti®-Histofix 4 %	Carl Roth, Karlsruhe, Germany
Roti-Safe GelStain	Carl Roth, Karlsruhe, Germany
siRNA Transfection Medium	Santa Cruz, Dallas, USA
siRNA-A	Santa Cruz, Dallas, USA
siRNA-Claudin-1	Santa Cruz, Dallas, USA
siRNA-DJ1	Santa Cruz, Dallas, USA
Sodium chloride	Sigma Aldrich, St. Louis, USA
Sodium deoxycholate	Sigma Aldrich, St. Louis, USA
Sodium dodecyl sulfate	Sigma Aldrich, St. Louis, USA
Sodium fluoride	Sigma Aldrich, St. Louis, USA
Sodium hydroxid	Sigma Aldrich, St. Louis, USA
SuperScript® III First-Strand Synthesis SuperMix	Invitrogen, Carlsbad, USA
SYBR Green I Master	Roche, Basel, Switzerland
Toluidin blue	Merck, Darmstadt, Germany
Tris-base	Carl Roth, Karlsruhe, Germany
Tris-hydrochloric	Sigma Aldrich, St. Louis, USA
Triton X-100	Sigma Aldrich, St. Louis, USA
Tween 20	Sigma Aldrich, St. Louis, USA
Yeast extract	Carl Roth, Karlsruhe, Germany
ZellShield	Minerva Biolabs, Berlin, Germany
β-Mercaptoethanol	Sigma Aldrich, St. Louis, USA

Enzymes, polymerase, ligase and restriction buffer

Table 8: Enzymes, ligase and restriction buffer for molecular biological applications

Name	Supplier
BamHI	Thermo Scientific, Waltham,USA
DpnI	Agilent Technologies, Santa Clara, USA
HindIII	Thermo Scientific, Waltham, USA
Pfu Polymerase	Agilent Technologies, Santa Clara, USA
Restriction buffer	Thermo Scientific, Waltham, USA
T4 DNA Ligase	New England Biolabs, Ipswich, USA
Taq Polymerase	Invitrogen, Carlsbad, USA

Kits

Table 9: Kits for molecular biological-, protein biochemical- and cell biological applications

Name	Supplier
5-Bromo-2‘-deoxy-uridine Labeling and Detection Kit III	Roche, Basel, Switzerland
Caspase-3/ CPP32 Colorimetric Protease Assay	Invitrogen, Carlsbad, USA
EndoFree Plasmid Maxi Kit	Quiagen, Hilden, Germany
Pierce™ BCA Protein Assay Kit	Thermo Scientific, Waltham, USA
QIAprep Spin Miniprep Kit	Quiagen, Hilden, Germany
Quick Change site directed mutagenesis Kit	Agilent Technologies, Santa Clara, USA
RNeasy Fibrous Tissue Mini Kit	Quiagen, Hilden, Germany
Subcellular Protein Fractionation Kit	Thermo Scientific, Waltham, USA

Cells

For *in vitro* experiments the human follicular carcinoma cells lines FTC-133 and FTC-238 and the rat thyroid follicular cell line PCCL3 were used. The human cell lines FTC-133 (Hoelting *et al*., 1997) and FTC-238 (Hoelting *et al*., 1997) are derived from the same male patient and harbor a tp53 mutation, whereas a homozygous PTEN inactivating mutation is only present in FTC-133 cells (Weng *et al*., 2001; Morani *et al*., 2001). FTC-133 cells are derived from a regional lymph node metastasis, whereas the FTC-238 cells are derived from a lung metastasis. Both cell lines were purchased from the European Collection of Cell Cultures (ECACC, Salisbury, UK). The PCCL3 cells are derived from Fisher rat thyroid follicular cells (Fusco *et al*., 1997). They are dependent on TSH for growth and they retain differentiated properties as they express thyroid specific markers like thyroglobulin, thyroid peroxidase and the TSH receptor.

Bacterial cells

For generation of the used constructs the XL-1 blue chemically competent cells were used.

Antibodies

Table 10: Primary antibodies for Western blot, IHC and IF

Name	Host	Number	Application	Supplier
Alexa Fluor 555 Phalloidin	-	#8953	IF	Cell Signaling, Danvers, USA
Anti-Akt	Rabbit	#9272	WB	Cell Signaling, Danvers, USA
Anti-alpha 1 Sodium Potassium ATPase	Mouse	#7671	WB	Abcam, Cambridge, UK

Anti-alpha-Tubulin	Mouse	#05-829	WB	Merck-Millipore, Darmstadt, Germany
Anti-claudin-1	Rabbit	#717800	WB, IHC, IF	Invitrogen, Carlsbad, USA
Anti-DJ-1 (D29E5) XP	Rabbit	#5933	WB, IF	Cell Signaling, Danvers, USA
Anti-Foxo3a	Rabbit	#2497	WB, IF	Cell Signaling, Danvers, USA
Anti-GAPDH	Mouse	#ACR001P	WB	Acris antibodies, Herford, Germany
Anti-Lamin A/C (4C11)	Mouse	#4777	WB	Cell Signaling, Danvers, USA
Anti-LAT2	Rabbit	#0142-10	IHC	Immunoglobe, Himmelstadt, Germany
Anti-P44/42 MAPK (Erk1/2)(137F5)	Rabbit	#4695	WB	Cell Signaling, Danvers, USA
Anti-PARK7/DJ1 antibody (prediluted)	Rabbit	#74317	IHC	Abcam, Cambridge, UK
Anti-Phospho-Akt (Ser473) (D9E) XP®	Rabbit	#4060	WB	Cell Signaling, Danvers, USA
Anti-Phospho-p44/42 (Erk1/2)	Rabbit	#4370	WB	Cell Signaling, Danvers, USA
Anti-Phospho-P70S6K	Rabbit	#9204	WB	Cell Signaling, Danvers, USA
Anti-phospho-PKC	Rabbit	#AB577-3451	WB	PromoKine, Heidelberg, Germany

Anti-PKC	Mouse	#P5704	WB	Sigma Aldrich, St. Louis, USA
Anti-PTEN (D4.3) XP	Rabbit	#9188	WB	Cell Signaling, Danvers, USA
Anti-RasV12	Rabbit	#140571	WB	Abcam, Cambridge, UK
Anti-SLC16A2/ MCT8	Rabbit	#HPA003 353	WB, IHC, IF	Atlas Antibodies, Stockholm, Sweden
Anti-SLC43A1/ LAT3	Rabbit	#HPA018 826	IHC	Atlas Antibodies, Stockholm, Sweden
Anti-SLC43A2/ LAT4	Rabbit	#HPA021 564	IHC	Atlas Antibodies, Stockholm, Sweden
Anti-β-Actin (8H10D10)	Mouse	#4970	WB	Cell Signaling, Danvers, USA
Draq5TM	-	#62251	IF	Invitrogen, Carlsbad, USA
FITC AnnexinV	-	#556419	FACS	Becton Dickinson, Franklin, Lakes, USA
Hoechst 33342	-	#62249	IF	Thermo Fischer, Waltham, USA

Table 11: Secondary antibodies for IF and WB

Name	**Application**	**Supplier**
Anti-mouse IgG, DyLight488 conjugate	WB	Thermo Scientific, Waltham, USA
Anti-mouse IgG, HRP-linked Antibody	WB	Cell Signaling, Danvers, USA
Anti-rabbit IgG, DyLight488 conjugate	WB	Thermo Scientific, Waltham, USA
Anti-rabbit IgG, HRP-linked Antibody	WB	Cell Signaling, Danvers, USA

Anti-rabbit, Alexa Fluor 488	IF	Cell Signaling, Danvers, USA

Solutions and buffers

Table 12: Solutions and buffers for protein biochemical applications

Name	**Composition**
APS (10 %)	10 g Ammoniumpersulfate 100 ml H_2O
SDS (10 %)	10 g SDS 100 ml H_2O
Tris/ Glycin (TG) Buffer (10x)	30.8 g Tris-base 144 g Glycin 800 ml H_2O Bring up to a final volume of 1 l with H_2O.
TBS-T (1x)	50 ml TBS (20x) 2 ml Tween 20 (0.1 %) Bring up to a final volume of 2 l with H_2O.
Transfer Buffer (1x, Wet Blot)	100 ml 10x Tris/Glycin Puffer 200 ml Ethanol 700 ml H_2O
TBS (20x)	48 g Tris-base 160 g NaCl 800 ml H_2O Adjust pH to 7.6. Bring up to a final volume of 1 l with H_2O.
BSA (5 %)	2.5 g BSA 50 ml 1x TBS-T
Milk (5 %)	2.5 g Milk powder 50 ml 1x TBS-T

TAE (50x)	242 g Tris-Base 57.1 ml Acetic acid 18.6 g EDTA 800 ml H_2O Adjust pH to 8.0-8.3 with HCl. Bring up to a final volume of 1 l with H_2O.
Matrigel coating Buffer	0.06 g Tris-Base (0.01 M) 0.35 g NaCl (0.7 %) 50 ml deionized water Adjust pH to pH 8.0 .
RIPA buffer	3 ml 5 M NaCl (150 mM) 0.788 g Tris-HCl (50 mM) 1 ml NP-40 (1 %) 0.5 g Sodium deoxycholate (0.5 %) 100 mg SDS (0.1 %) 0.075 g EDTA (2mM) 0.21 g Sodium fluoride (50 mM) 100 ml H_2O
Crystal violet staining solution	2.5 g Crystal violet (0.5 %) 5 ml Formaldehyde (1%) 5 ml Methanol (1%) 500 ml PBS
1.0 M Tris/HCl	157.6 g Trizma Hydrochlorid (1.0 M) 800 ml H_2O Adjust pH to 6.8. Bring up to a final volume of 1 l with H_2O.
1.5 M Tris/HCl	236.4 Trizma Hydrochlorid (1.5 M) 800 ml H_2O Adjust pH to 8.8. Bring up to a final volume of 1 l with H_2O.

Table 13: Solutions and buffers for molecular biological applications

Name	Compostition
LB-Agar	10 g Peptone 5 g Yeast extract 10 g NaCl 15 g Agar 800 ml H_2O Adjust pH to 7.0. Bring up to a final volume of 1 l with H_2O.
LB-Medium	10 g Peptone 5 g Yeast extract 10 g Sodium chloride 800 ml H_2O Adjust pH to 7.0. Bring up to a final volume of 1 l with H_2O.

Cell culture

Table 14: Buffers and chemicals used for cell biological applications

Name	Supplier
Dulbecco’s Phosphate Buffered Saline	Invitrogen, Carlsbad, USA
Fetal bovine serum	Invitrogen, Carlsbad, USA
Forskolin	Sigma Aldrich, St. Louis, USA
Ham’s F12 Nutrient Mix	Invitrogen, Carlsbad, USA
Hank's Balanced Salt Solution	Invitrogen, Carlsbad, USA
Hydrocortison	Sigma Aldrich, St. Louis, USA
Insulin	Sigma Aldrich, St. Louis, USA
OptiMem	Invitrogen, Carlsbad, USA
Somatostatin	Sigma Aldrich, St. Louis, USA

Thyroid stimulating hormone	Sigma Aldrich, St. Louis, USA
Trypsin/EDTA (0.25 %)	Invitrogen, Carlsbad, USA

Table 15: Composition of cell culture media

Name	Composition
FTC-133 Medium	Ham's F12 10 % FBS
FTC-133 starvation medium/ serum-low	Ham's F12 2 % FBS
Methocel medium (hanging drop culture)	0.012 g/ml Methylcellulose 50 ml warm Ham's F12 Take 2 ml of this and mix with 8 ml PCCL3 medium
PCCL3 Medium	Ham's F12 5 % FBS 5 µg/ml Transferrin 1 mU/ml TSH 10 µg/ml Insulin 10 nM Hydrocortison 10 ng/ml Somatostatin (Medium is stable for 1 week)
PCCL3 starvation medium	Ham's F12

SDS gels

Table 16: Composition of 10 % SDS gel

Name	Composition
Separating Gel (10 %), mini	1.665 ml H2O 1.3 ml Rothiphorese Gel A (30 % Acrylamide)

	0.78 ml Rothiphores Gel B (2 % Bis-Acrylamide) 1.5 ml 1.5 M Tris HCl 60 µl 10 % SDS 60 µl 10 % APS 6 µl TEMED
Stacking gel (10 %), mini	1.875 ml H_2O 0.48 ml Rothiphorese Gel A (30 % Acrylamide) 0.195 ml Rothiphores Gel B (2 % Bis-Acrylamide) 0.39 ml 1.0 M Tris HCl 30 µl 10 % SDS 30 µl 10 % APS 3 µl TEMED

Software

Table 17: Software used for analysis and statistics

Name	**Supplier**
Blast	NCBI, Bethesda, USA
Graph Pad Prism 5	GraphPad Software Inc., La Jolla, USA
Image J 1.48 v	National Institute of health, Bethesda, USA
ImageLab™	BioRad, Hercules, USA
Quantity One	BioRad, Hercules, USA
TScratch	CSE Lab, Zurich, Switzerland

Oligonucleotides

Oligonucleotides were designed using PrimerBlast (National Center for Biotechnology, Bethesda, USA) and were synthesized by Eurofins (Eurofins MWG Synthesis, Ebersberg, Germany).

Table 18: Sequences of primer for qRT-PCR

Name	**Sequence for**	**Sequence rev**
r*Tg*	GCAGCCAACATCTTTGAGTACC	CACACACCAGCAAGATTGGC
r*Tpo*	CACGGCTTACCAGGCTACAA	GCCTCCCAACCAGACATCAA
r*Nis*	TCTTGCCGATCTTCTACCGC	CCGGTCACTTGGTTCAGGAT
r*Thox1*	ACATTTCCCCCATTACCATTTTCA	AGCCGAGAGCCTTTGCTG
r*bActin*	ACCCGCCACCAGTTCG	ACCCATACCCACCATCACAC
r*Ppia*	CTGAGTGGCTGGATGGCAA	ACAGAAGGAATGGTTTGATG
r*DJ-1*	CCATCTGTGCGGGTCCTAC	GCTGCCGTTCATCATTTTGTC
h*DJ-1*	ATCTGAGTCTGCTGCTGTGA	TGACCTCCATTCATCATTTTG
h*PPIA*	AACGTGGTATAAAAGGGGCGG	CTGCAAACAGCTCAAAGGAG
18S	CGGCTACCACATCCAAGGAA	GCTGGAATTACCGCGGCT
h*bACTIN*	AGAGCTACGAGCTGCCTGAC	AGCACTGTGTTGGCGTACAG
h*MCT8*	CTCCTTCACCAGCTCCCTAAG	ACTTCCAGCAGATACCACAC
h*LAT2*	AACAACACCGCGAAGAACCA	GGAGCCAATGATGTTCCCTA
h*LAT3*	GGACGTGGAAGCTCTGTCTC	CCGGCATCGTAGATCAGCT
h*LAT4*	GACCAGAAGACAGTTGGCCT	GGCGTCTTCACACTCCTTCA

Table 19: Sequences of primer for mutagenesis

Name	**Sequence for**	**Sequence rev**

HRas-flanc	GCCACCATGACGGAATATAAGCTGGTGG	TCAGGAGAGCACACACTTGCAGCTC
RasT40	CTATAGAGGATTCCTACCGGAAGCAGGTGGT	ACCACCTGCTTCCGGTAGGAATCCTCTATAG
DJ1-hu	TCTGGTCATCCTGGCTAAAGG	CTGAATGGCAAGGAGGTGGC

Table 20: Primer for control PCRs and sequencing

Name	**Sequence**	**Application**
DJ1-for	AAGGAGCAGGAAAACCGG	Control PCR transfection
HRAS_1_for	ATGACGGAATATAAGCTGGT	Sequencing
HRAS_2_for	GCAAGTGTGTGCTCTCCTGA	Sequencing
HRAS_3_for	TTGTCGGGCACAGATGGGA	Sequencing
PAX8_PPARg_1	CAGTGATCAGGATAGCTGCC	Sequencing
PAX8_PPARg_2	CCAAAGTGCAATCAAAGTGG	Sequencing
pcDNA3.1_BAMHI_rev	TTTAAACGGGCCCTCTAGACTC	Control PCR transfection Sequencing
PPFPctr_for	GACAATGACACTGTGCCCAG	Control PCR transfection
PPFPctr_rev	CGATGGCAGAGGAGGCATA	Control PCR transfection
RasV12ctl_for	GAGTGCGCTGACCATCC	Control PCR transfection
SV40 Promotor	GCCCCTAACTCCGCCCATCC	Sequencing

Expendable materials

Table 21: Expendable materials used for molecular biological, protein biochemical and cell biological applications

Name	**Supplier**

Any kD Criterion TGX SDS polyacryklamide gel	BioRad, Hercules, USA
Cell culture inserts ThinCerts™ 24-well	Greiner, Essen, Germany
Cell Scraper 25 cm	Sarstedt, Nümbrecht, Germany
Cellstar® 24 Well Multiwell plates	Greiner, Essen, Germany
Cellstar® 6 Well Multiwell plates	Greiner, Essen, Germany
Cellstar® Cell culture dishes, 100/20 mm	Greiner, Essen, Germany
Cellstar® Cell culture flasks, 75 cm^2	Greiner, Essen, Germany
Cellstar® Serological pipette, 10 ml	Greiner, Essen, Germany
Cellstar® Serological pipette, 25 ml	Greiner, Essen, Germany
Cellstar® Serological pipette, 5 ml	Greiner, Essen, Germany
Cellstar® Serological pipette, 50 ml	Greiner, Essen, Germany
Centrifuge tubes, 15 ml	Greiner, Essen, Germany
Centrifuge tubes, 50 ml	Greiner, Essen, Germany
Cover Slides (Ø13mm)	Knittel Gläser GmbH, Braunschweig, Germany
Cyro mold	NeoLab, Heidelberg, Germany
Microscope Slides SuperFrost ®	R. Langenbrinck, Emmendingen, Germany
Microtome Blade A35	Feather, Tokio, Japan
PCR SoftTubes, 0.2 ml	Biozym, Hessisch Oldendorf, Germany
Reaction tubes, 0.5 ml	Carl Roth, Karlsruhe, Germany
Reaction tubes, 1.5 ml	Carl Roth, Karlsruhe, Germany
Reaction tubes, 2.0 ml	Carl Roth, Karlsruhe, Germany
Weighing pan	NeoLab, Heidelberg, Germany

D) Supplemetal Data

Chapter 2

1 Sequence analysis

The sequence of the constructs DJ-1, RASV12, PAX8/PPARγ and pcDNA3.1/Hygro were verified by sequence analysis using the primer listed in Appendix C (Material, Table 17).

pcDNA3.1/Hygro-DJ-1

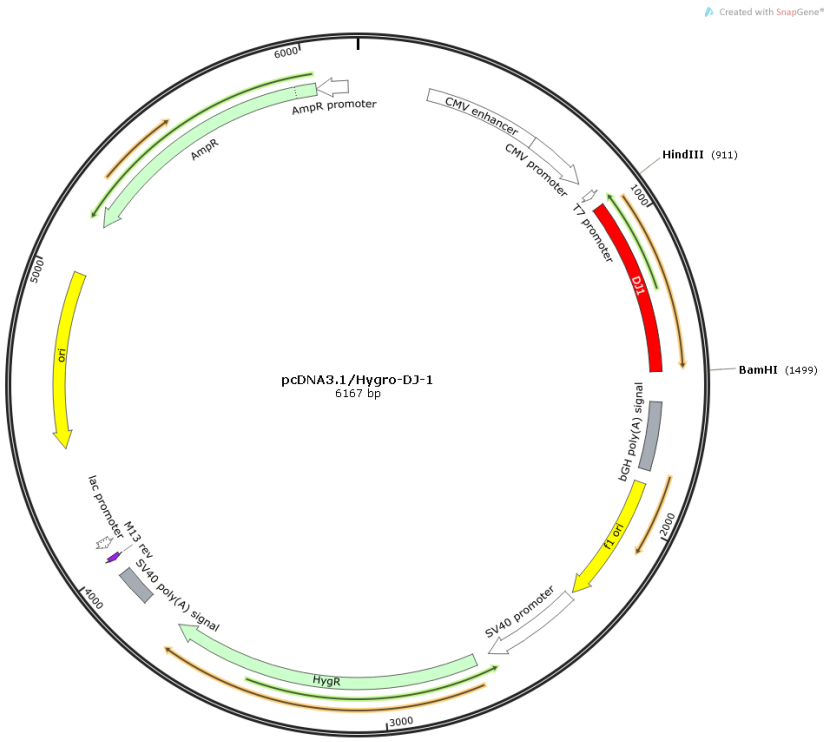

Figure 33: Map of the plasmid pcDNA3.1/Hygro-DJ-1.

Verification of the plasmid sequence was done by comparison to the published sequence (NM_007262.4, PARK7 transcript variant 1). Consistently bases are highlighted in yellow. The restriction enzymes HindIII and BamHI are highlighted in green.

GGCTAGCGTTTAAACTT**AAGCTT**GGTACCGAGCTCGATGGCTTCCAAAAGAGCTCTGGTCATCCT
GGCTAAAGGAGCAGAGGAAATGGAGACGGTCATCCCTGTAGATGTCATGAGGCGAGCTGGGATT
AAGGTCACCGTTGCAGGCCTGGCTGGAAAAGACCCAGTACAGTGTAGCCGTGATGTGGTCATTT
GTCCTGATGCCAGCCTTGAAGATGCAAAAAAAGAGGGACCATATGATGTGGTGGTTCTACCAGGA
GGTAATCTGGGCGCACAGAATTTATCTGAGTCTGCTGCTGTGAAGGAGATACTGAAGGAGCAGG
AAAACCGGAAGGGCCTGATAGCCGCCATCTGTGCAGGTCCTACTGCTCTGTTGGCTCATGAAATA

GGTTTTGGAAGTAAAGTTACAACACACCCTCTTGCTAAAGACAAAATGATGAATGGAGGTCATTAC
ACCTACTCTGAGAATCGTGTGGAAAAAGACGGCCTGATTCTTACAAGCCGGGGGCCTGGGACCA
GCTTCGAGTTTGCGCTTGCAATTGTTGAAGCCCTGAATGGCAAGGAGGTGGCGGCTCAAGTGAA
GGCTCCACTTGTTCTTAAAGACTA**GGATCC**ACT

pcDNA3.1-RASV12

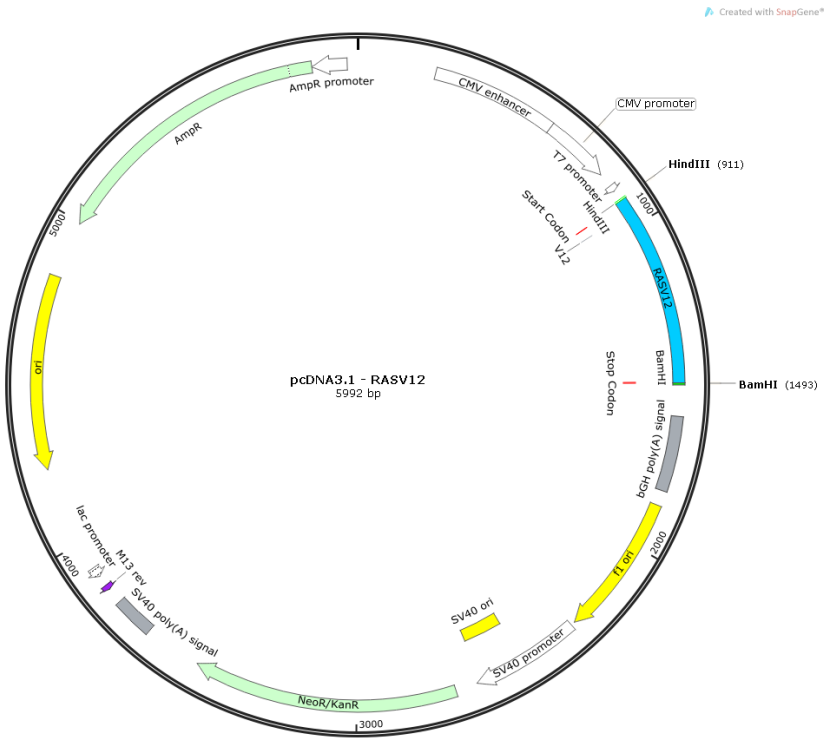

Figure 34: Map of the plasmid pcDNA3.1-RASV12.

Verification of the plasmid sequence was done by comparison to the published sequence (NM_005343.2, HRAS transcript variant 1). Consistently bases are highlighted in yellow. The restriction enzymes HindIII and BamHI are highlighted in green. The G12V mutation is highlighted in red.

CTAGCGTTTAAACTT**AAGCTT**GCCACCATGACGGAATATAAGCTGGTGGTGGTGGGCGCCG**G**CG
GTGTGGGCAAGAGTGCGCTGACCATCCAGCTGATCCAGAACCATTTTGTGGACGAATACGACCC
CACTATAGAGGATTCCTACCGGAAGCAGGTGGTCATTGATGGGGAGACGTGCCTGTTGGACATC
CTGGATACCGCCGGCCAGGAGGAGTACAGCGCCATGCGGGACCAGTACATGCGCACCGGGGA
GGGCTTCCTGTGTGTGTTTGCCATCAACAACACCAAGTCTTTTGAGGACATCCACCAGTACAGGG
AGCAGATCAAACGGGTGAAGGACTCGGATGACGTGCCCATGGTGCTGGTGGGGAACAAGTGTG
ACCTGGCTGCACGCACTGTGGAATCTCGGCAGGCTCAGGACCTCGCCCGAAGCTACGGCATCC
CCTACATCGAGACCTCGGCCAAGACCCGGCAGGGAGTGGAGGATGCCTTCTACACGTTGGTGC
GTGAGATCCGGCAGCACAAGCTGCGGAAGCTGAACCCTCCTGATGAGAGTGGCCCCGGCTGCA
TGAGCTGCAAGTGTGTGCTCTCCTGA**GGATCC**ACTAGTCCAGTGTGGTGGAATTCTGCAGATATC
CAGCACAGTGGCGGCCGCTCGAGTCTAGAG

pcDNA3.1-PPFP

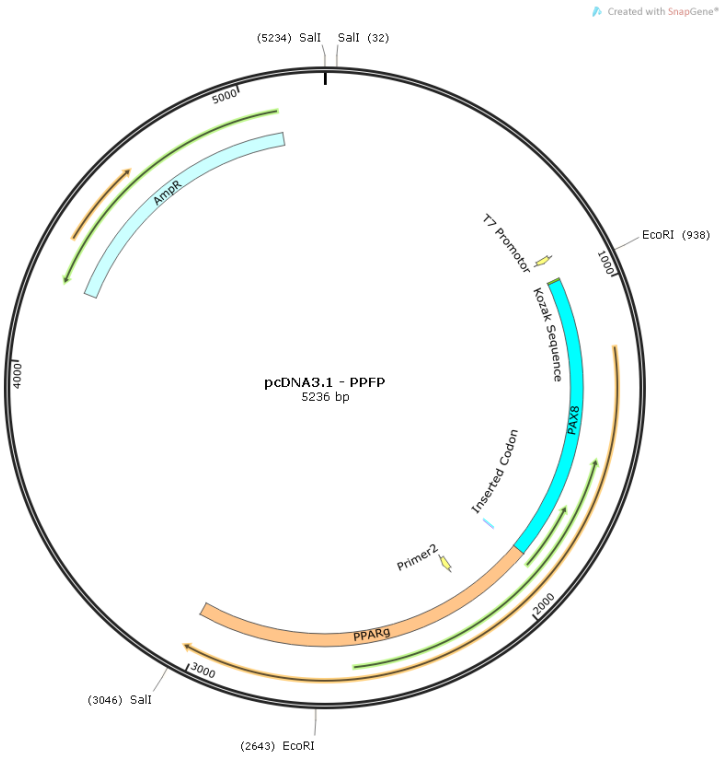

Figure 35: Map of the plasmid pcDNA3.1-PPFP.

Verification of the plasmid sequence was done by comparison to the published sequence. Consistently bases are highlighted in yellow. The restriction enzymes EcoRI and SalI are highlighted in green.

tagtaacggccgccagtgtgctgGAATTCGCCACCATGGCAGACCTCTGCCGGAAGTGGTCCGCCAGCGCA
TCGTAGACCTGGCCCACCAGGGTGTAAGGCCCTGCGACATCTCTCGCCAGCTCCGCGTCAGCCA
TGGCTGCGTCAGCAAGATCCTTGGCAGGTACTACGAGACTGGCAGCATCCGGCCTGGAGTGATA
GGGGGCTCCAAGCCCAAGGTGGCCACCCCCAAGGTGGTGGAGAAGATTGGGGACTACAAACGC
CAGAACCCTACCATGTTTGCCTGGGAGATCCGAGACCGGCTCCTGGCTGAGGGCGTCTGTGACA
ATGACACTGTGCCCAGTGTCAGCTCCATTAATAGAATCATCCGGACCAAAGTGCAGCAACCATTC
AACCTCCCTATGGACAGCTGCGTGGCCACCAAGTCCCTGAGTCCCGGACACACGCTGATCCCCA
GCTCAGCTGTAACTCCCCCGGAGTCACCCCAGTCGGATTCCCTGGGCTCCACCTACTCCATCAA
TGGGCTCCTGGGCATCGCTCAGCCTGGCAGCGACAAGAGGAAAATGGATGACAGTGATCAGGAT
AGCTGCCGACTAAGCATTGACTCACAGAGCAGCAGCAGCGGACCCCGAAAGCACCTTCGCACG
GATGCCTTCAGCCAGCACCACCTCGAGCCGCTCGAGTGCCCATTTGAGCGGCAGCACTACCCAG
AGGCCTATGCCTCCCCCAGCCACACCAAAGGCGAGCAGGGCCTCTACCCGCTGCCCTTGCTCAA
CAGCACCCTGGACGACGGGAAGGCCACCCTGACCCCTTCCAACACGCCACTGGGGCGCAACCT
CTCGACTCACCAGACCTACCCCGTGGTGGCAGGGCGAGAGATGGTGGGGCCCACGCTGCCCGG
ATACCCACCCCACATCCCCACCAGCGGACAGGGCAGCTATGCCTCCTCTGCCATCGCAGGCATG
GTGGCAGAAATGACCATGGTTGACACAGAGATGCCATTCTGGCCCACCAACTTTGGGATCAGCT
CCGTGGATCTCTCCGTAATGGAAGACCACTCCCACTCCTTTGATATCAAGCCCTTCACTACTGTT
GACTTCTCCAGCATTTCTACTCCACATTACGAAGACATTCCATTCACAAGAACAGATCCAGTGGTT
GCAGATTACAAGTATGACCTGAAACTTCAAGAGTACCAAAGTGCAATCAAAGTGGAGCCTGCATC
TCCACCTTATTATTCTGAGAAGACTCAGCTCTACAATAAGCCTCATGAAGAGCCTTCCAACTCCCT
CATGGCAATTGAATGTCGTGTCTGTGGAGATAAAGCTTCTGGATTTCACTATGGAGTTCATGCTTG
TGAAGGATGCAAGGGTTTCTTCCGGAGAACAATCAGATTGAAGCTTATCTATGACAGATGTGATC

TTAACTGTCGGATCCACAAAAAAAGTAGAAATAAATGTCAGTACTGTCGGTTTCAGAAATGCCTTG
CAGTGGGGATGTCTCATAATGCCATCAGGTTTGGGCGGATGCCACAGGCCGAGAAGGAGAAGCT
GTTGGCGGAGATCTCCAGTGATATCGACCAGCTGAATCCAGAGTCCGCTGACCTCCGGGCCCTG
GCAAAACATTTGTATGACTCATACATAAAGTCCTTCCCGCTGACCAAAGCAAAGGCGAGGGCGAT
CTTGACAGGAAAGACAACAGACAAATCACCATTCGTTATCTATGACATGAATTCCTTAATGATGGG
AGAAGATAAAATCAAGTTCAAACACATCACCCCCCTGCAGGAGCAGAGCAAAGAGGTGGCCATC
CGCATCTTTCAGGGCTGCCAGTTTCGCTCCGTGGAGGCTGTGCAGGAGATCACAGAGTATGCCA
AAAGCATTCCTGGTTTTGTAAATCTTGACTTGAACGACCAAGTAACTCTCCTCAAATATGGAGTCC
ACGAGATCATTTACACAATGCTGGCCTCCTTGATGAATAAAGATGGGGTTCTCATATCCGAGGGC
CAAGGCTTCATGACAAGGGAGTTTCTAAAGAGCCTGCGAAAGCCTTTTGGTGACTTTATGGAGCC
CAAGTTTGAGTTTGCTGTGAAGTTCAATGCACTGGAATTAGATGACAGCGACTTG

pcDNA3.1/Hygro-RASV12

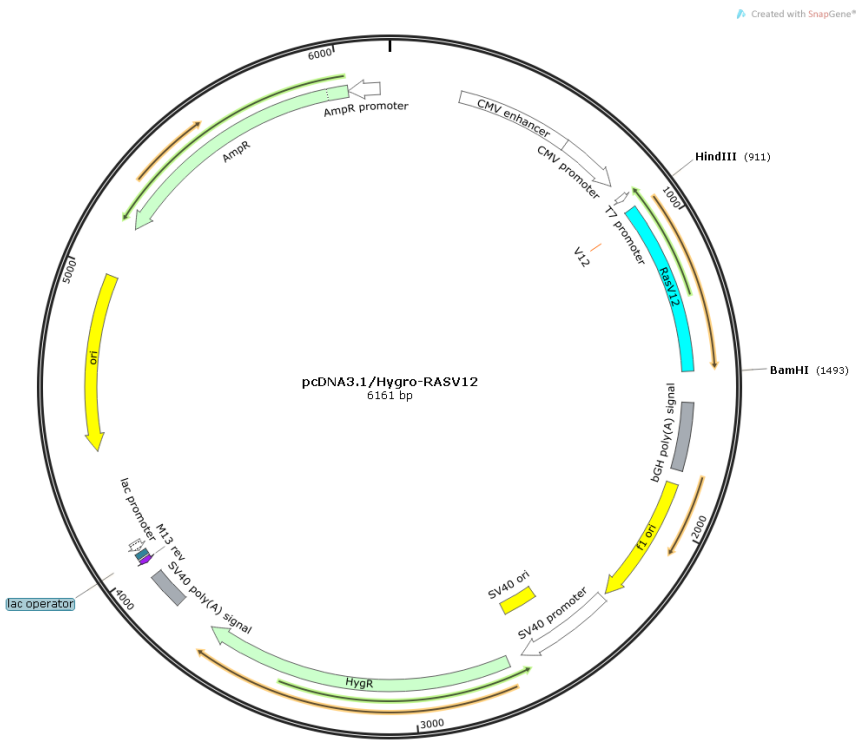

Figure 36: Map of the plasmid pcDNA3.1/Hygro-RASV12.

Verification of the plasmid sequence was done by comparison to the published sequence (NM_005343.2, HRAS transcript variant 1). Consistently bases are highlighted in yellow. The restriction enzymes HindIII and BamHI are highligted in green. The G12V mutation is highlighted in red.

CTAGCGTTTAAACTT**AAGCTT**GCCACCATGACGGAATATAAGCTGGTGGTGGTGGGCGCCG**G**CG
GTGTGGGCAAGAGTGCGCTGACCATCCAGCTGATCCAGAACCATTTTGTGGACGAATACGACCC
CACTATAGAGGATTCCTACCGGAAGCAGGTGGTCATTGATGGGGAGACGTGCCTGTTGGACATC
CTGGATACCGCCGGCCAGGAGGAGTACAGCGCCATGCGGGACCAGTACATGCGCACCGGGGA
GGGCTTCCTGTGTGTGTTTGCCATCAACAACACCAAGTCTTTTGAGGACATCCACCAGTACAGGG
AGCAGATCAAACGGGTGAAGGACTCGGATGACGTGCCCATGGTGCTGGTGGGGAACAAGTGTG
ACCTGGCTGCACGCACTGTGGAATCTCGGCAGGCTCAGGACCTCGCCCGAAGCTACGGCATCC

CCTACATCGAGACCTCGGCCAAGACCCGGCAGGGAGTGGAGGATGCCTTCTACACGTTGGTGC
GTGAGATCCGGCAGCACAAGCTGCGGAAGCTGAACCCTCCTGATGAGAGTGGCCCCGGCTGCA
TGAGCTGCAAGTGTGTGCTCTCCTGA**GGATCC**ACTAGTCCAGTGTGGTGGAATTCTGCAGATATC
CAGCACAGTGGCGGCCGCTCGAGTCTAGAG

2 Apoptosis induction (PCCL3)

Before starting to investigate the Caspase-3 activity of DJ-1, RASV12 and PPFP single transfected cells as well as DJ-1-RASV12 and DJ-1-PPFP co-transfected cells (see 3.3.3, Fig. 16), we performed tests to find the optimal etoposide concentration. PCCL3 wt cells were incubated with 10 µM, 20 µM, 50 µM, 70 µM and 150 µM etoposide for 24 h (Fig. 29A) or 48 h (Fig. 29B). Then cells were detached with trypsin/EDTA, absorbed in trypan blue and living cells were counted using a cell counter system (BioRad TC 20).

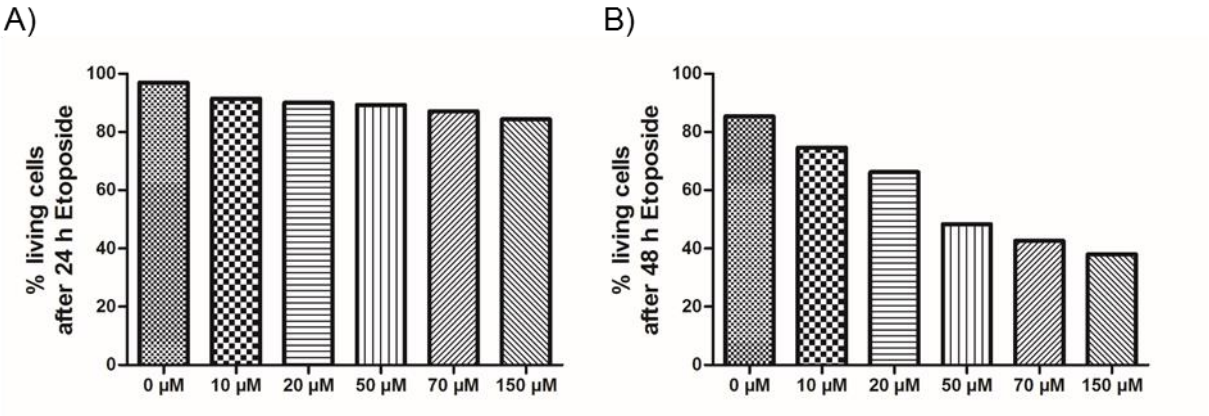

Figure 37: Test for apoptosis induction by etoposide. A) PCCL3 wt cells were incubated with indicated etoposide concentrations for 24 h. Living cells were counted using the BioRad TC20 cell counter system. B) PCCL3 wt cells were incubated with indicated etoposide concentrations for 48 h. Living cells were counted using the BioRad TC20 cell counter system.

The results showed, that 24 h incubation with etoposide does not induce cell death within the PCCL3 cells. So, we repeated the experiment and incubated the cells for 48 h with etopside. With a concentration of 50 µM Etoposide 50 % of the cells were still living.

E) List of figures

F) List of tables

G) Acknowledgement

My great thanks goes to Prof. Dr. Dr. Dagmar Führer-Sakel for giving me the pleasure to work in her lab and to give my very best for my projects. Your knowledge and motivation inspired me and I would like to thank you for your trust in me and for taking time for me whenever it was necessary.

My special thanks go to my lab manager Dr. Denise Zwanziger for having always an open ear and for giving me new ideas. Moreover, I would like to thank her for proofreading my manuscripts, congress contributions and also parts of this thesis. Thanks to Dr. Judith Hönes who helped me with the last experiments and to bring this to an end. Thanks to pathologist Dr. Saskia Ting who helped me with the immunohistochemistry of thyroid tumours and to Dr. med. Vera Tiedje who gave me an insight into the clinical point of view and who made me laugh whenever I met her.

Furthermore, I would like to thank Prof. Klaudia Brix (Jacobs University Bremen, Campus Ring 1, 28759 Bremen) who was a great cooperation partner and who made it possible to get such nice immunofluorescence pictures. Moreover, I would like to thank Prof. Georg Brabant (Universitätsklinikum Schleswig-Holstein, Ratzeburger Allee 160, 23538 Lübeck) for providing us thyroid tumour samples and who made it possible to investigate such a large series of thyroid tissue samples for immunohistochemistry. Thanks to Dr. H.V. Reddy (The Jackson Laboratory, Farmington, USA) who offered our group the PAX8/PPARγ plasmid, to Dr. I.E. Blasig (Leibniz-Institut für Molekulare Pharmakologie, Robert-Roessle-Str.10, 13125 Berlin) for providing us the Claudin-1 plasmid, to Dr. Kerstin Krause (University of Leipzig, Brüderstraße 34, 04103 Leipzig) for the DJ-1 and RASV12 plasmids and to Prof. Pilar Santisteban (Autonomous University of Madrid, Biomedical Research Institute *Alberto Sols*, Madrid, Spain) who made it possible to work with the PCCL3 cells. Thanks also to Dr. Bernd Kölsch (University Hospital Essen, Institute of Pathology, Hufelandstr.55, 45147 Essen) who offered us the thyroid of a 8 month old male rat for verification of our PCCL3 cell line.

Thanks to all of the members of the endocrine research lab at the University Hospital Essen: Helena, Kathrin, Sebastian, Sören, Steffi, Andrea, Hannah and Julius. Thanks for having great discussions and ideas for further experiments. I think we had a great

time together job-related but also private. Thanks especially to Steffi who gave every day a good beginning and who made working in this lab as easy as possible.

My greatest thanks go to my parents who made it possible to go this way and who supported me every time. Without them I wouldn’t be the person I am.

At last I would like to thank Kevin who was my tower of strength during the last years and who confirmed me everytime to go my way. You are one of my biggest supporters, my big love and my best friend.

H) Bestätigung der Betreuerin

Bestätigung:

Hiermit bestätige ich die Darstellung zu den Anteilen von Frau Julia Badziong an Konzeption, Durchführung und Abfassung jeder Publikation (Chapter 2-5) gemäß der Promotionsordnung der Fakultät für Biologie zur Erlangung des Dr. rer. nat.

Essen, den_____ _____

Prof. Dr. Dr. Dagmar Führer-Sakel

I) Eidesstattliche Erklärungen

Erklärung zu früheren Promotionsversuchen:

Hiermit erkläre ich, dass ich gemäß der Promotionsordnung der Fakultät für Biologie, § 6 Abs. (2) e) keine andere Promotion bzw. Promotionsversuche in der Vergangenheit durchgeführt habe.

Essen, den_____ _____

Julia Badziong

Erklärung zur kommerziellen Promotionsberatung (§ 6 Abs. 2 Buchstabe f)

Ich gebe folgende Erklärung ab:

Die Gelegenheit zum vorliegenden Promotionsverfahren ist mir nicht kommerziell vermittelt worden. Insbesondere habe ich keine Organisation eingeschaltet, die gegen Entgelt Betreuerinnen und Betreuer für die Anfertigung von Dissertationen sucht oder die mir obliegenden Pflichten hinsichtlich der Prüfungsleistungen für mich ganz oder teilweise erledigt. Hilfe Dritter wurde bis jetzt und wird auch künftig nur in wissenschaftlich vertretbarem und prüfungsrechtlich zulässigem Ausmaß in Anspruch genommen. Mir ist bekannt, dass Unwahrheiten hinsichtlich der vorstehenden Erklärung die Zulassung zur Promotion ausschließen bzw. später zum Verfahrensabbruch oder zur Rücknahme des Titels führen können.

Essen, den_____ _____

Julia Badziong

Erklärung:

Hiermit erkläre ich, gem. § 6 Abs. 2, g der Promotionsordnung der Fakultät für Biologie zur Erlangung der Dr. rer. nat., dass ich das Arbeitsgebiet, dem das Thema **„Relevance of the oncogene DJ-1, the tight junction protein Claudin-1 and the thyroid hormone transporter MCT8 for follicular thyroid carcinogenesis“** zuzuordnen ist, in Forschung und Lehre vertrete und den Antrag von Frau **Julia Badziong** befürworte.

Essen, den_____ _____

Prof. Dr. Dr. Dagmar Führer-Sakel

Erklärung:

Hiermit erkläre ich, gem. § 7 Abs. 2, d und f der Promotionsordnung der Fakultät für Biologie zur Erlangung des Dr. rer. nat., dass ich die vorliegende Dissertation selbständig verfasst und mich keiner anderen als der angegebenen Hilfsmittel bedient habe und alle wörtlich oder inhaltlich übernommenen Stellen als solche gekennzeichnet habe.

Essen, den_____ _____

Julia Badziong

Erklärung:

Hiermit erkläre ich, gem. § 7 Abs. 2, e und g der Promotionsordnung der Fakultät für Biologie zur Erlangung des Dr. rer. nat., dass ich keine anderen Promotionen bzw. Promotionsversuche in der Vergangenheit durchgeführt habe, dass diese Arbeit von keiner anderen Fakultät abgelehnt worden ist, und dass ich die Dissertation nur in diesem Verfahren einreiche.

Essen, den_____ _____

Julia Badziong

J) Curriculum vitae

Der Lebenslauf ist in der Online-Version aus Gründen des Datenschutzes nicht enthalten.

K) Publications

Denise Zwanziger*, **Julia Badziong***, Saskia Ting, Lars C Moeller, Kurt Werner Schmid, Udo Siebolts, Claudia Wickenhauser, Henning Dralle, and Dagmar Fuhrer, 2015, The impact of claudin-1 in follicular thyroid carcinoma aggressiveness, *Endocrine Relatated Cancer* **22** 819-30

*contributed equally

Tiedje V, Ting S, Walter R, Herold T, Worm K, **Badziong J**, Zwanziger D, Schmid KW, Fuhrer D, 2016, Prognostic markers and response to vandetanib therapy in sporadic medullary thyroid cancer patients, *Eur J Endocrinol* **175** 173-180

Julia Badziong, Saska Ting, Sarah Synoracki, Vera Tiedje, Klaudia Brix, Georg Brabant, Lars Christian Möller, Kurt Werner Schmid, Dagmar Führer and Denise Zwanziger, 2017, Differential regulation of monocarboxylate transporter 8 expression in thyroid cancer and hyperthyroidism, *European Journal of Endocrinology* **177 243-250**

Judith Hönes, **Julia Badziong**, Denise Zwanziger, Saskia Ting, Kurt Werner Schmid, Kerstin Krause, Lars Christian Moeller, Dagmar Fuehrer, Relevance of the oncogene DJ-1 in follicular thyroid carcinogenesis – *in preparation*

L) Congress contributions

Molecular discrimination of cold thyroid nodules (oral)

29th Arbeitstagung Experimentelle Schilddrüsenfoschung, Essen, Germany, 13.12.-15.12.13

MCT8 and LAT2 expression in thyroid tumours (poster)

38th Annual Meeting of the European Thyroid Association, Santiago de Compostela, Spain, 06.09.-10.09.14

Expression of DJ-1 in follicular thyroid tumours (poster)

13th Forschungstag der Medizinischen Falkultät, University Hospital Essen, Essen, Germany, 21.11.14

TH transporters in thyroid tumourigenesis (oral)

30th Arbeitstagung Experimentelle Schilddrüsenforschung, Bremen, Germany, 04.12.-05.12.14 & 1st International Conference TTA-IC, Bremen, Germany, 05.12.-07.12.14

TH transporter expression in differentially functioning benign and malignant thyroid tumours (Poster)

1st Essen Conference for Hematology and Oncology (ECHO), Essen, Germany, 10.04.-12.04.15

DJ-1 in follicular thyroid cancer (poster)

14th Forschungstag der Medizinischen Fakultät, University Hospital Essen, Essen, Germany, 20.11.15

Thyroid hormone transporter expression in differentially functioning benign and malignant thyroid tumours (oral)

Annual Meeting Graduate School of Biomedical Science (BIOME), 02.12.15

Relevance of the oncogene DJ-1 in follicular thyroid carcinogenesis (oral)

31th Arbeitstagung Experimentelle Schilddrüsenforschung, Berlin, Germany, 11.12.-13.12.15

DJ-1 in follicular thyroid carcinogenesis (flashtalk)

D·A·CH-Tagung der DGE, ÖGES und SGED, München, Germany, 26.05.-28.05.16